Role of Flexibility in Grid Connection Capacity Planning of Large Urban Living Spaces

MSc Thesis project

Stefano Carraro

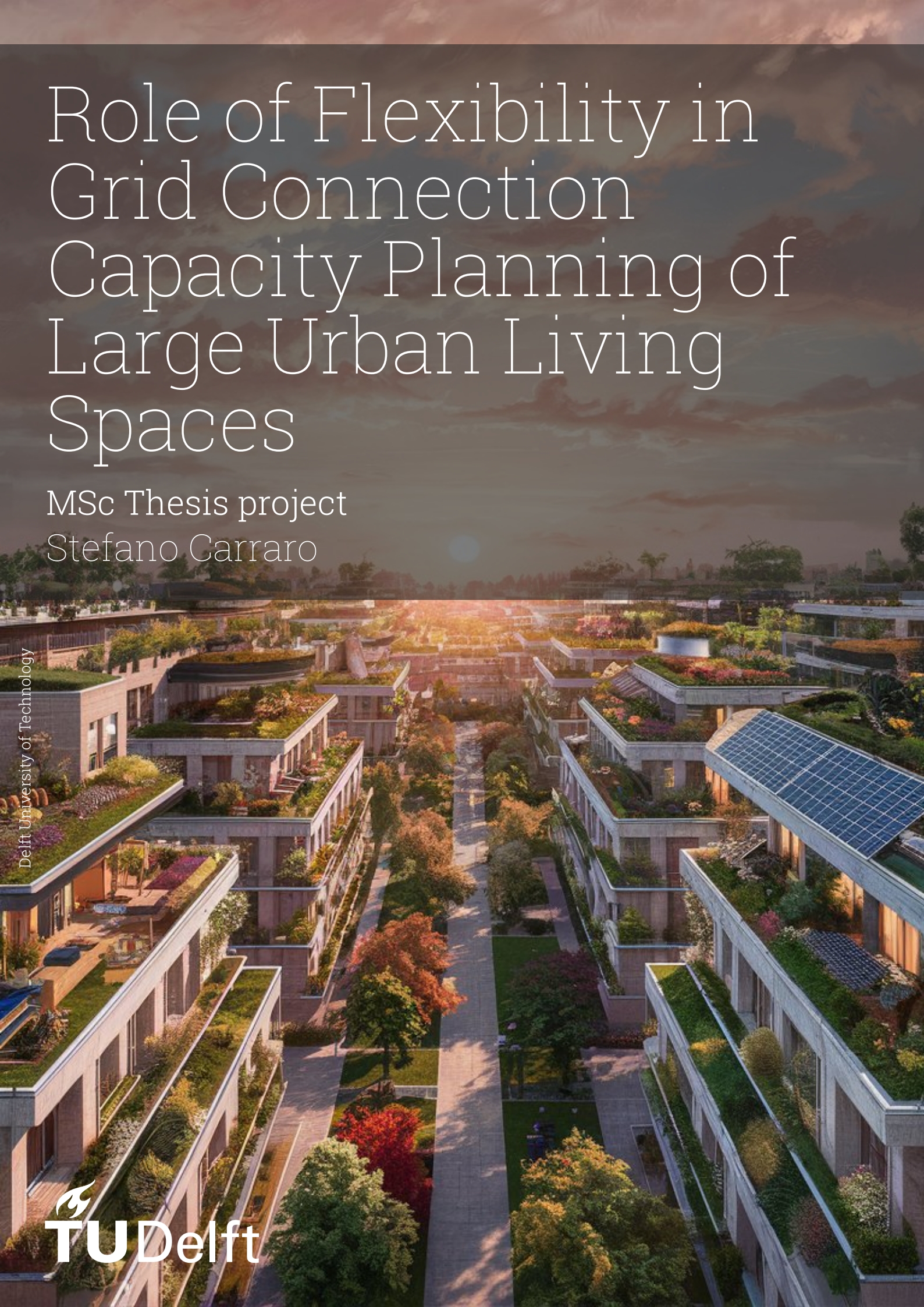

Delft University of Technology

TU Delft

Role of Flexibility in Grid Connection Capacity Planning of Large Urban Living Spaces

by

Stefano Carraro

to obtain the degree of Master of Science
at the Delft University of Technology,
to be defended publicly on Monday July 10, 2024 at 10:00 AM.

Student number:	5848229
Project duration:	December 4, 2023 – July 10, 2024
Supervision:	Dr. S.H. Tindemans - responsible supervisor, EEMCS
	N.K. Panda (MSc.) - daily supervisor, EEMCS
Thesis committee:	Dr. S.H. Tindemans - chair, EEMCS
	Dr. ir. Ö. Okur - committee member, TPM

This thesis is confidential and cannot be made public until December 31, 2024.

Cover:	Sustainable Urban Living at Sunset, AI-generated using Ideogram 1.0.
Style:	TU Delft Report Style

An electronic version of this thesis is available at `http://repository.tudelft.nl/`.

TU Delft

Acknowledgement

This work marks the culmination of my studies at the Technical University of Delft. The journey has not always been easy, but it has been both fascinating and inspiring.

I would like to express my deepest gratitude to all those who provided support and guidance throughout the completion of this thesis. First, I would like to thank my supervisor Prof. Simon Tindemans and colleague Nanda Panda for their time and patience. Their expertise and insightful feedback were fundamental in guiding me during this research. I would like to extend this also to the team in the ROBUST project, who provided me with useful information and support.

Finally, I wish to express my deepest gratitude to my families, girlfriends and friends, who are the most beautiful thing of all. Without your support, I would have not loved my studies as much.

Stefano Carraro
Delft, July 2024

The work in this thesis was partly fulfilled in the context of the ROBUST project. For more information: https://tki-robust.nl/. ROBUST received funding from the *MOOI 2020* Top Sector Energy subsidy by the Ministry of Economic Affairs and Climate Policy, executed by the Netherlands Enterprise Agency.

All rights reserved. No part of the material protected by this copyright notice may be reproduced or utilised in any form or by any means, electronic or mechanical, including photocopying, recording or by any information storage and retrieval system, without written permission of the author.

An electronic version of this dissertation is available at https://repository.tudelft.nl/.

More about the code and plots can be found at the following link:
https://github.com/stefanocarrraro/MSc_Thesis_2024.git

Abstract

In recent years, the rapid increase in energy demand and the threat of climate change have pushed the energy sector towards electrification. Despite this being the first step to a more sustainable future, a new problem arises with the growing demand: grid congestion. This project explores innovative strategies within energy system design and operational framework to enhance operation efficiency in large urban energy systems. A model was established that allows the optimization and analysis of the performance of a residential energy community with energy systems supplied by renewable sources. The design focuses on the flexibility of the system to operate with an integrated planning framework exploiting batteries, thermal storage and shared Electric Vehicles (EVs). By investigating these technologies' design and operational conditions, the project seeks to optimize the system's functioning and minimize its impact on the electricity grid to mitigate congestion. Focusing on a new residential area in Utrecht (NL), the study investigates the role of flexibility for new capacity connection challenges in a highly populated urban area with a vulnerable infrastructure. This research provides useful insights that can guide the development of more adaptable energy infrastructures capable of meeting the growing demands of modern cities. The findings aim to inform future urban energy areas to facilitate the transition towards a more sustainable residential landscape.

Contents

Acknowledgement **i**

Abstract **ii**

1 Introduction **1**
1.1 Research Questions . . . 2

2 Background **3**
2.1 Introduction to Grid Congestion . . . 3
2.1.1 Types of Grid Congestion . . . 3
2.1.2 The Causes of Grid Congestion . . . 4
2.1.3 Occurrence of Grid Congestion . . . 5
2.1.4 Implications of Grid Congestion . . . 6
2.1.5 Power Grid Congestion in Low-voltage Grids . . . 7
2.1.6 Mitigating Grid Congestion in Low-Voltage Energy Systems . . . 7
2.1.7 New Connection Capacity Mechanisms in the Dutch Context . . . 9
2.2 Energy Communities and Energy Hubs . . . 11
2.3 Energy system modelling . . . 13

3 Methodology **18**
3.1 Scope of the model . . . 18
3.2 Optimization method . . . 18
3.3 Modelling tools . . . 19
3.4 Energy system resources and modelling . . . 19
3.4.1 PV system . . . 19
3.4.2 Heating system . . . 21
3.4.3 Battery energy storage system . . . 28
3.4.4 Electric vehicle fleet . . . 29
3.4.5 Energy system balance . . . 30
3.5 Model of the energy system . . . 31

4 Description of the case study **34**
4.1 Case Study Description . . . 34
4.2 Data Description . . . 36
4.3 Grid Connection Agreements: cases description . . . 40
4.3.1 Base case: no peak reduction . . . 42
4.3.2 *Current system* case: simple peak reduction . . . 42
4.3.3 *Moderate EV charging* case . . . 42
4.3.4 *V2G* case: integration of vehicle-to-grid . . . 42
4.3.5 *TES* case: increased size of the thermal storage . . . 42
4.3.6 *BESS* case: integration of a battery storage system . . . 43

5 Analysis of results **44**
5.1 Base case scenario . . . 46
5.2 Scenario 2: day-long curve flattening . . . 48
5.3 Scenario 3: morning peak hours . . . 52
5.4 Scenario 4: evening peak hours . . . 56
5.5 Scenario 5: morning and evening peak hours . . . 59
5.6 Conclusions of results analysis . . . 61

6 Discussions **63**
6.1 Techno-economic considerations . . . 63
6.1.1 Financial Considerations . . . 63
6.1.2 Scenario Analysis . . . 65

6.2 Role of Flexibility in Different Connection Agreements 68
6.3 Limitations and data sensitivity 69
6.4 Further studies 70

7 Conclusions **71**

References **73**

1 Introduction

In recent years, renewable energy has become the centre of attention due to the escalation problem of climate change. The rapid and continuous increase in energy demand, driven by technological evolution and population growth, is straining the current energy infrastructure since more and more energy must be provided and distributed.

The growing importance of sustainability in urban areas has become a critical focus in modern urban planning and development. As cities continue to expand and populations increase, the need for sustainable practices to minimize environmental impact and improve the quality of urban life is fundamental. Renewable energy integration, efficient resource management and environmentally friendly infrastructure have thus become top priorities on governmental agendas.

The introduction of Distributed Energy Resources (DERs) has proven to be an effective strategy for increasing the penetration of renewables in total energy consumption. DERs, which include technologies such as solar panels, district heating, energy storage and Electric Vehicles (EVs), allow power generation and consumption at the consumer's site, making the energy structure decentralized. While this brings generation closer to the user, it also increases system complexity, making it challenging to define the roles and responsibilities of each involved party.

However, the unpredictable nature of renewable energy sources and the fluctuating demand behaviour require innovative solutions to ensure reliable and efficient grid operation. One of the primary challenges, especially concerning low-voltage energy systems within urban areas, is grid congestion, particularly during peak demand periods. Although the integration of DERs brings the generation closer to the load, their fluctuating nature can worsen the problem as the network has to manage the variability and intermittency of these resources. This can lead to situations where the grid is unable to efficiently distribute electricity, resulting in increased operational costs and reduced reliability.

Additionally, expanding grid capacity and accommodating new connections in areas with limited space and high population density brings in further significant challenges in managing congestion. The increasing difficulty for new energy systems to find space on congested grids is becoming a pressing issue, particularly in urban and industrial zones. This not only hinders societal development but also presents a substantial governmental challenge, slowing the process of energy transition to meet the goals stated in the 2015 Paris Agreement.

Concerning the issue of grid congestion, traditional energy systems present significant limitations when confronted with the dynamic demands of modern urban environments. These systems were originally designed for mono-directional power flow from large centralized power plants to consumers, lacking the flexibility needed to efficiently manage the congested network.

As a result, the electricity grid is thus facing a dual problem: from one side, the integration of DERs in decentralized energy systems to handle the fluctuating nature of generation and demand, and on the other an outdated transmission and distribution infrastructure unable to handle this decentralized structure.

This study aims to address the critical issue of grid congestion by exploring how the intrinsic flexibility of DERs can be exploited to mitigate peak power demands in low-voltage urban energy systems. By developing a comprehensive model to analyze a specific case study, this research investigates the potential of various DERs in reducing peaks in the grid power withdrawal, to alleviate congestion and investigate

new capacity connections. The findings of this study will contribute to a better understanding of how to optimize the integration and operation of DERs in urban grids, ensuring a more stable and efficient energy supply and assisting in the integration of new energy communities into existing grids. This research includes important implications for grid operators and urban planners, providing insights that can guide the development of more adaptable energy infrastructures capable of meeting the growing demands of modern cities.

1.1. Research Questions

To provide structure and coherence to the project, the thesis aims to answer the following research question:

How can an integrated scheduling framework optimize the design of large urban neighbourhood energy systems by utilizing the flexibility of Distributed Energy Resources (DERs) to mitigate grid congestion?

To address the research question and meet the project's objectives, different chapters of this master's thesis elaborate various sub-questions, allowing for a comprehensive examination of each aspect. The main research question has been deconstructed into five sub-questions, allowing for a thorough exploration of each aspect. These are:

- *What is grid congestion and what are its implications?*
- *How can flexibility of DERs be modelled in a residential neighbourhood energy system?*
- *What are the different designs that can be employed for solving grid congestion in a general large urban living space?*
- *How does the flexibility of the system assist in the final goal of peak power withdrawal reduction?*
- *To which extent can the flexibility be used to fit within power envelopes that can be agreed with a DSO?*

2 Background

Concerns regarding the sustainability of present energy usage are spreading around the world. While the impacts of various energy sources are increasingly recognized and researched, the growing energy demand has not been matched by an equal focus on grid development, instead overlooking the essential role of the energy grid. Recently, a revolution in the power grid sector has been driven primarily by the urgent need to address climate change. However, this progress is jeopardized by the disparity between the rising of energy demand and the slow grid infrastructure development.

Shifting towards renewable energy is critical for creating sustainable and resilient grid infrastructures that can meet growing urban demands while mitigating environmental impacts. Given their lower costs and longer lifespan, distributed renewable energy resources are becoming more and more common in the urban sector [8]. Currently, numerous efforts are being made to address the pressing issue of grid congestion, which the following chapter aims to explore. This literature review will introduce the topics of grid congestion, how this affects energy communities and how these latter can be modelled and studied.

2.1. Introduction to Grid Congestion

Facing the challenge of climate change, the whole world's energy sector is transforming rapidly. On a global level, scientists and policymakers are directing their efforts toward reducing carbon emissions and minimizing environmental impact by upgrading technologies to sustainable alternatives, in particular electrical energy. To achieve sustainability goals set by the Paris agreement in 2015, electrification emerges as a primary strategy. By electrifying various sectors such as transportation, heating, and industrial processes, societies aim to reduce reliance on fossil fuels and embrace cleaner energy sources [47].

However, as electricity demand continues to grow, the current transmission and distribution infrastructures are becoming outdated and incapable of meeting the power loads. When the technical limitations of the grid hinder system operators in consistently delivering electricity to consumers, the grid is defined as congested.

Chuang et al. [14] visualize this concept by comparing the grid to a funnel. In this analogy, the outgoing flow, representing energy delivery, is limited to a much lower value than the incoming flow, representing generation. As suppliers continuously feed the grid with electricity, similar to filling a funnel, users can only receive a reduced portion due to the network's limitations. As a result, if the demand is higher than what the grid can deliver, part of the loads cannot rely on the electricity infrastructure and therefore require an alternative source of power. Hence, the electricity grid emerges as the primary bottleneck in the flow of energy.

2.1.1. Types of Grid Congestion

Power grid congestion can be divided into two categories. The first type is known as *in-feed* grid congestion and is registered on the supply side of the grid. Due to outdated infrastructure, operational decision framework and governmental policies, several energy generators may be forbidden from feeding all or part of their capacity into the energy grid during certain periods.

Alternatively, grid congestion can be on the demand side of the grid, defining the so-called *consumption* grid congestion. In this case, the energy requested by the connected load cannot be provided due to too

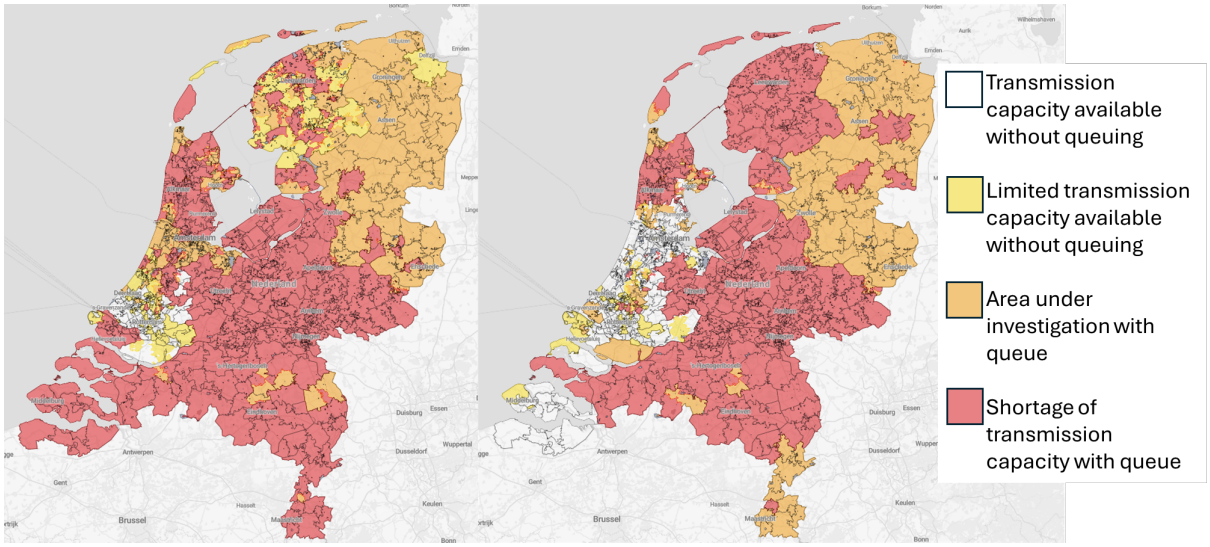

Figure 2.1: Electricity capacity congestion map of the Netherlands, in-feed congestion (left) and consumption congestion (right). Update: June 2024 [53].

high capacity or, again, due to the infrastructure of the transmission network.

This problem is particularly common in highly dense developed countries. Considering, for instance, the case of the Netherlands, information about grid congestion is of public access by *Netbeheer Nederland* (NBNL) [53], as shown in figure 2.1. The *in-feed map* on the left shows the grid connection availability for new generation projects with significant connection requirements[1], such as PV parks or wind farms. In this map, coloured areas indicate locations where the grid has troubles or cannot accommodate additional electricity supply. Conversely, the *consumption map* on the right displays the grid's capacity to accommodate large load connections[1].

It is easy to notice the actual magnitude of the problem. The figures show only a few areas in the country where capacity is available without congestion problems. This means that in all the remaining zones, orange and red, the grid system operators cannot accommodate any energy system that desires to establish or expand its connection.

2.1.2. The Causes of Grid Congestion

To effectively mitigate grid congestion, the first step is to understand its causes and mechanisms of occurrence.

Renewable energy sources are currently driving the energy transition thanks to their reduced cost and carbon footprint. However, the integration of intermittent generation, such as solar and wind, introduces variability and unpredictability into the energy balancing system, particularly during periods of high renewable generation and low electricity demand.

This irregularity can lead to periods where the energy supply exceeds the grid's capacity, then causing congestion. With the increasing popularity of DERs, renewable energy generation has become geographically dispersed, with many small-scale projects, such as rooftop PV, connected to the distribution network rather than the transmission network. When many small producers inject power into the grid simultaneously, for instance during high solar penetration, midday production can surpass the local grid's capacity, leading to congestion and even potential outages in severe cases.

A study conducted by Shabbir et al. [73] investigated the effect of rooftop PV generation on the low-voltage distribution grid, highlighting how exceeding capacity can overload the network and lead to overvoltage and congestion issues. Hence, the current electricity network is not able to efficiently handle the fluctuating nature of these renewable energy systems.

Schmietendorf et al. [71] argue the impact of variable renewable generation on grid stability and electricity quality, proposing a mathematical procedure to generate realistic feed-in fluctuations with temporal correlations. The study shows how the fluctuation of wind and solar power, which consists of the largest share of renewable electricity in Germany and the Netherlands, challenges system operators to successfully manage the electricity distribution due to excess of generation [36, 37].

[1]Connection larger than 3x80 A.

Moreover, grid congestion can be influenced significantly by market dynamics. In markets where electricity prices are set based on real-time supply and demand conditions, congestion can occur when there is limited transmission capacity to deliver electricity from areas of surplus generation to areas of high demand. This mismatch can lead to price disparities between regions and inefficient utilization of generation resources.

As stated in Verzijlbergh et al. [81], the variability of renewable energy generation makes the correlation between the electricity market and electricity prices less strong since renewable energy production does not follow the demand profile. The study argues a mutual correspondence between grid congestion and energy markets: as imbalance occurs, the energy market responds amplifying the congestion problem and vice versa. As a result, in periods with high supply and low demand, the electricity price drops in order to redistribute the energy in excess.

This regional issue is then amplified within countries. Due to market transparency regulations, not all information is equally available to the system operators in the various EU countries. Rausch et al. [64] conduct an overview of the available data about transmission grid congestion and how this affects feed-in management mechanisms, marking the importance of data quality and availability for an efficient analysis of the market response to electricity imbalance.

Besides the economic mechanisms acting on the energy markets, grid congestion is related to the physical limitation of the transmission technology. The electricity grid was primarily designed to support centralized power generation from large power plants. Shifting this to a decentralized structure, the current network infrastructure is incapable of handling the bi-directional and variable flow of energy. As a result, the grid system operators struggle to efficiently distribute electricity to the user and congestion is experienced.

Moreover, inadequate grid planning and geographic constraints can further lead to congestion, especially in densely populated regions undergoing rapid population growth or significant renewable energy deployment. Therefore, as supply and demand grow, the transmission grid must improve. Hoicka et al. [33] give a broad overview of the electricity grid structure as it is and is expected to change, both in technical and socio-political terms. The research highlights the importance of constant improvement in the electricity infrastructure to keep up with the times and analyzes the foreseen impact on society that this grid transformation will have.

Finally, a common cause of grid congestion is related to new Distributed Energy Resources (DERs) that are becoming more and more popular at the consumer site. Besides the aforementioned distributed generation, the integration of storage facilities, district heating systems and electric vehicles introduces additional loads to the total electricity demand, pushing the distribution network closer to the designed limits. These loads are characterized by high flexibility that can be exploited to module the final profile and thus flatten the electricity demand curve.

However, a thorough scheduling framework must be implemented in order to efficiently exploit their potential. If, for instance, a large number of consumers simultaneously shift their electricity consumption to off-peak hours or respond to real-time pricing signals, the total distribution grid demand profile may experience concentrated spikes and easily lead to localized grid congestion [85]. Hussain et al. [35] argue the effect of large EV fleets on the distribution grid, highlighting how incorrect scheduling framework may lead to line overload and consequently congestion. The study reviews different management strategies implemented to minimize the impacts of the integration of EVs, highlighting the need for accurate EV affluence forecasting in decentralized coordination.

2.1.3. Occurrence of Grid Congestion

The second challenge for efficiently designing congestion management mechanisms is to accurately predict when and for how long the grid will be congested.

The occurrence of grid congestion can be attributed to a combination of different factors from the electricity demand profile and the integration of intermittent renewable generation to limitations in grid infrastructure and market dynamics. These factors interact with each other in complex ways, influencing the probability and magnitude of congestion in different areas and contexts.

At the distribution grid level, grid congestion typically occurs during peaks in the electricity demand. Depending on different factors, such as geographical location and type of loads, the occurrence of these peaks can be more or less frequent, of different magnitudes and more or less difficult to manage.

In residential areas, for instance, the demand profile commonly follows the so-called *duck curve*, registering a first hump in the morning and a larger one in the evening [63]. The first peak is usually

registered around 08:00, when citizen turn on their appliances and the industries start to open, on average until noon, while the evening one usually occurs between 18:00 - 22:00, coinciding with residents returning home [56, 16]. Conversely, industrial areas' demand is usually low during the night and high and constant during the day shift. Hence, the prediction of such profiles becomes crucial for efficiently mitigating congestion.

In their research, Gürses et al. [29] argue that this issue typically repeats with daily patterns, making it possible to identify a sort of algorithm able to predict an approximated time range in which management mechanisms will be required. The study offers a machine learning-based model for probabilistic demand forecasting to assist Distributor System Operators (DSOs) to perform a more accurate congestion management.

It is important to mention that these time ranges are not universal and each country, as well as each different area, may experience different demand curves. This area is still open to research and DSOs are experimenting with different methods to better define the concept of peak hour [77].

Alternatively, grid congestion can be caused due to large renewable generation at the consumer site. During periods of high production, such as summer days for PV or winter for wind farms, the power supply can easily exceed the grid capacity limits causing in-feed congestion.

To avoid this, advanced forecast methods can be developed and integrated into the system operators' operational algorithms. In their study, Srivastava et al. [76] propose a thorough PV production forecast based on sky images to foresee the overproduction of solar energy and consequently allow re-scheduling of local DERs to avoid curtailment and losses, showing how this can potentially assist a better electricity network functioning.

As mentioned in the previous section, grid congestion can be related to the energy markets. Indeed, the fluctuation in price can influence both generation and consumption patterns.

For example, demand response programs, designed to shift electricity usage away from peak times, can also contribute to congestion if not properly managed. These programs rely on price signals to incentivize consumers to adjust their usage. However, if a large number of consumers respond to the same price signal simultaneously, this can create new peaks in demand at different times, potentially leading to congestion in other parts of the grid.

Attar et al. [7] argue how dislocated generation can exercise strong market power during periods of congestion, discussing how market-based congestion management mechanisms can be effective at the local level.

2.1.4. Implications of Grid Congestion

Besides understanding the nature of grid congestion, it is important to highlight why its mitigation is crucial. Indeed, the implication of network unavailability poses significant challenges across various sectors, including economic, environmental, technological, and social aspects.

Grid congestion has significant economic repercussions that affect both utilities and consumers. One of the primary economic impacts is the increased cost of electricity. Considering different energy price areas, between countries for instance, during peak congestion periods prices can spike dramatically, leading to economic uncertainty for businesses and consumers as well as a drastic rise in the final energy bills. Conversely, from a generation power plant point of view, the reduced transportation capacity may lead to curtailment or negative price, resulting in losses for the supply firm.

Schermeyer et al. [70] investigate the effect of grid congestion on wind curtailment in Germany, which has proven a steep growth in the past decade, pointing out the actuality of the problem. This suggests that better management of the grid would avoid losses due to exceeded generation and consequently their final income.

As previously mentioned, the current electricity grid infrastructure does not match the variable nature of renewable energy generation plants. As a result, the integration of these becomes challenging, leading to a smaller renewable penetration in the energy mix and therefore a generally higher carbon footprint.

Such problem concerns first the small-scale distributed generation but also affects large wind and solar farms, hindering their connection to the electricity system. This problem is deeply analyzed by McAllister et al. [49]. The study provides a broad overview of the procedure for obtaining new connections for large solar parks in the European case, highlighting how the congested nature of the grid drastically slows down the energy transition challenge. In addition, due to curtailment or power readjustments, renewable

generation projects may encounter technological issues that compromise the efficiency of operation. Millstein et al. [50] researched the impact of network congestion on wind and PV farm operations. The study shows that besides the energy loss due to the incapability of grid feeding, the functioning of the generators can be highly compromised depending on the region depending congestion occurs more or less often.

In addition to the implication of grid congestion on existing connected loads and generation, another significant issue concerns the new capacity connection. Referring again to figure 2.1, the *consumption map* on the right-hand side shows that a large part of the territory of the Netherlands is currently unable to welcome new large capacity connections. This means that new energy systems asking for connections and connected parties willing to expand find themselves in an extremely long "waiting queue" with the DSO [54]. As a result, the societal impact is significant for the general society development. Considering, for instance, the lack of living spaces the Dutch case is currently facing, grid congestion indirectly affects the rental pricing and the whole residential market. Such implication, as argued later in the report, is the direct effect of the case study analyzed in this research, currently in the queue for reaching an agreement for a new connection to the distribution grid.

2.1.5. Power Grid Congestion in Low-voltage Grids

As observed, among the different actors penalized, low-voltage energy grids are often the first to suffer from grid congestion. This type of electricity grid is usually found in urban residential neighbourhoods or industrial areas. It is characterized by single or multiple connections to other distribution grids or directly to the transmission networks through medium voltage transformers, making the grid operate at a range of 230/400 V [83]. These grids typically consider radial distribution and are susceptible to localized congestion due to high demand density and variable power flow.

The latter can indeed be seen as a degree of freedom of the DSO for congestion management on the demand side. Depending on the load nature, whether residential or industrial, the system operator may invite the low-voltage grid to shift or avoid part of the demand, depending on its flexibility and the agreement with the regulator. Such an approach is better known as Demand-Side Management (DSM), which is proven to be significantly effective for local congestion management (CM) [74].

Furthermore, feed-in grid congestion can also be experienced in low-voltage networks. Consider, for instance, a system with high production of solar energy. During periods of high renewable penetration, curtailment may also be required on the user side, for, again, both technical and non-technical constraints [73]. This is often experienced in industrial areas, where the rated PV capacity designed is higher than the agreed capacity of the transformer.

As a result, low-voltage energy grids are the first to experience the implications related to grid congestion from the demand side.

In their research, van Westering et al. [83] discuss the implication of grid congestion in low-voltage electricity grids, exploring how these can be overcome with the integration of battery storage systems. Their study provides theoretical insights and experimental validation, using a receding horizon charge path optimizer to manage voltage and overload issues effectively.

2.1.6. Mitigating Grid Congestion in Low-Voltage Energy Systems

Despite the large variety of reasons and different kinds of nature for which grid congestion occurs, TSOs and DSOs are constantly experimenting and researching mechanisms to efficiently address the problem and relieve the electricity grid from these bottlenecks [27].

While engineers explore new technologies to reinforce the grid infrastructure, economists and policymakers focus on designing and testing frameworks to prevent and manage power congestion problems.

In their research, Hennig et al. [32] offer a broad overview of the most used mechanisms to mitigate grid congestion. The study divides the CM methods into categories based on the load-controlling party, meaning who has the responsibility to control and apply the framework, and the DSO position of network access, meaning whether the control is included in the initial connection "offer" or the DSO has to "buy-back" the capacity needed to resolve congestion. Following these two characteristics, the CM methods can be classified in:

- **Network access prices**, including all the mechanisms for which the DSO applies the CM based on charges for network access. It can be further divided depending on the time frame considered, identifying the sub-groups of static tariffs and dynamic tariffs;
- **Local Flexibility Markets (LFMs)**. This category includes all CM methods controlled by the end users and based on the DSO's buy-back of network access;
- **Direct Load Control (DLC) schemes**, for which the DSO can directly control the non-critical loads or maximum connection capacity allowed during peak hours.

The classification procedure can be visualized below in figure 2.2. Following the flowchart, the natural differences of the various CM methods can be analyzed. For example, if the DSO is in control of the operation of non-critical electrical loads, during peak hours, it can decide to reduce overall demand on the grid and thus avoid congestion. Such a mechanism falls into the DLC category. Conversely, when considering Demand-Side Management (DSM) methods, such as the critical peak pricing program, the DSO sends an advance notice a few hours before the price spike occurs and the end-user is responsible for adjusting its demand profile accordingly. In this case, the CM method falls is a dynamic network access price mechanism.

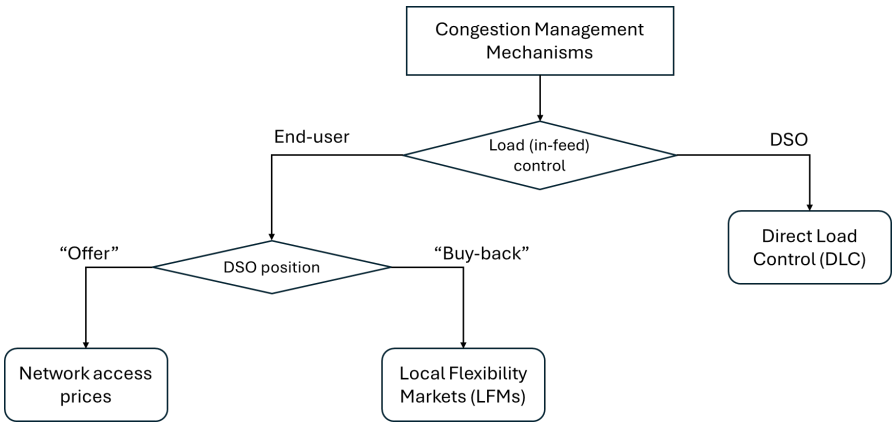

Figure 2.2: Flowchart for classification of Congestion Management (CM) methods, based on [32].

The implementation of Congestion Management (CM) mechanisms is proven to successfully assist the grid operators in providing electricity to the final user. However, identifying the most suitable method to apply in each case depends on several factors. The local grid characteristics, such as line capacity or voltage level, strictly constrain the size of available power. On the other side, different demand profiles, which vary, for instance, from a residential to an industrial area, are expected to affect the peak hours occurrence. Hence, it becomes challenging to predict which mechanism is more effective and which other could penalize the involved parties.

When considering CM frameworks for mitigating grid congestion at the distribution level, it is common to involve the Distributed Energy Resources (DERs) installed at the local user site. For this purpose, Demand-Side Management (DSM) approach is very effective.

In their work, Paulus et al. [59] conducted a comparison between DSM and other mechanisms for daily dispatch of generation, focusing on the uprising integration of variable renewable energy from the supply side. The study investigates the impact of DSM on the German electricity grid showing the potential of such a method on a large scale.

The integration of demand-side mechanisms often needs to be assisted by local management actors, able to correctly forecast the demand and adjust the scheduling according to the congestion timing as communicated by the DSO. Considering the load side, Siano et al. [74] argue the effects of demand response frameworks at the small-medium grid scale. They point out how DSM requires the integration of smart devices, such as smart meters, communication technologies and monitoring systems, for the correct functioning of the energy system. It is thus proven that the implementation of CM mechanisms on the user side asks for an efficient DER management system to efficiently mitigate grid congestion.

2.1.7. New Connection Capacity Mechanisms in the Dutch Context

As mentioned earlier, besides the implication of congestion on the existing connected parties, the issue of new connection capacity has emerged as a top priority.

For the case of the Netherlands, the current situation considers a single type of agreement between the Distributor System Operator (DSO) and the party requesting connection: the so-called Firm - Connection and Transmission Agreement (CTA), *aansluit- en transportovereenkomst* (ATO) in Dutch [42]. With this contract, the connected party has the right to use the transmission capacity agreed with the system operator, which is estimated based on the maximum peak load and the expected load profile [42]. Thus, it figuratively owns a part of the electricity grid. When the sum of all agreed CTAs in a certain grid section matches the maximum load capacity of the area, the grid is defined as "full" and no more CTAs, and consequently new connections, can be signed.

However, as previously discussed, grid congestion does not occur continuously, and cases where all connected parties simultaneously require their designated peak power are rare. This indicates that the electricity grid is not being utilized optimally.

In order to overcome these problems and enable more CTAs, the Dutch Authority for Consumers and Markets (ACM) recently announced the design of new types of connection contracts that will make the electricity grid capable of accepting more parties and efficiently distributing the capacity during off-peak hours.

In their article, Klapwijk and van Bergeijk [42] summarize the current situation regarding the Dutch electricity grid future plans.

The first move towards a less congested grid was mentioned in the National Grid Congestion Action Program, *Landelijk Actieprogramma Netcongestie* (LAN) in Dutch, published on the 20th of December 2022. With this program, the involved parties disclosed the intended actions of the Dutch electrification sector for grid congestion mitigation and better use of the electricity grid. This was then confirmed by the National Energy grid Plan (NPE) on the 1st of December 2023, which showed how the future energy grid should look like. A few months later, on the 13th of March 2024, the Authority for Consumers and Markets (ACM) published the Draft Decision ATR, following the proposal drafted by all the grid operators united in *Netbeheer Nederland* (NBNL). This aimed to introduce three new flexible contract and transmission agreements: Alternative Transmission Rights (ATR), Non-Firm ATO (NFA) and Group CTA, or *Groep ATO* (G-ATO) in Dutch.

In ATR, the availability of transmission capacity to the connected party is not continuously guaranteed. This means that during certain time periods, electricity power withdrawal (or grid in-feeding in the case of prosumers) may not be available to the customer. In exchange, a discount is applied to the transmission capacity consumption tariff. According to the draft, two types of ATRs are designed: Time-based Transmission Rights (TTRs) and Time-Block-based Transmission Rights (TBTRs). Their characteristics are summarized in table 2.1 below.

Category	Standard CTA	Time-based Transmission right (TTR)	Time-Block-based Transmission Right (TBTR)	Non-Firm ATO (NFA)	Groep ATO (G-ATO)
Transmission Guarantee	All time.	85% of the time (7446 h/yr).	During defined time blocks.	During off-peak hours.	All time.
Scheduling	-	Defined one day ahead.	Time blocks are agreed with the DSO when signing the contract. They must be during off-peak hours.	Defined one day ahead.	-
Pricing	No discounts.	Discount on the transmission-dependent consumption.	Discount on the transmission-dependent consumption.	Discount to zero.	Discounts may be available based on group negotiations.
Availability	HV and LV grids.	Only available on the national HV grid both in congested and non-congested areas.	Time blocks may vary depending on the area, both on HV and MV grids.	Available based on connected party-specific conditions.	Available based on group-specific conditions.
Date	Active.	Estimated effective date 1st of April 2026.	Estimated effective date 1st of April 2025.	Estimated effective date 31st of December 2024.	Active.

Table 2.1: Comparison of the different transmission agreements, based on [42, 54].

Non-Firm ATO (NFA) is defined as a fully variable transmission right, specifically designed for customers with flexible transmission needs. This means that the connected party is only entitled to transmission capacity during off-peak hours, while during peak hours the right of transmission is null. The advantage of such a mechanism is that the tariff per kW contracted is zero. This means the connected parties with an NFA do not pay for a reserved transport capacity, reflecting their non-guaranteed access status [15].

In case of multiple neighbouring parties asking for connection, the Dutch system operators can suggest a group CTA (G-ATO). By forming a group and making contractual agreements with the grid operator, individual transmission rights are abolished. This allows individuals to use more transport capacity than their original CTA, as long as the group remains within the contracted limit. The G-ATO offers more certainty for the grid operator by optimizing grid capacity through coordinated group behaviour. This concept can be visualized in figure 2.3 below.

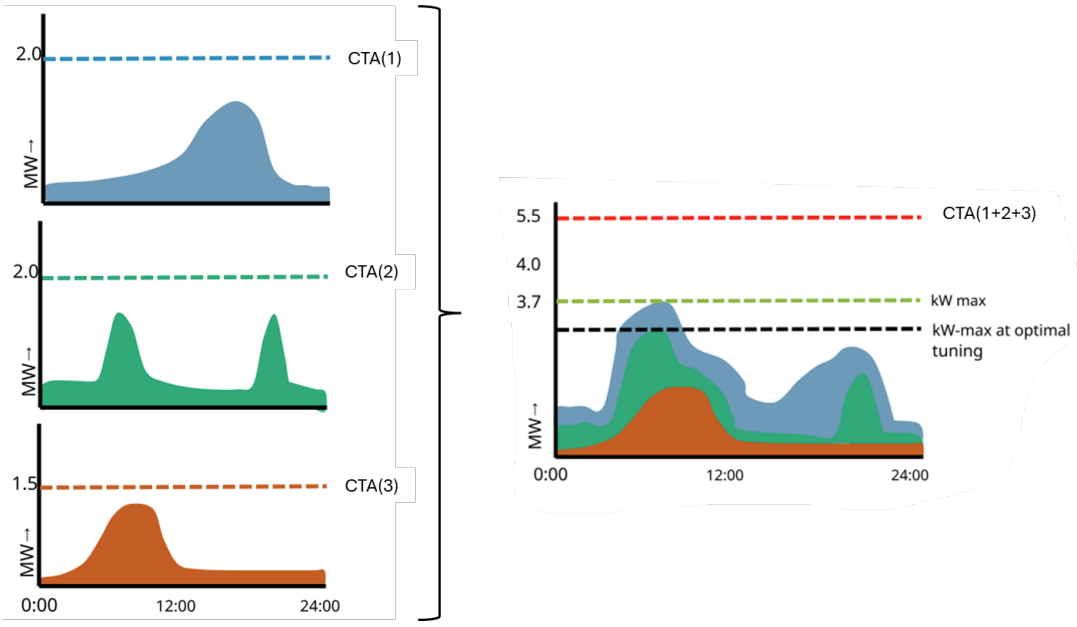

Figure 2.3: Example of implementation of the Groep ATO agreement, based on [54].

In addition, the Dutch grid connection field provides two other possible ideas on top of the CTAs:

Capacity Reduction Contract, *capaciteitsbeperkingscontract* (CBC) in Dutch, and UIOLI, which stands for "Use It On time or Lose It".

CBC is an additional contract on top of the normal CTA that provides a payment to the connected party in case of reduction during the peak hours activated at least one day ahead. The time window for reduction can be either agreed the day before or predefined, depending whether the CBC includes or not the "call-off" (*afroep*) option. This contract is designed as an incentive for consumers to reduce their consumption during periods of high demand. The terms of the agreement, including the compensation rates and the specific conditions under which capacity reductions will occur, are defined in the contract between the connected party and the grid operator. CBC can be an attractive option depending on the party's activity of connection, when and how often the restriction is applied as well as how much time is between two activations.

Differently, the UIOLI is an approach for avoiding unused connections. It aims to redistribute unused but already contracted, hence "reserved", capacities to other potential customers, following the approach of first come first served. This concept ensures that transmission capacity that has been reserved but is not being utilized is made available to other users who may need it.

Despite the choice of the connection contract in a liberal market being free, the implementation of ATR or NFA cannot be always defined as "voluntary" since the other option may be not obtaining a connection at all. Moreover, the implementation of UIOLI mechanisms implies that parties that do not use their full capacity risk losing it completely. Hence, political debate is still open regarding how to limit the authority of system operators and preserve the connected parties' rights.

It is important to mention that the different new connection agreements discussed, meaning CTA, TTR, TBTR and NFA, differ from congestion management mechanisms. While the first are measures applied with the primary goal of accommodating new parties, CM mechanisms are specifically designed to actively manage and mitigate congestion on the grid in real time [42]. Hence, applying congestion management does not directly empty the saturated grid. As a result, the two tools can co-exist and operate in a complementary manner.

2.2. Energy Communities and Energy Hubs

As the energy field keeps changing, the general view of an energy system is experiencing a radical revolution. The old centralized energy scheme as a mono-directional flow of energy from the power plants to the consumers has become outdated and unpractical for the nowadays society, often leading to congestion issues. As part of this change, the end consumers, once passive, are now encouraged to play an active role by reducing their consumption, or by locally generating or storing energy. Therefore, a side of producer and consumer, this concept defines the role of the prosumer. A prosumer is defined as a consumer of energy vectors that also produces its own energy making it capable of covering at least a fraction of its energy demand [8]. Consequently, the involvement of a new actor forces the energy system to be reconfigured in a way in which both power and value streams can operate bi-directionally [26]. These new systems are commonly referred to as energy hubs or energy communities. Although these are usually considered synonyms, they refer to two very different concepts.

The energy hub concept was presented for the first time in the "Vision Of Future Energy Networks (VOFEN)" project, conducted by ETH Zurich in 2005 [22]. The project defined an energy hub as the integration in a single unit of energy conversion and storage carriers [51].

In their research, Mohammadi et al. [51] provide an extensive literature review on the topic identifying inputs, converters, storage systems and outputs as main components of an energy hub.

With inputs, we refer to the various energy carriers the system receives, for instance, solar and wind power, biomass, hydrogen and geothermal heat. The incoming energy carriers are then converted into different types of energy, such as electrical or heat. This category includes all the technologies used for transforming energy, such as heat exchangers, fuel cells and electronic converters. The crucial characteristic of energy hubs concerns the storage systems. This includes batteries, thermal storage, compressed air and hydrogen. Finally, outputs are the various forms of energy delivered to consumers to meet their demands, such as electricity, heat, cooling, water, and other energy products like compressed air and hydrogen.

Energy hubs mainly focus on the technical interaction of different DERs within a defined energy system. When designing these, the main objective is to achieve optimal design and enhance efficiency of operation.

Energy Communities (ECs) follow a different definition. According to the European Directive 2018/2001, a Renewable Energy Community is a legal entity based on open and voluntary participation. It is autonomous and effectively controlled by shareholders (located in the proximity of the renewable energy projects), operating based on the applicable national law [20].

According to Barabino et al. [8], energy communities can be classified depending on the energy uses, such as electricity or heating, the type of users, for instance residential, public, industrial, commercial, and the business model implemented. Focusing on the latter, the study highlights six main classes:

- **Prosumers**. The EC is exclusively formed by prosumers who produce and consume (part of) their electricity selling and buying the extra needs from the electricity grid;
- **Collective generation**. EC based on a share generation system, usually PV, and (eventually) a storage system. In this case, the members remain passive consumers except when generation exceeds the demand;
- **Aggregator**. Producers, prosumers and consumers are grouped by an entity referred to as an aggregator. This is responsible to manage the energy and value streams within the community and to communicate with the external parties;
- **Third party sponsored**. The EC is created by the support of external entities, such as public governmental actors or energy service companies. This business model typically sees the third party maintaining the ownership while the users stay passive members;
- **Local energy markets**. The members of the EC share the self-generated energy through a local market;
- **Cooperatives**. The EC members are shareholders and hold the governance over the community system. The revenues and expenses are shared among the members depending on their level of involvement.

As a result, unlike energy hubs, which consider the energy system solely in a technical manner, energy communities integrate the socio-economic aspects of the system. The objective is to provide a functioning system with responsibilities clearly defined among the shareholders.

Therefore, an energy system can potentially combine features of both an energy hub and an energy community, addressing both technical efficiency and socio-economic integration perspectives.

The key characteristics and differences between the two concepts are summarized below in table 2.2.

Aspect	Energy Hubs	Energy Communities
Definition	Centralized system integrating various energy sources and carriers for optimal production, conversion, storage, and distribution of energy.	Group of individuals or organizations producing, distributing, and consuming energy collectively.
Focus	Technical optimization and efficiency.	Social, economic, and environmental benefits for community members.
Objectives	Improve energy efficiency, enhance flexibility and reduce environmental impact.	Empower local communities, increase renewable energy use, enhance energy security and provide economic benefits.
Ownership and Participation	(Typically) managed by utilities or specialized companies.	Owned and managed by community members (in most of the cases).

Table 2.2: Comparison of Energy Hubs and Energy Communities, based on [8, 45].

Therefore, there exists a substantial difference between energy communities and energy hubs. For the scope of this research, it is important to highlight the role of the energy system type, whether energy hub or community, when discussing grid congestion.

In the context of optimizing large urban neighbourhood energy systems, the concepts of energy hubs and energy communities play a crucial role. Energy hubs, with their integration of various energy sources and carriers, provide the technical optimization and efficiency necessary for an effective scheduling framework. This aligns well with the aim of utilizing Distributed Energy Resources (DERs) to mitigate grid congestion and optimize the energy system's functioning. On the other hand, energy communities

emphasize the socio-economic aspects and explores the role of each involved party. This concept aligns well with the research on CM methods and new capacity connection contracts mentioned in the previous section.

As a result, this research aims to consider part of both energy community and energy hub concepts to efficiently describe the whole energy system characteristics.

2.3. Energy system modelling

To effectively investigate how to exploit the flexibility of Distributed Energy Resources (DERs) for managing grid congestion, it is crucial to employ robust modelling methods. Accurate models facilitate simulations and optimizations across various scenarios, allowing the identification of effective strategies to reduce grid dependency and manage peak demand depending on its timing and magnitude.

Energy system modelling, as defined by Keirstead et al. [40], consists of a formalized representation of an energy system with internally consistent rules, which are integrated through computational tools designed to simulate real system behaviour under different scenarios and objectives.

Different types of modelling techniques can be employed to describe the complexities and dynamics of energy generation, distribution, and consumption. Based on this, energy system models can be grouped into two main categories: simulations and optimization.

A simulation model can be defined as the representation of a system used to reproduce and predict its behaviour under specific set conditions [84]. The goal is to analyze the system's functioning and show its behaviour when subjected to the same circumstances that could experience in reality.

In contrast, optimization seeks the optimal performance under certain conditions using a set of decision variables, typically design characteristics of the energy system [44]. The objective is to determine how the system can adjust its variables within given limits to achieve a specified goal, such as minimizing costs or maximizing efficiency.

For the scope of the research, it is important to highlight the main differences between the two modelling types. Lund et al. [44] and Tozzi et al [78] provide a comparison review between simulation and optimization models highlighting the main differences as:

- **Final solution**: while optimizations seek a unique optimal solution, simulations are not expected to converge to a single outcome;
- **Economic involvement**: Simulation modelling does not imply the monetisation of all consequences. The implicit assumption is that decisions can be made rationally without common denominators;
- **Scope of the research**: optimization modelling aims to find an optimal design and operation of the energy system while simulation modelling is a better fit for backcasting and forecasting for political decision-makers and the need for major changes.

Another key difference is the practical modelling approach. Simulations often use Monte Carlo and agent-based methods.

Monte Carlo simulation consists of probabilistic modelling where variables are assigned random values based on their probability distributions, allowing analysts to assess a range of possible outcomes and their probabilities. The final solution is found after a large number of iterations that converge to the final value, requiring thus high computational cost.

Agent-based simulation, on the other hand, represents the behaviour of individual agents within a system, each bounded by its own set of rules and interactions. This approach is particularly useful for modelling decentralized systems or scenarios where individual decision-making affects system dynamics.

Monte Carlo simulations are largely used in the energy system simulation field. Focusing on describing an energy system in Popova Island, Uwineza et al. [80] conduct a deep techno-economic analysis, providing a valuable reference for stakeholders showing the potential of renewable energy integration in reducing costs.

In another research, Akhatova et al. [4] discusses decarbonization in terms of policies, technologies, processes, and the different stakeholder roles for a general urban energy system following an agent-based simulation approach. The research highly emphasises the need for thorough specification of the agents' characteristics for the correct functioning of the model.

Mathematically, similar approaches may be applied for optimization models as for simulation models, though with the integration of decision parameters [44]. Vilen et al. [82] provide an overview of the most

used tools for district-level optimization modelling, discussing the effectiveness of different optimization approaches on district heating systems.

Depending on the level of detail and the goal of the research, energy system optimization can address one or multiple objectives. Generally, the complexity and multi-dimensionality of district-level energy systems often lead the model to have a set of optimal solutions. Hence, additional constraints and boundaries must be included in order to get a single and unique optimal output. As a result, multi-objective optimization is usually preferred in the field of energy system modelling. In their work, Chen et al. [13] review the effectiveness of multi-objective optimization for long-term energy system modelling, highlighting how this can effectively include economic, environmental and societal factors in the mathematical problem statement.

However, representing these factors mathematically can be challenging. To address this, depending on the case, different approaches can be employed. These can be divided into prior, posterior and interactive models depending on when in the process the optimal is sought [13].

In prior methods, the decision maker prioritizes the objective functions and then converts multiple objectives into a single objective. This can be done using the weighted-sum method, where each objective is multiplied by a coefficient w_i representing its priority weight, as represented in equation 2.1.

$$O.F. \quad \min \sum_{i=1}^{N} w_i \cdot f_i(x) \tag{2.1}$$

Another approach is the ε-constrained method, which highlights one main objective function while treating the others as secondary constraints, as expressed in equation 2.3 below.

$$\begin{gathered} O.F. \quad \min f_m(x) \\ s.t.\ f_i(x) \leq \varepsilon_i \quad \forall i = 1, 2, ..., n \text{ and } i \neq m \\ x \in D \end{gathered} \tag{2.2}$$

Alternatively, the Analytic Hierarchy Process (AHP) method can be implemented. This divides the target objectives through a hierarchical tree based on their relative importance, proceeding then to solve each of them accordingly.

The first two methods are characterized by relatively easy implementation, only requiring thorough initialization of coefficients. In contrast, the AHP approach provides more accurate solutions in exchange for a more intricate definition of each objective and its importance.

Prior methods are undoubtedly the most popular approach for energy system optimization thanks to their low computational cost and sufficient precision [13, 82]. Their implementation is indeed efficient for general modelling projects. In the research conducted by Alabi et al. [5], an emission-free multi-energy system modelling investigates the potentiality of storage combined with comprehensive demand response through the weighted sum method. When including multiple factors of different natures, the ε-constrained method results efficient, as highlighted in Javadi et al. [39]. The research analyzes the functioning of a home management energy system in a multi-objective optimization considering energy price and user discomfort applied to a modern house case study. Zong et al. [87] proposed and applied an AHP-improved entropy weight method to assign weights to the targets for performing multi-objective optimization of a multi-energy flow coupling system.

When more accurate results are required, meaning deeper analysis of the optimal solutions and their nature, posterior methods are typically employed. These approaches select the optimal solution from a Pareto set that has been previously calculated. This method allows the system to identify all feasible solutions and then narrow them down to the optimal one(s).

The solutions can be found through mathematical programming methods, typically Normal Boundary Intersection (NBI), which resolve the problem generating uniformly distributed points on the Pareto surface without being affected by the scale of the objective function [3]. Despite the high computational cost, it often results in optimal choice for non-convex and high dimensional multi-objective problems.

Alternatively, Multi-Objective Evolutionary Algorithms (MOEAs) allow thorough research of the optimal solution by implementing iterative algorithms capable of detecting solutions on non-convex surfaces. A popular algorithm in this category is the NSGA-II [13]. Although MOEAs produce highly accurate outcomes, their computational cost and complexity require deep knowledge of the problem, making them less applicable to large energy systems.

The implementation of posterior modelling approaches allows the modelling of non-linear problems with highly complex physics. Unlike prior models, which often rely on fixed assumptions, posterior modeling refines these assumptions based on findings and adapts parameters iteratively. This is shown, for instance, in Secchi et al. [72]. The study implements the NSGA-II iterative algorithm to perform a bi-objective optimization for maximising the self-sufficiency of an Energy Community (EC) from the distribution grid while minimising the BESS capacity, showing how the MOEA approach allows a deep sensitivity analysis for the EC's energy system optimal design.

Finally, interactive methods allow the selection of optimal solutions during the optimization process itself. These methods involve decision-makers, who interact with the optimization algorithm providing feedback and adjusting settings as the optimization continues. This iterative process allows the decision-maker to explore trade-offs between different objectives while the system is still solving, to then ultimately converge to a solution that best meets their initial goals. However, due to their complexity, these are hardly used in the field of energy modelling [13].

When focusing on low-voltage energy systems, modelling can be further divided into two categories: district-level models, where a large group of DERs are interconnected to operate in an efficient manner, and building-level system models, which focus on a smaller system scale but with higher precision and accuracy of results [78]. The choice between these models depends on the scope of the research, with one being preferred over the other based on specific research objectives.

A broad overview of the different tools for district-level simulations is argued in Allegrini et al. [6], while Crawley et al. [17] highlight the most used for district-level and building-level energy system optimization, discussing more than 230 modelling approach in their research.

Recalling the problem statement introduced in chapter 1, this research aims to investigate how the flexibility of several DERs in an energy system can be exploited to achieve efficiency of design and operation, given the goal of congestion mitigation. As a result, the modelling method used in this thesis will follow an optimization approach at the district level.

In addition, further considerations regarding the uncertainty issue must be discussed before proceeding with the modelling part. As discussed in Feng et al. [23], uncertainties can be related to the model parameters or to the model structure itself. For model parameters, this can include, for instance, demand forecasting, renewable energy generation, electricity prices, weather forecast or unscheduled maintenance. On the other hand, uncertainty can be related to the structure of the model, meaning the incorrect definition of the objective or of the decision variables.

The impact of uncertainties on the final model results mainly concerns the reliability of the solution found. This can dangerously affect decision-making, policy and strategy formulation as well as risk assessment of the optimal found. As a result, it is crucial to address this problem to enhance the correctness of results. Feng et al. [23] provide an overview of different methods used to mitigate uncertainties, identifying three main categories of modelling: deterministic, stochastic and hybrid.

Deterministic modelling assumes the input data as fixed providing exact solutions based on the specification given. Conversely, in stochastic models, part of the input data is characterized by a random behaviour related to certain probability functions. Hence, these aim to address uncertainties through the variability of the given data, resulting thus in a range of possible outcomes. Deterministic approaches, on the other hand, assess uncertainties through the specified data and deliver a single solution for each input given. Moreover, when the system in analysis is characterized by high uncertainty factors, such as energy markets or high renewable fluctuation, stochastic modelling results in optimal for a correct description of the system. In contrast, deterministic approaches are preferred when data is well-defined and the system is characterized by reduced uncertainty, making the model sufficiently simple to be implemented. As a result, deterministic methods are typically simpler to implement, while stochastic analyses are generally more computationally expensive. As the name suggests, hybrid models consider a combination of the stochastic and deterministic approaches.

In their work, Hu and Ryan [34] compare a two-stage stochastic programming and a deterministic model with forecast-based wind reserves for short-term planning of a combined natural gas and power system with uncertain wind energy. While the combined gas power plant is efficiently described by the deterministic approach, the highly fluctuating behaviour of the wind farm makes the stochastic programming more attractive despite its complexity. Hence, the research shows the advantages and disadvantages of both approaches, concluding that the best method depends on many characteristics of the problem in analysis.

To address uncertainties, a common approach used in the literature associated with forecasting is scenario analysis. Each scenario represents a storyline about how the system would perform in the future along with a set of exogenous assumptions considered [18]. Scenario analysis allows researchers and policymakers to explore a variety of possible options by considering different combinations of key variables and assumptions, such as economic growth rates, technological advancements, policy changes, and market dynamics. The most critical step in this analysis consists of the identification of scenarios, which must be feasible and match the specification of the case study. Once this is defined, the model is run for each case to simulate the system response and eventually optimize the functioning or design.

Scenario analysis improves the robustness of the research enabling a secondary analysis of parameters that cannot be included in the mathematical model. However, as mentioned by Morgan and Keith [52], scenarios with detailed storylines can contribute to cognitive biases by appearing more probable than they are in reality. To overcome this, further analysis can be performed through iterative processes that provide a broader view of the optimal solution found. In their research, DeCarolis et al. [18] aim to show how an iterative approach computed through the technique of Modelling to Generate Alternatives (MGA) can lead to insights that may not be achieved with normal optimization. Such a tool represents a useful way to explore the decision landscape given the complexity and uncertainties associated with energy systems. MGA can be seen as an extensive sensitivity analysis. While sensitivity analysis is performed on a single decision variable to prove the robustness of a single solution, MGA explores multiple alternatives to provide decision-makers with a variety of options that are significantly different from each other but still meet the problem's constraints [18]. An example of modelling to generate alternatives approach is observed in Pedersen et al. [60], where the framework is applied to study a range of technical and socioeconomic metrics on a model of the European electricity system. From the optimal solution found, the research reveals that large variations are observed for the near-optimal solutions for small variations in total system cost.

However, the existing modelling methods present limitations that may reduce the accuracy and reliability of energy system modelling. Technical limitations include computational constraints, meaning the time and density of the model in representing the real system, and model scalability, referring to the size and type of information the model can handle. Moreover, methodological limitations are typically an issue. These concerns, for instance, the oversimplification of complex physics and lack of real-world validation. Additionally, the accuracy and availability of data are often a strong limitation. It is indeed common for energy system modelling to consider data from different projects and adapt them to the case study.

Being these limitations unique case by case, there is no single solution to the problem. However, by acknowledging this challenge, engineering consideration can be made and a sufficiently accurate result can be achieved.

In the past years, many modelling tools have been developed for the different approaches mentioned in this chapter. Allegrini et al. [6] provide an extensive review of the most used software for energy modelling in the last years, dividing them by modelled Distributed Energy Resource (DER).

For what concerns the modelling of energy community systems as in this research, the reference summarizes the tools as in figure 2.4. For the scope of this research, the following groups are defined:

- High-level tools (Modelica libraries): *KULeuven IDEAS lib* and *LBNL District lib*;
- Heating network-focused models: *Termis*, *Neplan*, *EnerGis* and *NetSim*;
- Simulation of city quarters: *CitySim* and *Solene*;
- Techno-economic simulator: *energyPRO* and *RETScreen*;
- Microgrids design optimization: *HOMER* and *EnergyPLAN*;
- Programming language for model development: *MatLab*, *Python* and *Java*.

In order to focus the model functioning on the research question introduced in chapter 1, for this research, a dedicated model is designed. In this way, the aforementioned technical and methodological limitations can be better addressed.

To summarize, this chapter provided an in-depth overview of the problem of grid congestion and its implications, specifically focusing on low-voltage energy systems at the urban level.

The research divided the problem into two sub-categories: congestion for existing connections and issues related to new connection capacity. The first discusses the issue of the DSO in efficiently

X	Not included	External air flow	short-wave radiation	Long-wave radiation	Building thermal	User behaviour	Building system	Thermal network	Electrical network	Gas network	District plant	Thermal storage	Wind power	PV	Ground source	Spatial	Transportation
L	Link to another program																
S	Simplified model																
D	Detailed model																
KULeuven IDEAS lib		S	D	D	D	D	D	S	D	X	S	S	X	D	D	X	X
LBNL District lib		S	D	D	D	X	D	S	D	X	S	S	S	D	D	X	X
Termis		X	X	X	L	X	X	D	X	X	S	S	X	X	X	L	X
Neplan		X	X	X	L	X	X	D	D	D	S	S	D	X	X	L	X
NetSim		X	X	X	L	X	X	D	X	X	D	X	X	X	X	L	X
EnerGis		X	X	X	S	X	S	S	X	X	S	X	X	S	S	D	X
CitySim		X	D	D	S	D	S	S	X	X	X	S	S	S	S	D	X
Solene		L	D	D	S	S	X	X	X	X	X	X	X	X	X	D	X
energyPRO		X	X	X	L	X	D	D	D	X	D	D	D	D	S	S	X
RETScreen		X	X	X	S	X	S	S	X	X	S	S	S	S	S	X	X
HOMER		X	X	X	L	X	X	X	X	X	S	X	D	D	X	X	X

Figure 2.4: Table of common programs used for energy system modelling, based on [6].

distributing electricity to the connected parties and examines different methods for efficiently managing it, while the second argues how highly congested networks are incapable of accommodating new projects and how to overcome this.

Further discussion has then focused on the Dutch case, exploring the involved actors' plans to mitigate the problem of grid congestion in the Netherlands. The study suggested how the new connection capacity congestion problem is of high priority in the country and how policymakers and governmental entities are planning to address this issue.

Then, a brief overview of technical and socio-political aspects was explored through the concepts of energy hubs and energy communities, highlighting the characteristic differences and how these may apply to the research.

Finally, an overview of energy system modelling was presented, describing the different approaches used in literature and identifying their strengths and weaknesses for solving the problem stated in chapter 1. The literature review suggested that a deterministic approach, executed through an optimization model, is the most suitable for this study.

To define the details for resolving the optimization problem, the modelling tool must be first thoroughly explained. While existing modelling software offers a wide range of capabilities, their general nature does not enable the effective implementation of DSM for mitigating grid congestion. Therefore, to achieve more precise and effective results, a dedicated model is developed. In the next chapters, the assumptions and approaches followed are argued to provide a clear idea of the energy system model used in this research.

3 Methodology

As discussed in the previous chapter, energy system modelling can be approached using various methodologies, each suited to different scenarios. There is no universally optimal method applicable to all situations. This chapter describes the tools, the physics and the methodology followed to describe the energy system in this research. First, section 3.1 discusses the scope of the model for this research. Then, section 3.2 gives an overview of the optimization approach used in this research while section 3.3 gives an overview of the software used. Next, section 3.4 explores the equations to model the functioning of all energy resources. Finally, section 3.5 resumes the optimization structure and argues the different scenarios computed to achieve the research goal.

3.1. Scope of the model

In order to explore the potential of Distributed Energy Resources (DERs), a comprehensive model has been developed and implemented. The goal is to represent the operational dynamics of the energy system such that each DER can function autonomously then interacting with the broader system. In other words, the scope of the model is to accurately emulate the energy system's response to specified input parameters, to optimize the scheduling and utilization of various DERs.

The problem subject of the study consists of a small-medium energy system characterized by various DERs and a grid connection. These include photovoltaic (PV) generation, Electric Vehicles (EVs), district heating networks and possibly the installation of a battery storage system. The problem revolves around the connection to the distribution grid as it may not be available during congestion periods. For this reason, the optimization will focus on grid connection, while the different DER variables will be adjusted to achieve the optimal solution. It is easy to expect several constraints for modelling each single resource, resulting in a complex optimization problem with an important computational cost. To make the modelling easier to implement, simplifications and linearization of constraints will be argued for each DER modelling. The objective is to determine the optimal configuration to achieve peak power reduction during defined peak hours. To ensure robustness and accuracy, hourly simulations are performed for each day of the year, allowing a good representation of (most of) the different possible conditions the real system may encounter.

3.2. Optimization method

Mathematical optimization is a broad and complicated subject that can be developed through many different methodologies and strategies. In the previous chapter, an overview of the approaches used in the field of low-voltage energy systems was discussed. The research highlights how the decision of the type of optimization method is strictly dependent on the nature of the study case as well as the goal of the research. Indeed, for the scope of this thesis, a few considerations can be argued.

Due to its multi-dimensional nature, the system is expected to be defined by several variables and consequently multiple degrees of freedom. This may lead to an issue of non-unique solutions if the objective of the optimization is not well defined. Following the trend in the literature, the energy system modelling will consider a multi-objective optimization approach. Therefore, besides the primary goal of peak power reduction, secondary goals will be specified.

Furthermore, the integration of variable DERs, for instance, PV, introduces uncertainties to the problem. In order to solve this issue, this research follows a deterministic prior resolution approach. This is further elaborated in section 3.5.

3.3. Modelling tools

Among the different programs available for solving optimization problems, this research will use *Pyomo v6.7.0* (Python Optimization Modelling Objects), a package for *Python*, installed in *v3.11.5*. The reason for this choice was led by the high versatility, efficiency and user-friendliness of *Pyomo* as well as the fact of it being open-source. Moreover, *Pyomo* is largely used in industries in several fields, among which also energy system modelling. Indeed, its functionalities are preferred over others by important research entities such as the National Energy Technology Laboratory or the National Renewable Energy Laboratory[1].

Besides the easy interface that allows a simple implementation of the problem, *Pyomo* solve functions depend on the type of solver used. Thanks to its multiple advantages, the software *Gurobi* was chosen for the project. It is primarily a mathematical optimization solver, specifically focusing on Linear Programming (LP), Mixed-Integer Linear Programming (MILP), Quadratic Programming (QP), and convex optimization problems. This software uses different mathematical methods to perform optimizations, including cutting-plane methods, branch-and-cut algorithms, and interior-point methods. Unlike other types of solvers, such as heuristic or decision-rule based, *Gurobi* allows a full range analysis able to find both optimal and sub-optimal solutions [28]. Finally, its speed and quality of performance fit best the scope of the research.

To exploit the friendly user interface of *Pyomo*, the modelling part of the project was written in *Python*, in which the optimization tool is an additional library available to import. *Pyomo* solves optimization problems working on a *model* in which all characteristics are specified. First, the initialization of *Sets*, such as the time set $\mathcal{T}$, allows the introduction of *Parameters* and *Variables* used then in the model. Secondly, *constraints* are specified in order to generate the feasible region. Finally, the objective function is initialized and through the use of a solver, as *Gurobi* in this case, the optimal solution is found.

3.4. Energy system resources and modelling

Modelling of energy systems can simply be seen as shaping the physics described in equations into computational expressions that can be solved by a computer simulator. Therefore, in order to understand the computation, the physics must be discussed first.

This chapter discusses the assumptions, equations and formulas used to describe the technical part of a general energy community, focusing on the technologies considered in the case study. Every subsection argues the physical principles and considerations of every side of the energy system to then explain more in detail the method of modelling. Photovoltaic physics is described in subsection 3.4.1 while subsection 3.4.2 carefully explains the methodology followed for district heating system modelling. Then, subsection 3.4.3 and subsection 3.4.4 focus on equations used for the battery storage system and the EV fleet, respectively. Finally, the general system balancing is modelled in subsection 3.4.5.

3.4.1. PV system

The integration of renewable energy resources into small-medium energy systems is proven to drastically reduce the system's carbon footprint as well as grid congestion issues. In particular, the installation of PV panels allows the penetration of cheap and clean power that positively affects the system's sustainability [2]. On the other side, PV modules can be considered as a variable current source in the electrical layout that may cause instability of voltage and power supply. Indeed, photovoltaic technology generates electricity only when sun radiation is registered. Thus, the power produced is strongly dependent on time and weather conditions. The output power properties depend on different factors, such as the solar cell characteristics, its temperature and the irradiation it is posed. For the scope of this research, the integration of a PV system will be defined by only one dimension of interest: the PV power output.

For simplicity of modelling, PV panels can be grouped in subgroups, identified as *PV strings*, identified by the subscript p from now on. A string, or array, is defined as a connection in series of two or more

[1]Reference: https://www.pyomo.org/impact

panels, usually mounted with the same tilt and azimuth angles [75]. It can be assumed that all panels in a string have the same power output. In reality, shading, cleanness and position of the modules affect each other's energy production. However, these details are outside the scope of the project and can be neglected.

As well explained in Smets et al. [75] the total irradiance that a PV module experiences during daylight is given by the sum of direct, diffuse and ground irradiance, respectively expressed as $G_{t,p}^{dir}$, $G_{,t,p}^{dif}$ and $G_{t,p}^{ground}$ in equation 3.1.

$$G_{t,p} = G_{t,p}^{dir} + G_{t,p}^{dif} + G_{t,p}^{ground} \tag{3.1}$$

The highest contribution is given by the direct irradiance term, which expresses the solar energy that reaches the surface of the solar panel directly from the source, the sun. It is computed as shown in equation 3.2 below.

$$G_{t,p}^{dir} = DNI_t \cdot [sin(\theta_p^{panel}) \cdot cos(a_t^{sun}) \cdot cos(\gamma_p^{panel} - \gamma_t^{sun}) + cos(\theta_p^{panel}) \cdot sin(a_t^{sun})] \tag{3.2}$$

Here, DNI_t represents the Direct Normal Irradiance, measured in $\frac{kW}{m^2}$, while γ_p^{panel} and θ_p^{panel} are the module's azimuth[2] and tilt angles, both expressed in degrees. Similar parameters are defined for the sun position, which depends on time t. These are expressed as a_t^{sun} and γ_t^{sun} in the equation above and represent sun elevation and azimuth respectively, again measured in degrees.

The second term of equation 3.1 is the diffuse irradiance term, which represents the scattered light generated when sun rays enter the atmosphere. This can be described with the so-called *sky models*, physics models that take into account clouds and particles floating in the air. For the scope of this research, a good representation of the diffuse irradiance is obtained with the simplified model called *isotropic sky diffuse model*, shown below in equation 3.3 [69].

$$G_{t,p}^{dif} = DIF_t \cdot SVF_p \tag{3.3}$$

$$SVF_p = \frac{1 + cos(\theta_p^{panel})}{2} \tag{3.4}$$

in which DIF_t is the Diffuse horizontal Irradiance, in $\frac{kW}{m^2}$. This component is strongly dependent to the Sky View Factor (SVF), defined in equation 3.4 by the tilt angle of the panels mounting. Depending on the installation tilt, the portion of the sun visible by the module changes drastically, hence, the importance of designing the correct inclination depending on the location.

Finally, the last type of irradiance is given by the reflection of light from the building surfaces and the ground. Indeed, depending on the surroundings of the PV module, the albedo coefficient α_p of reflection can vary and so affect the power output of the solar system. For urban areas, α_p assumes values that can vary between 0.05 and 0.2 [75]. Therefore, the final component of the total irradiance can be computed through equation 3.5.

$$G_{t,p}^{ground} = GHI_t \cdot \alpha_p \cdot (1 - SVF_p) \tag{3.5}$$

$$GHI_t = DNI_t \cdot cos(a_t^{sun}) + DIF_t \tag{3.6}$$

in which GHI_t is known as Global Horizontal Irradiance, expressed in equation 3.6.

Once the total irradiance is defined, it is easy to calculate the power output of the PV system as in equation 3.7:

$$p_{t,p}^{PV} = G_{t,p} \cdot \eta_p^{panel} \cdot A_p^{panel} \cdot N_p^{panel} \tag{3.7}$$

$$\eta_p^{panel} = \frac{P_{mpp}^{panel}(STC)}{G(STC) \cdot A^{panel}} \tag{3.8}$$

[2] γ = 0° (South), γ = + 90° (West), γ = - 90° (East) and γ = ± 180° (North)

where η_p^{panel} represents the efficiency of the panel in use, A_p^{panel} is the module's area m^2 and N_p^{panel} is the number of modules used.

It is important to mention that the module efficiency coefficient strongly depends on different factors, both operational (cell temperature, irradiance) and technical (type of cell) [75]. For the scope of this project, this parameter is estimated through equation 3.8, making results less precise but easier to compute. The dimension P_{mpp}^{panel} is the maximum power output that can be achieved by the solar panel in Standard Test Conditions (STC)[3], measured in kWp, while $G(STC)$ is the total irradiance in STC, assumed as 1'000 $\frac{W}{m^2}$.

This concept can be applied to every string p, assuming that the converters are sized to process all available power. As a result, when modelling a PV system composed of $\mathcal{P}$ strings, the total PV power production can be modelled by simply summing all the strings' power outputs.

3.4.2. Heating system

Since the early 2000s, the shift to developing more sustainable systems with lower or zero carbon emissions has been the main focus in relation to district heating system evolution [57]. The main driver of this change is the increased availability of heat pumps, which allow heating by using only electric power.

A heat pump is defined as a thermodynamic machine that can transfer thermal energy from a cold source to a hotter one, called sink, by the introduction of work. It can be theoretically idealized as shown in figure 3.1. The heat Q_C is extracted from a cold source and through the assistance of external work W, electrical in the case of heat pumps, it is, indeed, pumped to the sink, again in form of thermal energy Q_H. The efficiency of a heat pump is defined by the Coefficient of Performance (COP), theoretically computed as shown in equation 3.9.

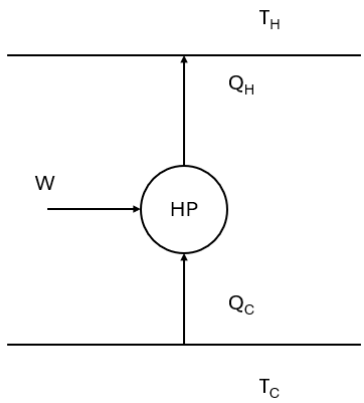

Figure 3.1: Thermodynamic scheme of an ideal heat pump.

$$COP(t) = \frac{Q_H(t)}{W(t)} = \frac{W(t) + Q_C(t)}{W(t)} = 1 + \frac{Q_C(t)}{W(t)} \tag{3.9}$$

As clear in the expression above, unlike the other most known thermodynamic machines, heat pumps are characterized by an "efficiency" always greater than 1 and whose value depends both on the type of HP as well as the external conditions [79]. As a result, it is easy to notice that the higher the HP's COP, the lower the electrical power needed for the same heating goal. Hence, this parameter plays a crucial role in determining when it is optimal to use the heat pump. In reality, this parameter depends on multiple factors such as the temperatures, type of source, type of sink and efficiency of the internal technology used for transforming energy. Further consideration regarding the COP will be argued later in section 4.2. Defining the group of heat pump $h \in \mathcal{H}$, this concept is shown in equation 3.10.

$$COP_{t,h} \cdot p_{t,h}^{HP} = |q_{t,h}^{HP}| \tag{3.10}$$

Where $p_{t,h}^{HP}$ is the heat pump electric power, bounded by its rated power $\overline{P}_h^{HP}$ as in equation 3.11, while $q_{t,h}^{HP}$ represents the HP power in the form of thermal energy. The expression includes the absolute value

[3]STC is characterized by 1'000 $\frac{W}{m^2}$ of irradiance, AM1.5 spectrum and cell temperature of 25 °C as specified in the IEC 60904-3.

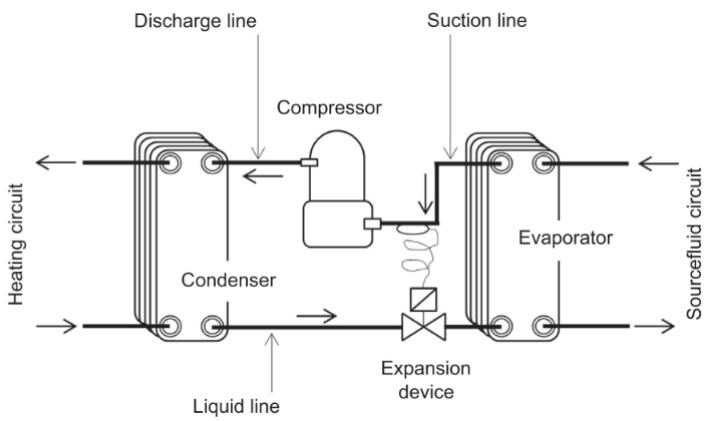

Figure 3.2: Vapour compression heat pump scheme [79].

of thermal power to represent the case in which the heat pump operates as a cooling device, hence, negative $q_{t,h}^{HP}$.

$$0 \leq p_{t,h}^{HP} \leq \overline{P}_h^{HP} \tag{3.11}$$

In reality, the theoretical thermodynamic cycle of a heat pump can be emulated by using the bi-phase property of a fluid, usually water solutions or hydrofluorocarbons, which allows heat pumping thanks to forced circulation. An example scheme of the primary loop functioning is shown in figure 3.2, while figure 3.3 reports the respective thermodynamic cycle. The fluid is brought from the bi-phase state point A to a super-heated vapour through an evaporator in point B. Then, the compressor brings the fluid to a higher pressure state in point C, introducing the aforementioned external work W. The heat is thus transferred to the condenser, which leads heat to the hot sink, bringing the flow to point D. Finally, an expansion valve adjusts the pressure closing the cycle again in point A.

Nowadays, there are several types of heat pumps available in the industry. They can be distinguished by the origin of cold and hot sources. These can be air, water, ground or waste heat for the source side and air, water, steam or heated material for the sink side. When considering residential heating and cooling, the optimized designs usually see Air-Source Heat Pumps (ASHPs) and/or Ground-Source Heat Pumps (GSHPs) [11]. The first ones are usually preferred for single household installation, being smaller, cheaper and easier to install. On the other hand, their COP is generally lower making them inadequate for big residential areas with centralized heating systems. Furthermore, their functioning bases on a ventilation fan that may result too loud for highly populated urban areas [79].

A more efficient and reliable heating system is provided by GSHPs, which fit best for district networks of heating and cooling. Despite the cost and difficulty of installation may be crucial for already existing areas, GSHPs are the optimal choice for new residential neighbourhoods [11]. Ground-source heat pumps use earth, groundwater, or both as a source of heat during cold seasons and as a reservoir for house cooling during summer. Their design includes a ground heat exchanger, usually a long metal pipe installed in the soil that transfers heat to/from the circulating fluid (commonly an anti-freeze solution or water).

Here there are two methods of operation. With a closed loop, the circulating fluid is constantly pumped into the ground pipes to be warmed up (or cooled down). At the end of the cycle, heat transfer happens in the so-called primary heat exchanger (the evaporator) inside the house, which transfers the heat gained from the ground to the primary loop and thus to the dwelling.

Conversely, when considering an open loop, the heat source is a groundwater reservoir. The water flowing in the ground is thus extracted from an aquifer, which is a more stable sink than the ground. Hence, this latter configuration makes the system more efficient. A schematic of GSHP for both loops is shown in figure 3.4.

Although GSHPs are the most efficient way to exploit geothermal energy in residential areas, limitations regarding soil integrity must be considered. Indeed, it is important to mind the effects of extracting/injecting heat on soil's temperature, moisture and properties. Especially in the northern countries, heating demand is abundantly higher than the designed cooling, meaning that the heat extracted from the soil is

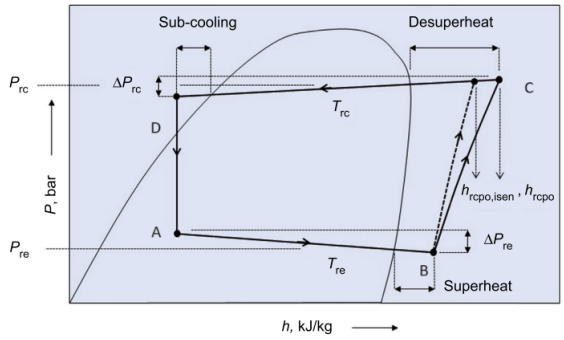

Figure 3.3: Thermodynamic cycle for vapour compression heat pumps [79].

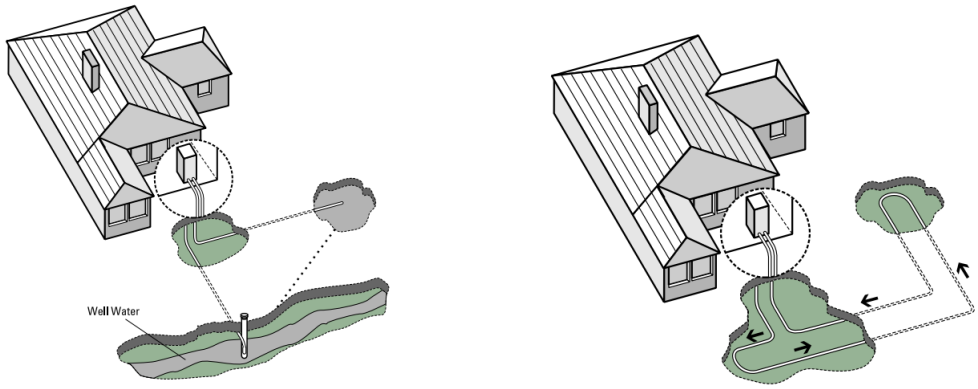

Figure 3.4: Scheme of the secondary open-loop (left) and closed-loop (right) of ground-source heat pump for dwellings [11].

more than the one re-injected. As a result, many years of system operation will affect a decrease in the heat pump COP, as well as degradation of the earth [12]. For this reason, regulations are strictly applied by governmental entities in ground heat usage. Besides permits for construction, it is often required to periodically re-inject heat in the ground, resulting in higher cooling demand during the warm season. More detailed considerations about the data used will be discussed later in section 4.2.

Modelling of heating systems is a complicated subject that often requires non-linear equations and a high level of computation. However, the scope of this research is to describe the energy system from a bigger picture and therefore some simplification can be considered.

A schematic design of the heating system model used in this project is shown in figure 3.5. It consists of a flux of water that periodically circulates in a closed loop pipe. Along this, different heat exchangers are placed to allow thermal energy transmission. To the left side of the picture, the pink arrow expresses the heat transferred from the heat pumps to the water flow, defined as $q^{HP}_{t,h}$. As a result, the flow is heated from temperature $T^4_{t,h}$ to temperature $T^1_{t,h}$, according to equation 3.12. Similarly happens on the right-hand side, where a heat exchanger passes heat from the water flow to the house heating, defined as $Q^d_{t,h}$, cooling it from $T^2_{t,h}$ to $T^3_{t,h}$ as in equation 3.13. The mass flow $\dot{m}$ and the specific heat Cp_w are assumed to be constant. This is a valid assumption if the district heating demands, meaning space heating, hot water and space cooling, can be considered always required, and therefore circulation is constantly needed.

$$q^{HP}_{t,h} = \dot{m} \cdot Cp_w \cdot (T^1_{t,h} - T^4_{t,h}) \tag{3.12}$$

$$Q^d_{t,h} = \dot{m} \cdot Cp_w \cdot (T^2_{t,h} - T^3_{t,h}) \tag{3.13}$$

Considering now more in-depth the physics of water flowing in the heating system pipes, it is important to highlight the complexity of the problem due to losses. Indeed, depending on the chemical properties and speed of the circulating water, as well as the material, size and condition of the pipe, energy losses will be experienced during operation, mainly connected to friction. In addition to that, one or more

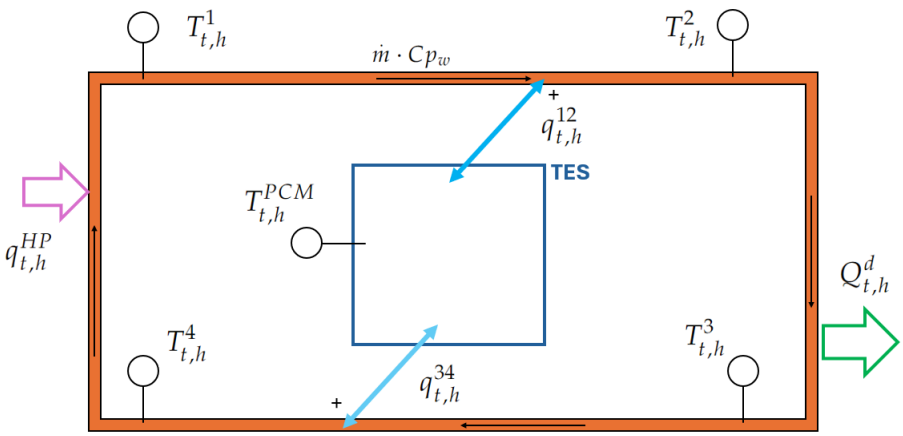

Figure 3.5: Schematic representation of the h-th heating system network.

water pumps are constantly needed in operation for the fluid to circulate. These devices' efficiency is usually difficult to estimate since it is proportional to the condition of operation, location and technology involved. Hence, a detailed and precise analysis of the fluid system becomes very complex. Despite the fact this may strongly affect the results, it is assumed that all aforementioned losses are taken into account within the house heating demand $Q^d_{t,h}$, shown in equation 3.14, defined as the union of space heating $Q^{sh}_{t,h}$, hot water $Q^{hw}_{t,h}$ and space cooling $Q^{cool}_{t,h}$ demands at each time t. Such an assumption is valid if the data used in simulations is measured at the user's end.

$$Q^d_{t,h} = Q^{sh}_{t,h} + Q^{hw}_{t,h} - Q^{cool}_{t,h} \tag{3.14}$$

Moreover, it is important to mention that in district heating networks, pipelines can reach up to several kilometres in length and therefore the temperature changes in the water flow do not happen instantaneously. For the scope of this project, though, a strong simplification will be considered in order to avoid describing temperature transients over time. This can be assumed valid when the heating network is relatively small, for instance, a single neighbourhood, and simulations consider a sufficiently large time step t. Therefore, it is assumed that every infinitesimal volume of water circulating in the network is in equilibrium with each other, such that every change happening in one section simultaneously affects the others. This allows to treat the heating system as an electrical circuit, which is subject to instant changes. Although this hypothesis may significantly affect the final results, the lack of information about the exact dimensions of the heating system and pipe specifications makes such simplification valid for the final goal of the research.

As described so far, such a heating system results in a simple demand-response network in which the heating/cooling load pulls into operation the heat pumps right when needed. In residential households, it is proved that the highest share of energy use is for space heating and hot water [24]. For this reason, when addressing load shifting and demand management, it is crucial to include a flexibility term. As a result, the heating system model shown before in figure 3.5 considers a Thermal Energy Storage (TES) as a heat buffer, shown in blue.

Thermal energy storage (TES) technologies stand out as one of the most prevalent methods for storing energy in residential areas. In district heating systems, two primary types of TES are typically distinguished: domestic TES, also known as short-term buffers, and seasonal TES, alternatively referred to as long-term buffers [57].

As the name suggests, domestic TES is frequently installed within individual houses and consists of devices capable of storing heat at elevated temperatures for load-shifting purposes, typically for up to two weeks. On the other hand, the integration of long-term thermal storage units is becoming increasingly popular in new residential districts. These are usually installed close to the dwellings and designed to store heat for several weeks.

Furthermore, besides the design purpose, thermal energy storage is categorized into three distinct types based on the technology employed. The oldest and simplest unit is Sensitive Thermal Energy Storage (STES), typically consisting of a well-insulated water tank. While its straightforward design

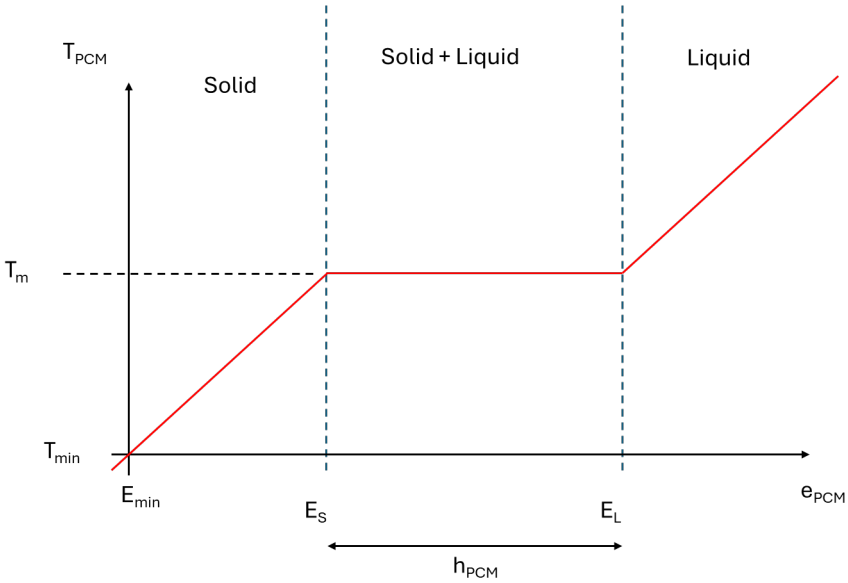

Figure 3.6: Temperature of PCM function of the internal energy $e_{t,h}^{PCM}$.

makes it relatively cheap and easy to install, it experiences losses making it less suitable for seasonal storage applications. An improved version is the Phase-Change Material (PCM) thermal unit, which exploits the bi-phase properties of the used composite to store heat in both sensitive and latent forms. This allows for lower operating temperatures compared to STES, resulting in higher efficiency. Lastly, thermochemical TESs take advantage of the composite material's chemical properties and store heat through chemical reactions. However, the materials used increase safety risks in domestic installations, and their higher cost places this type of TES as the least popular choice for current district heating systems [57].

Thanks to its lower average temperature and contained costs, a phase change material storage unit has been included in the model design. PCM buffers are designed such that the bi-phase state is exploited most of the time. This is because when in this state, the temperature of the whole composite is constant and uniform, hence, temperature control becomes more simple. This latter characteristic results in a non-linear temperature function, following three different equations depending on the state of energy (and thus the phase). This concept is expressed mathematically in equation 3.15 and shown in figure 3.6.

$$T_{t,h}^{PCM} = \begin{cases} \frac{1}{c_h^{PCM}} \cdot e_{t,h}^{PCM} \cdot \frac{3600}{m_h^{PCM}} & \text{if } e_{t,h}^{PCM} \leq E_h^S \\ T_h^{melt} & \text{if } E_h^S < e_{t,h}^{PCM} \leq E_h^L \\ \frac{1}{c_h^{PCM}} \cdot (e_{t,h}^{PCM} \cdot \frac{3600}{m_h^{PCM}} - h_h^{PCM}) & \text{if } e_{t,h}^{PCM} > E_h^L \end{cases} \tag{3.15}$$

Therefore, the internal temperature of the PCM, $T_{t,h}^{PCM}$, expressed in Celsius, depends on the internal State of Energy (SOE), $e_{t,h}^{PCM}$, expressed in kWh. When in mono-phase, either liquid or solid, the temperature follows a linear function in which slope depends on the specific heat c_h^{PCM} of the composite and intercept defined through the specific latent heat h_h^{PCM}, expressed in $\frac{kJ}{kgK}$ and $\frac{kJ}{kg}$ respectively.

According to the thermodynamics principles, every object can be characterized with its internal energy ΔU, strictly connected to its defined temperature T [19]. As a result, for thermal energy storage, it is convenient to define the SOE as relative to a set internal energy of reference. For simplicity of use, the reference is set as SOE for zero degrees Celsius, allowing the expression of the temperature in Celsius degrees instead of Kelvin. This concept is mathematically expressed in equation 3.16 and equation 3.17 below, in which $\overline{T}_h$ and $\underline{T}_h$ represent the bounding temperature of the heating system, and therefore of the thermal buffer.

Furthermore, the phase-change thresholds, defined through E_h^S and E_h^L and also measured in kWh, are inherent characteristics of the composite use and depend only on the PCM mass m_h^{PCM}, in kg, and

the melting temperature T_h^{melt}. Hence, knowing these characteristics of the composite, the phase-change SOE are determined as in equation 3.18 and equation 3.19.

$$\overline{E}_h^{PCM} = (c_h^{PCM} \cdot (\overline{T}_h - T(0°C)) + h_h^{PCM}) \cdot \frac{m_{PCM}}{3600} \tag{3.16}$$

$$\underline{E}_h^{PCM} = (\underline{T}_h - T(0°C)) \cdot \frac{c_h^{PCM} \cdot m_h^{PCM}}{3600} \tag{3.17}$$

$$E_h^S = (T_h^{melt} - T(0°C)) \cdot \frac{c_h^{PCM} \cdot m_h^{PCM}}{3600} \tag{3.18}$$

$$E_h^L = (c_h^{PCM} \cdot (T_h^{melt} - T(0°C)) + h_h^{PCM}) \cdot \frac{m_h^{PCM}}{3600} \tag{3.19}$$

In order to make the PCM storage model linear, the temperature gradient throughout the buffer is assumed to be negligible during single-phase states. Hence, only one parameter, $T_{t,h}^{PCM}$, communicates with the water flow of the heating system. Referring again to equation 3.5, the charging and discharging of the thermal storage happens on two fronts: after the water has been heated up by the heat pumps and after it has been cooled down by the household heat exchangers. From now on in the report, these will be referred to as *hot side*, between points 1 and 2, and *cold side*, between points 3 and 4, respectively. On both sides, heat is transferred to and from the TES depending on the system's defined internal temperature. According to the second law of thermodynamics:

"Heat does not flow spontaneously from a colder region to a hotter region, or, equivalently, heat at a given temperature cannot be converted entirely into work." [19].

As a result, if at a certain time t^* the temperature of the composite, $T_{t^*,h}^{PCM}$, is higher than the temperature of the water after being heated up by the HPs, $T_{t^*,h}^1$, there will be a transfer of thermal energy from the buffer to the water flow, which will result then warmer in section 2 than in section 1 ($T_{t^*,h}^2 \geq T_{t^*,h}^1$), and vice versa. Therefore, the thermal energy transfer per unit of time $q_{t,h}^{12}$ can be defined positive when outgoing, or discharging, the TES and negative when ingoing, or charging, the thermal storage. This concept is resumed below from equation 3.20 to equation 3.23.

$$q_{t,h}^{12} = \dot{m} \cdot Cp_w \cdot (T_{t,h}^2 - T_{t,h}^1) \tag{3.20}$$

$$q_{t,h}^{34} = \dot{m} \cdot Cp_w \cdot (T_{t,h}^4 - T_{t,h}^3) \tag{3.21}$$

$$q_{t,h}^{12} \geq 0 \quad \text{if } T_{t,h}^1 \leq T_{t,h}^{PCM} \tag{3.22}$$

$$q_{t,h}^{34} \geq 0 \quad \text{if } T_{t,h}^3 \leq T_{t,h}^{PCM} \tag{3.23}$$

$$Q_{t,h}^d = q_{t,h}^{HP} + q_{t,h}^{12} + q_{t,h}^{34} \tag{3.24}$$

It is important to mention that the thermal losses of charging and discharging are considered negligible for the research goal, meaning that the heat exchangers can ideally transfer the whole energy instantaneously. Although this is a significant simplification, the non-linearity of the heat transfer physics drastically increases the model complexity, making the computational cost of the model out of the research scope [57].

Moreover, for the same law of thermodynamics, the end temperature of the heat exchange process must be between the values of the other two temperatures. This is explained in the following equation 3.25.

$$\begin{aligned}
&\text{if} \quad T_{t,h}^1 \geq T_{t,h}^{PCM} \quad \text{then} \quad T_{t,h}^1 \geq T_{t,h}^2 \geq T_{t,h}^{PCM} \\
&\text{if} \quad T_{t,h}^1 \leq T_{t,h}^{PCM} \quad \text{then} \quad T_{t,h}^1 \leq T_{t,h}^2 \leq T_{t,h}^{PCM} \\
&\text{if} \quad T_{t,h}^3 \geq T_{t,h}^{PCM} \quad \text{then} \quad T_{t,h}^3 \geq T_{t,h}^4 \geq T_{t,h}^{PCM} \\
&\text{if} \quad T_{t,h}^3 \leq T_{t,h}^{PCM} \quad \text{then} \quad T_{t,h}^3 \leq T_{t,h}^4 \leq T_{t,h}^{PCM}
\end{aligned} \tag{3.25}$$

Thermal storage can be considered to have a similar nature to a battery, meaning that a State of Energy (SOE) can be defined and modelled to monitor the charging and discharging of the TES during operation. Equation 3.26 shows the discrete expression for charging and discharging the thermal buffer. The negative sign in front of the heat power exchanged is due to the definitions of $q^{12}_{t,h}$ and $q^{34}_{t,h}$ mentioned before.

$$e^{PCM}_{t,h} = L^{PCM}_{h,t} \cdot e^{PCM}_{t-1,h} - (q^{12}_{t,h} + q^{34}_{t,h}) \cdot \delta t \tag{3.26}$$

In order to consider thermal losses through the buffer walls, the coefficient $L^{PCM}_{h,t} \in (0, 1]$ is introduced. Although this parameter depends on the temperature difference between inside the buffer and outside, it is possible to approximate it to a constant value. More detailed information can be found in section 4.2.

Finally, the union of equation 3.12 to equation 3.26 fully describes the heating system model. Despite the problem appears linear and easily computable, the if conditions must be re-adapted in order to be included as constraints in the optimization problem. This can be done with the introduction of binary variables.

First, PCM temperature described in equation 3.15 is treated. By introduction the binary variables for solid-state $u^S_{t,h}$ and liquid-state $u^L_{t,h}$, as in equation 3.27, the composite's temperature can be constrained as in equation 3.28 to equation 3.31.

$$u^S_{t,h} = \begin{cases} 1 & \text{if } e^{PCM}_{t,h} \leq E^S_{t,h} \quad \text{(Solid-state)} \\ 0 & \text{otherwise} \end{cases} \qquad u^L_{t,h} = \begin{cases} 1 & \text{if } e^{PCM}_{t,h} \geq E^L_{t,h} \quad \text{(Liquid-state)} \\ 0 & \text{otherwise} \end{cases} \tag{3.27}$$

$$e^{PCM}_{t,h} \leq E^L_h + (E^S_h - E^L_h) \cdot u^S_{t,h} + (\overline{E}^{PCM}_h - E^L_h) \cdot u^L_{t,h} \tag{3.28}$$

$$e^{PCM}_{t,h} \geq E^S_h + (E^L_h - E^S_h) \cdot u^L_{t,h} + (\underline{E}^{PCM}_h - E^S_h) \cdot u^S_{t,h} \tag{3.29}$$

$$u^S_{t,h} + u^L_{t,h} \leq 1 \tag{3.30}$$

$$T^{PCM}_{t,h} = \frac{1}{c^{PCM}_h} \cdot \left(\frac{3600 \cdot e^{PCM}_{t,h}}{m^{PCM}_h} - h^{PCM}_h \cdot u^L_{t,h} \right) \cdot (u^S_{t,h} + u^L_{t,h}) + T^{melt}_h \cdot (1 - u^S_{t,h} - u^L_{t,h}) \tag{3.31}$$

Accordingly, two more binary variables are defined for the condition expressed in equation 3.25, respectively $u^{12}_{t,h}$ and $u^{34}_{t,h}$, explained below in equation 3.32. These aim to represent the charging, when equal to 1, and discharging, when equal to 0, of the thermal buffer. In addition, in equation 3.33 to equation 3.40 eight more constraints are introduced to successfully model the physics shown before.

$$u^{12}_{t,h} = \begin{cases} 1 & \text{if } T^1_{t,h} \geq T^{PCM}_{t,h} \\ 0 & \text{otherwise} \end{cases} \qquad u^{34}_{t,h} = \begin{cases} 1 & \text{if } T^3_{t,h} \geq T^{PCM}_{t,h} \\ 0 & \text{otherwise} \end{cases} \tag{3.32}$$

$$T^1_{t,h} \leq T^{PCM}_{t,h} + Q_1 \cdot u^{12}_{t,h} \tag{3.33}$$

$$T^1_{t,h} \geq T^{PCM}_{t,h} - Q_2 \cdot (1 - u^{12}_{t,h}) \tag{3.34}$$

$$T^2_{t,h} \geq T^{PCM}_{t,h} \cdot u^{12}_{t,h} + T^1_{t,h} \cdot (1 - u^{12}_{t,h}) \tag{3.35}$$

$$T^2_{t,h} \leq T^1_{t,h} \cdot u^{12}_{t,h} + T^{PCM}_{t,h} \cdot (1 - u^{12}_{t,h}) \tag{3.36}$$

$$T^3_{t,h} \leq T^{PCM}_{t,h} + Q_1 \cdot u^{34}_{t,h} \tag{3.37}$$

$$T^3_{t,h} \geq T^{PCM}_{t,h} - Q_2 \cdot (1 - u^{34}_{t,h}) \tag{3.38}$$

$$T^4_{t,h} \geq T^{PCM}_{t,h} \cdot u^{34}_{t,h} + T^3_{t,h} \cdot (1 - u^{34}_{t,h}) \tag{3.39}$$

$$T^4_{t,h} \leq T^4_{t,h} \cdot u^{34}_{t,h} + T^{PCM}_{t,h} \cdot (1 - u^{34}_{t,h}) \tag{3.40}$$

The parameters Q_1 and Q_2 are defined to constraint the temperatures $T^1_{t,h}$ and $T^3_{t,h}$ within the bounds of $\overline{T}_h$ and $\underline{T}_h$ of the system and the temperature of the buffer $T^{PCM}_{t,h}$ by non-linear expressions. To avoid further complications, coefficients Q_1 and Q_2 are set to 10^4 and the boundary conditions of the system temperatures are then included through equation 3.41 to equation 3.45.

$$\underline{T}_h \leq T^1_{t,h} \leq \overline{T}_h \tag{3.41}$$

$$\underline{T}_h \leq T^2_{t,h} \leq \overline{T}_h \tag{3.42}$$

$$\underline{T}_h \leq T^3_{t,h} \leq \overline{T}_h \tag{3.43}$$

$$\underline{T}_h \leq T^4_{t,h} \leq \overline{T}_h \tag{3.44}$$

$$\underline{T}_h \leq T^{PCM}_{t,h} \leq \overline{T}_h \tag{3.45}$$

To summarize, the heating system is the DER that demands the highest computational level within the overall energy system model described in this chapter. This section has outlined various assumptions made to accurately represent the heating system's physical behaviour. For clarity, these assumptions are summarized below:

- The energy losses related to the water flow, pumping devices and fluid dynamical frictions are included in the final heating and cooling demands;
- All points in the heating network are in constant equilibrium, meaning instant propagation is assumed. This implies that within each time step t, the system experiences infinite speed and infinitesimal mass of water, resulting in a constant mass flow rate $\dot{m}$. As a result, temperature changes are considered instantaneous;
- The heat exchanger is assumed to transfer thermal energy without any losses.

3.4.3. Battery energy storage system

In energy systems, the incorporation of PV energy systems introduces environmental benefits alongside challenges due to weather-dependent fluctuations. While solar power offers green energy, its availability strongly depends on weather conditions, resulting in variable output. This variability arises because electrical energy must be consumed as soon as it's generated and in the quantity it is produced. Hence, integrating storage technology becomes imperative, enabling the buffering of surplus electricity generated during peak sunlight for use during periods of scarcity.

In the context of on-grid energy systems, such concerns are no longer necessary thanks to the connection to an "unlimited" source of power. However, integrating storage technologies still offers advantages such as load shifting and maintaining consistent power draw throughout the day. During periods of high solar production, grid power withdrawal decreases, only to rise again after sunset. Incorporating storage technologies here ensures steadier grid power and facilitates the delayed consumption of PV-generated energy.

One of the primary challenges facing the energy industry today is identifying the most efficient, cost-effective, and sustainable methods for both short and long-term electricity storage. Concerning residential district energy systems, the prevalent storage technologies included are batteries, thermal energy storage, and hydrogen with fuel cells, ranked in order of popularity [45].

Batteries serve as devices enabling the storage of electrical energy in the form of chemical energy by exploiting the chemical properties of their constituent materials. The most common types are lithium-ion batteries thanks to their high energy capacity, long life cycles, low maintenance requirements and a reduced environmental impact [10].

Although the battery functionality strongly depends on the internal physics, the modelling at the scale of an energy system scale simplifies when only considering power flows.

The operational behaviour of a Battery Energy Storage System (BESS) depends mainly on the device's characteristics. First, the battery total capacity C^{BESS}, expressed in kWh, represents the size of the storage unit. To preserve the battery lifetime, it is common to introduce limits for the maximum and minimum state of energy, denoted respectively $\overline{E}^{BESS}$ and $\underline{E}^{BESS}$ in kWh. These constraints define the operational range within which the battery charges and discharges.

Additionally, limitations in power exchange must be specified. By defining $\overline{P}^{BESS}$ and $\underline{P}^{BESS}$, in kW, the charging and discharging power are bounded within physical limits. Therefore, the battery system State of Energy (SOE), e_t^{BESS}, charging power, $p_t^{BESS,ch}$, and discharging power, $p_t^{BESS,dch}$, change within these bounds, as shown in equation 3.46 to equation 3.48. It's important to define that the battery can only charge when not discharging. This is specified by the binary variable u_t^{BESS} in equation 3.49. This is computed through a non-linear constraint, as shown in equation 3.50 below. However, thanks to the binary nature of u_t^{BESS}, the problem can still be solved by the selected tools mentioned in section 3.3 despite the non-linearity.

$$\underline{E}^{BESS} \leq e_t^{BESS} \leq \overline{E}^{BESS} \tag{3.46}$$

$$0 \leq p_t^{BESS,ch} \leq \overline{P}^{BESS} \tag{3.47}$$

$$\underline{P}^{BESS} \leq p_t^{BESS,dch} \leq 0 \tag{3.48}$$

$$u_t^{BESS} = \begin{cases} 1 & \text{if BESS is charging} \\ 0 & \text{otherwise} \end{cases} \tag{3.49}$$

$$p_t^{BESS,ch} \cdot (1 - u_t^{BESS}) = p_t^{BESS,dch} \cdot u_t^{BESS} \tag{3.50}$$

The State of Energy (SOE) of the battery reflects the dynamic changes in stored energy across time. As a result, each time step is strictly dependent on the battery SOE at the time step before, and the difference is implemented by the power exchange to the energy system. This concept is illustrated in equation 3.51.

$$e_t^{BESS} = L^{BESS} \cdot e_{t-1}^{BESS} + (\eta^{BESS,ch} \cdot p_t^{BESS,ch} + \frac{1}{\eta^{BESS,dch}} \cdot p_t^{BESS,dch}) \cdot \delta t \tag{3.51}$$

Here, the terms L^{BESS}, $\eta^{BESS,ch}$ and $\eta^{BESS,dch}$ express the loss of energy in time and the charging and discharging efficiencies respectively. This is a complicated term that depends on the battery type and the State of Charge (SOC). However, for the scope of the project, this term can be neglected as in equation 3.52 [21].

$$e_t^{BESS} = e_{t-1}^{BESS} + (p_t^{BESS,ch} + p_t^{BESS,dch}) \cdot \delta t \tag{3.52}$$

As a result, the modelling of a BESS in the picture of an energy system can be resumed with equation 3.46 to equation 3.52.

3.4.4. Electric vehicle fleet

In recent years, electric vehicles have become one of the main points of focus for shifting the transportation sector to a more and more sustainable design. Among the different research that universities and companies are developing, residential car-sharing is the one that may have the greater benefit to the energy grid. The concept was initially designed to reduce the ownership of cars in cities and lower its expenses [43]. Nowadays, with the threat of climate change pushing for decarbonization, electric vehicles have taken over, changing thus also the whole concept of fueling the car. However, as well known, while a gasoline or diesel vehicle needs only a few minutes to completely fill the fuel tank, an electric counterpart may require hours to reach the charge for the same driving range. This is one of the crucial factors that make fuel vehicles still competitive.

When considering shared EVs, this issue becomes less significant. Thanks to the non-private ownership of the vehicle, customers can choose the car with the highest battery SOC at the moment they need it. This improves, from one side user satisfaction by having a shorter waiting time, and from the other side the charging process by extending the time of connection of each vehicle.

Recent studies have shown the high potential of shared EV as a tool to mitigate grid congestion [31]. In this section, the physical principles of EVs will be argued, focusing first on a general EV-grid connection to move then to the potential of V2G.

In energy terms, an electric vehicle can be easily represented by a union of a simple electric load and battery storage. First, an EV is characterized by a schedule and an electric demand, making it considerable as a non-critical load. Considering the vehicle s in the EV fleet $\mathcal{S}$, by the definition of an arrival time, T_s^{arr}, and a departure time, T_s^{dep}, a time slot of connection is defined. During this, the vehicle may or may not charge with a certain power, initialized as $p_{t,s}^{EV}$ and bounded by $\underline{P}_s^{EV}$ and $\overline{P}_s^{EV}$, all expressed in kW. This concept is mathematically shown in equation 3.53. Here, $\underline{P}_s^{EV}$ is usually set to zero, it is changed to a negative value in case V2G is implemented.

$$\begin{cases} \underline{P}_s^{EV} \leq p_{t,s}^{EV} \leq \overline{P}_s^{EV} & \text{if} \quad T_s^{arr} \leq t \leq T_s^{dep} \\ \\ p_{t,s}^{EV} = 0 & \text{otherwise} \end{cases} \tag{3.53}$$

At the same time, an EV can be considered as a battery able to store energy. As a result, a State of Energy (SOE), $e_{t,s}^{EV}$, in kWh, can be defined. As already discussed for the heating system and the BESS, the same physical principle of equation 3.26 and 3.52 can be applied to EVs as in equation 3.54.

$$\begin{cases} e_{t,s}^{EV} = L_s^{EV} \cdot e_{t-1,s}^{EV} + \eta_s^{EV} \cdot p_{t,s}^{EV} \cdot \delta t & \text{if} \quad p_{t,s}^{EV} \geq 0 \quad \text{(charging)} \\ e_{t,s}^{EV} = L_s^{EV} \cdot e_{t-1,s}^{EV} + \frac{1}{\eta_s^{EV}} \cdot p_{t,s}^{EV} \cdot \delta t & \text{if} \quad p_{t,s}^{EV} < 0 \quad \text{(discharging)} \end{cases} \tag{3.54}$$

The terms L_s^{EV} and η_s^{EV} are again introduced to express the battery losses. As discussed in the previous section, this term is set to one. As a result, the SOE expression can be merged into one as in equation 3.55 [21].

$$e_{t,s}^{EV} = e_{t-1,s}^{EV} + p_{t,s}^{EV} \cdot \delta t \tag{3.55}$$

In addition to equation 3.53 and equation 3.55, equation 3.56 allows expresses the charging behaviour of the general vehicle s.

$$\begin{cases} e_{t,s}^{EV} = 0 & \text{if} \quad t \leq T_s^{arr} \\ 0 \leq e_{t,s}^{EV} \leq \overline{E}_s^{EV} & \text{if} \quad T_s^{arr} < t \leq T_s^{dep} \\ e_{t,s}^{EV} = \overline{E}_s^{EV} \cdot \gamma_s^{EV} & \text{if} \quad t > T_s^{dep} \end{cases} \tag{3.56}$$

where the initial state of energy at the time of connection T_s^{arr} is set to zero while $\overline{E}_s^{EV}$ expresses the maximum energy of charge, or in other words 100% SOC.

It is important to mention that the SOE considered does not represent the real charging/discharging of the EV. Indeed, the variable $e_{t,s}^{EV}$ expresses the EV's battery behaviour only from the point of view of the charger and the energy system, able to detect changes only when the car is connected. In other words, when a vehicle connects, the charger registers only how much energy is needed to fully complete the car battery. As a result, for the scope of the model, other information about the vehicle is not needed.

Moreover, as expressed in equation 3.56, the maximum EV battery capacity $\overline{E}_s^{EV}$ is multiplied by the parameter γ_s^{EV}, which represents the final minimum SOC that vehicles need to reach. This is introduced in order to further increase flexibility in the system and make the charging boundaries a soft constraint. This variable is thus bounded as in equation 3.57. If, for instance, $\Gamma^{EV} = 0.7$, all vehicles will be charged at 70% minimum of the final state of charge.

$$\Gamma^{EV} \leq \gamma_s^{EV} \leq 1 \tag{3.57}$$

3.4.5. Energy system balance

Finally, the balancing of the system takes place. For every time step t, all electricity introduced in the energy system must be consumed by the loads. As discussed in this chapter, this can be resumed as in equation 3.58.

$$\sum_{p \in \mathcal{P}} p_{t,p}^{PV} - p_t^{BESS,dch} + p_t^{grid} = \sum_{s \in \mathcal{S}} p_{t,s}^{EV} + \sum_{h \in \mathcal{H}} p_{t,h}^{HP} + p_t^{BESS,ch} + \sum_{l \in \mathcal{L}} p_{t,l}^{el} \tag{3.58}$$

in which the power supply is expressed on the left-hand side while the power demand is on the right-hand side.

The parameter $p^{el}_{t,l}$ represents the electrical demand of load l at time t in kW. As a result, the power withdrawal from the grid at the generic time t can be defined as:

$$p^{grid}_t = \sum_{s \in \mathcal{S}} p^{EV}_{t,s} + \sum_{h \in \mathcal{H}} p^{HP}_{t,h} + p^{BESS,ch}_t + p^{BESS,dch}_t + \sum_{l \in \mathcal{L}} p^{el}_{t,l} - \sum_{p \in \mathcal{P}} p^{PV}_{t,p} \tag{3.59}$$

The energy system is designed to operate as an on-grid district-size system, characterized by one or multiple Points of Connection (POC). Each POC represents the device that connects the low-voltage energy feeder(s) of the energy system to the distribution grid. Accordingly, each of these must be constrained by a maximum power, expressed as $\overline{P}^{trafo}$ in kW, which defines the maximum technical or contracted limit of power withdrawal. This is expressed in equation 3.60. In the next chapter, consideration regarding this parameter is further argued.

$$p^{grid}_t \leq \overline{P}^{trafo} \tag{3.60}$$

3.5. Model of the energy system

In this chapter, the different resources integrated into the energy system were analyzed in theory and the respective models were argued. In the following section, the whole model design is summarized, showing the constraints and the objectives.

As shown along section 3.5, each DER integrated into the energy system can be modelled independently. However, these models must communicate with each other in order to describe the functioning of the full energy system. As a result, all defined constraints must be connected. In the list of equations below, the full base model constraints are gathered as mathematical expressions implemented in the *Python* code.

PV:

$$p^{PV}_{t,p} = G_{t,p} \cdot \eta^{panel}_p \cdot A^{panel}_p \cdot N^{panel}_p \quad \forall t \in \mathcal{T}, \forall p \in \mathcal{P} \tag{3.7}$$

Heating system:

$$COP_{t,h} \cdot p_{t,h}^{HP} = |q_{t,h}^{HP}| \quad \forall t \in \mathcal{T}, \forall h \in \mathcal{H} \tag{3.10}$$

$$0 \leq p_{t,h}^{HP} \leq \overline{P}_h^{HP} \quad \forall t \in \mathcal{T}, \forall h \in \mathcal{H} \tag{3.11}$$

$$q_{t,h}^{HP} = \dot{m} \cdot Cp_w \cdot (T_{t,h}^1 - T_{t,h}^4) \quad \forall t \in \mathcal{T}, \forall h \in \mathcal{H} \tag{3.12}$$

$$Q_{t,h}^d = \dot{m} \cdot Cp_w \cdot (T_{t,h}^2 - T_{t,h}^3) \quad \forall t \in \mathcal{T}, \forall h \in \mathcal{H} \tag{3.13}$$

$$Q_{t,h}^d = Q_{t,h}^{sh} + Q_{t,h}^{hw} - Q_{t,h}^{cool} \quad \forall t \in \mathcal{T}, \forall h \in \mathcal{H} \tag{3.14}$$

$$q_{t,h}^{12} = \dot{m} \cdot Cp_w \cdot (T_{t,h}^2 - T_{t,h}^1) \quad \forall t \in \mathcal{T}, \forall h \in \mathcal{H} \tag{3.20}$$

$$q_{t,h}^{34} = \dot{m} \cdot Cp_w \cdot (T_{t,h}^4 - T_{t,h}^3) \quad \forall t \in \mathcal{T}, \forall h \in \mathcal{H} \tag{3.21}$$

$$Q_{t,h}^d = q_{t,h}^{HP} + q_{t,h}^{12} + q_{t,h}^{34} \quad \forall t \in \mathcal{T}, \forall h \in \mathcal{H} \tag{3.24}$$

$$e_{t,h}^{PCM} = L_{t,h}^{PCM} \cdot e_{t-1,h}^{PCM} - (q_{t,h}^{12} + q_{t,h}^{34}) \cdot \delta t \quad \forall t \in \mathcal{T}, \forall h \in \mathcal{H} \tag{3.26}$$

$$e_{t,h}^{PCM} \leq E_h^L + (E_h^S - E_h^L) \cdot u_{t,h}^S + (\overline{E}_h^{PCM} - E_h^L) \cdot u_{t,h}^L \quad \forall t \in \mathcal{T}, \forall h \in \mathcal{H} \tag{3.28}$$

$$e_{t,h}^{PCM} \geq E_h^S + (E_h^L - E_h^S) \cdot u_{t,h}^L + (\underline{E}_h^{PCM} - E_h^S) \cdot u_{t,h}^S \quad \forall t \in \mathcal{T}, \forall h \in \mathcal{H} \tag{3.29}$$

$$u_{t,h}^S + u_{t,h}^L \leq 1 \quad \forall t \in \mathcal{T}, \forall h \in \mathcal{H} \tag{3.30}$$

$$T_{t,h}^{PCM} = \frac{\left(\frac{3600 \cdot e_{t,h}^{PCM}}{m_h^{PCM}} - h_h^{PCM} \cdot u_{t,h}^L\right)}{c_h^{PCM}} \cdot (u_{t,h}^S + u_{t,h}^L) + T_h^{melt} \cdot (1 - u_{t,h}^S - u_{t,h}^L) \quad \forall t \in \mathcal{T}, \forall h \in \mathcal{H} \tag{3.31}$$

$$T_{t,h}^1 \leq T_{t,h}^{PCM} + Q_1 \cdot u_{t,h}^{12} \quad \forall t \in \mathcal{T}, \forall h \in \mathcal{H} \tag{3.33}$$

$$T_{t,h}^1 \geq T_{t,h}^{PCM} - Q_2 \cdot (1 - u_{t,h}^{12}) \quad \forall t \in \mathcal{T}, \forall h \in \mathcal{H} \tag{3.34}$$

$$T_{t,h}^2 \geq T_{t,h}^{PCM} \cdot u_{t,h}^{12} + T_{t,h}^1 \cdot (1 - u_{t,h}^{12}) \quad \forall t \in \mathcal{T}, \forall h \in \mathcal{H} \tag{3.35}$$

$$T_{t,h}^2 \leq T_{t,h}^1 \cdot u_{t,h}^{12} + T_{t,h}^{PCM} \cdot (1 - u_{t,h}^{12}) \quad \forall t \in \mathcal{T}, \forall h \in \mathcal{H} \tag{3.36}$$

$$T_{t,h}^3 \leq T_{t,h}^{PCM} + Q_1 \cdot u_{t,h}^{34} \quad \forall t \in \mathcal{T}, \forall h \in \mathcal{H} \tag{3.37}$$

$$T_{t,h}^3 \geq T_{t,h}^{PCM} - Q_2 \cdot (1 - u_{t,h}^{34}) \quad \forall t \in \mathcal{T}, \forall h \in \mathcal{H} \tag{3.38}$$

$$T_{t,h}^4 \geq T_{t,h}^{PCM} \cdot u_{t,h}^{34} + T_{t,h}^3 \cdot (1 - u_{t,h}^{34}) \quad \forall t \in \mathcal{T}, \forall h \in \mathcal{H} \tag{3.39}$$

$$T_{t,h}^4 \leq T_{t,h}^4 \cdot u_{t,h}^{34} + T_{t,h}^{PCM} \cdot (1 - u_{t,h}^{34}) \quad \forall t \in \mathcal{T}, \forall h \in \mathcal{H} \tag{3.40}$$

$$\underline{T}_h \leq T_{t,h}^1 \leq \overline{T}_h \quad \forall t \in \mathcal{T}, \forall h \in \mathcal{H} \tag{3.41}$$

$$\underline{T}_h \leq T_{t,h}^2 \leq \overline{T}_h \quad \forall t \in \mathcal{T}, \forall h \in \mathcal{H} \tag{3.42}$$

$$\underline{T}_h \leq T_{t,h}^3 \leq \overline{T}_h \quad \forall t \in \mathcal{T}, \forall h \in \mathcal{H} \tag{3.43}$$

$$\underline{T}_h \leq T_{t,h}^4 \leq \overline{T}_h \quad \forall t \in \mathcal{T}, \forall h \in \mathcal{H} \tag{3.44}$$

$$\underline{T}_h \leq T_{t,h}^{PCM} \leq \overline{T}_h \quad \forall t \in \mathcal{T}, \forall h \in \mathcal{H} \tag{3.45}$$

BESS:

$$\underline{E}^{BESS} \leq e_t^{BESS} \leq \overline{E}^{BESS} \quad \forall t \in \mathcal{T} \tag{3.46}$$

$$0 \leq p_t^{BESS,ch} \leq \overline{P}^{BESS} \quad \forall t \in \mathcal{T} \tag{3.47}$$

$$\underline{P}^{BESS} \leq p_t^{BESS,dch} \leq 0 \quad \forall t \in \mathcal{T} \tag{3.48}$$

$$p_t^{BESS,ch} \cdot (1 - u_t^{BESS}) = p_t^{BESS,dch} \cdot u_t^{BESS} \quad \forall t \in \mathcal{T} \tag{3.50}$$

$$e_t^{BESS} = e_{t-1}^{BESS} + (p_t^{BESS,ch} + p_t^{BESS,dch}) \cdot \delta t \quad \forall t \in \mathcal{T} \tag{3.52}$$

EV fleet:

$$p_{t,s}^{EV} = 0 \quad \text{for } t < T_s^{arr} \text{ and } t > T_s^{dep} \ , \forall s \in \mathcal{S} \tag{3.53}$$

$$\underline{P}_s^{EV} \leq p_{t,s}^{EV} \leq \overline{P}_s^{EV} \quad \text{for} \quad T_s^{arr} \leq t \leq T_s^{dep} \ , \forall s \in \mathcal{S} \tag{3.53}$$

$$e_{t,s}^{EV} = e_{t-1,s}^{EV} + p_{t,s}^{EV} \cdot \delta t \quad \text{for} \quad T^{arr} < t < T^{dep} \ , \forall s \in \mathcal{S} \tag{3.55}$$

$$e_{t,s}^{EV} = 0 \quad \text{for} \quad t \leq T_s^{arr} \ , \forall s \in \mathcal{S} \tag{3.56}$$

$$0 \leq e_{t,s}^{EV} \leq \overline{E}_s^{EV} \quad \text{for} \quad T_s^{arr} < t \leq T_s^{dep} \ , \forall s \in \mathcal{S} \tag{3.56}$$

$$e_{t,s}^{EV} = \overline{E}_s^{EV} \cdot \gamma^{EV} \quad \text{for} \quad t > T^{dep} \ , \forall s \in \mathcal{S} \tag{3.56}$$

$$\Gamma^{EV} \leq \gamma_S^{EV} \leq 1 \quad \forall s \in \mathcal{S} \tag{3.57}$$

Balancing:

$$p_t^{grid} = \sum_{s \in \mathcal{S}} p_{t,s}^{EV} + \sum_{h \in \mathcal{H}} p_{t,h}^{HP} + p_t^{BESS,ch} + p_t^{BESS,dch} + \sum_{l \in \mathcal{L}} p_{t,l}^{el} - \sum_{p \in \mathcal{P}} p_{t,p}^{PV} \quad \forall t \in \mathcal{T} \tag{3.59}$$

$$p_t^{grid} \leq \overline{P}^{trafo} \quad \forall t \in \mathcal{T} \tag{3.60}$$

On top of the above-listed constraints, an extra constraint is defined:

$$p^{peak} \geq p_t^{grid} \quad \forall t \in \mathcal{T}^{peak} \tag{3.61}$$

Depending on the definition of the peak hour set, $\mathcal{T}^{peak}$, this additional constraint specifies the time period in which peak power reduction is performed, discussed further in the next chapter. Finally, the optimization problem is characterized by an objective function. This is expressed below.

$$\text{O.F.} \quad \min[\, p^{peak} - \varepsilon \cdot (\sum_{s \in \mathcal{S}} \gamma_s^{EV} \cdot \overline{E}_s^{EV} + \sum_{s \in \mathcal{S}} \sum_{t \in \mathcal{T}} e_{t,s}^{EV} - \sum_{t \in \mathcal{T}} (SOE_{goal}^{BESS} - e_t^{BESS})^2 - \sum_{h \in \mathcal{H}} \sum_{t \in \mathcal{T}} p_{t,h}^{HP}) \,] \tag{3.62}$$

Therefore, the problem is defined as multi-objective optimization, implemented as a Mixed-Integer Quadratic Programming (MIQP) and solved through a weighted-sum method. This is selected thanks to its simplicity and due to the bi-objective nature of the problem. Indeed, besides the main objective of peak power reduction, p^{peak}, secondary objectives must be included in order to obtain unique optimal solutions. To compute this, the weight parameter ε is introduced in front of the secondary aims, making them mathematically less important in the optimization objective. This is set to 10^{-6} in order to differentiate primary to secondary objectives. As expressed in equation 4.5, four secondary goals are introduce:

- **Maximized final EV SOE**. This is done through the variable γ_s^{EV}, which represents the final minimum state of charge and is bounded as equation 3.57;
- **EV fast charging**. By maximizing the area under the SOE curve, each vehicle aims to charge the fastest possible;
- **Minimized usage of the BESS**. The battery storage is constrained to be used only if necessary for the peak reduction. By minimizing the difference between the variable e_t^{BESS} and a set state of energy, SOE_{goal}^{BESS}, the BESS will try to operate as close as possible to a defined SOC. For simplicity, this set parameter is defined as 70% of the total battery capacity. This is selected to have a large margin of discharge and a smaller freedom of charge, computed to reduce possible charging power spikes right before the peak hours;
- **Minimized heat pumps energy usage**, done by minimizing the area under the curve of $p_{t,h}^{HP}$ over time for each heating network. This is expected to maximize the saving of energy and thus reduce the losses of the heating system.

4

Description of the case study

In order to obtain concrete results for real implementations, a specific energy system has been studied in the research. In this chapter, section 4.1 briefly describes the Energy Community of the case study, showing the technologies involved and adding information to what is modelled in chapter 3. Then, in section 4.2, all assumptions and reasoning followed during data acquisition are argued. Finally, section 4.3 argue the different system designs in order to address grid congestion issues within various scenarios according to the literature.

4.1. Case Study Description

The energy system of reference is a new residential area currently under construction in the city of Utrecht, the Netherlands. It consists of a pilot project for a new era of sustainable urban construction, including buildings with high energy classes.

The project's energy system integrates multiple Distributed Energy Resources (DERs) and technologies to meet the diverse energy demands. The primary sources of supply are the city electricity grid and photovoltaic (PV) panels mounted on the rooftops of the buildings. The generated electricity is then distributed to the various end-users, including residential houses, commercial spaces, and electric vehicle chargers. To promote sustainable transportation and increase the system's flexibility, EVs are part of a shared fleet available to the residents. In addition, a large part of the electrical flow is directed to a heating room where Ground-Source Heat Pumps (GSHPs) are installed. These are responsible for meeting the heating, cooling and hot water demands of houses and community spaces through separate heating networks. Finally, the system design considers a possible integration of battery storage solutions, in order to again increase flexibility and assist congestion management. A general scheme of the energy system considered in the research is shown in figure 4.1.

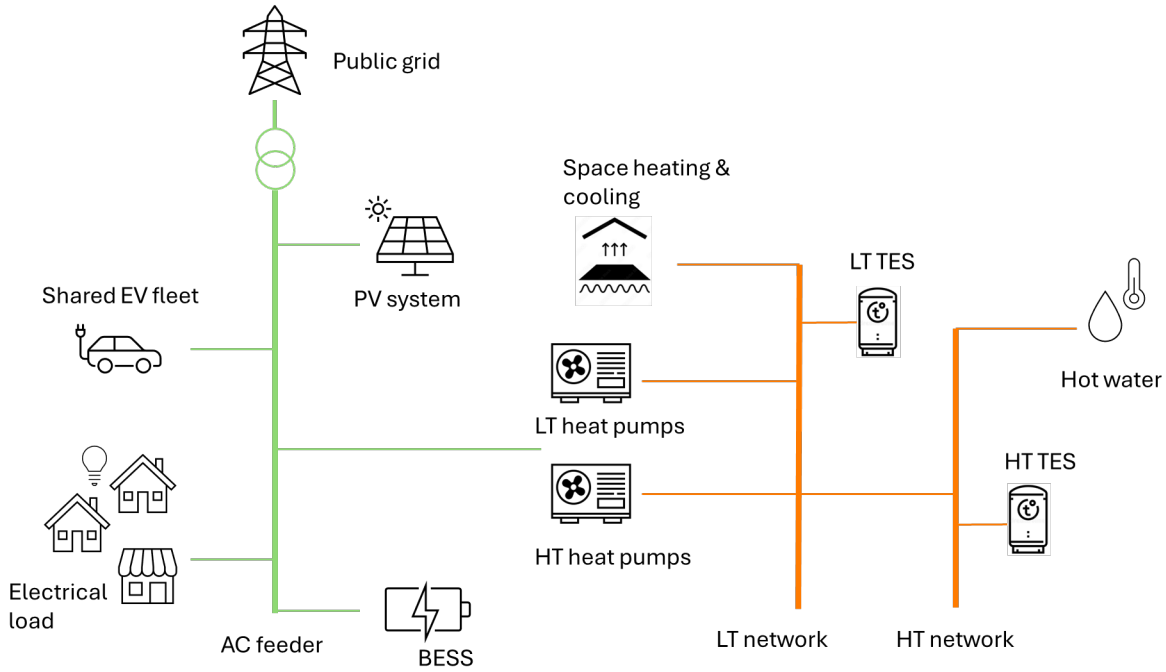

Figure 4.1: Scheme of the energy system in study

For what concerns the heating system, a 4-pipe change-over design has been implemented for the case study. It consists of two separate pipe networks that transport hot water at different temperatures. The High-Temperature (HT) network is responsible for demands that require high supply temperatures, such as hot water, while the Low-Temperature (LT) network is in charge of both space heating and cooling.

Thermal losses during hot water transport are proportional to the temperature difference between the water and the surrounding environment. Therefore, to increase system efficiency, the change-over mechanism is introduced in the LT network, allowing the system to provide low-temperature heating and high-temperature cooling. Each network operates with dedicated heat pumps, making the system more robust and reliable.

The heating system can then operate in two different modes:

- **Heating mode**. During cold seasons, when no space cooling is demanded and outdoor temperature is below 15°C[1], the system provides space heating through the LT network while hot water demand is met through the HT water flow. In case of failure of low-temperature HPs, the HT network can take over to provide the remaining space heating.
- **Cooling mode**. During warmer periods, when cooling is required and outdoor temperature exceeds 15°C[1] the system exploits the change-over design and the flow of water is reversed in the Low-Temperature (LT) network. This is thus responsible for meeting the space cooling demand. In parallel, space heating and hot water demands are fully met through the HT network. Since the outdoor temperature is generally higher in these cases, thermal losses experienced with HT are reduced compared to the winter months.

For simplicity, no interaction is considered between the two heating networks. This concept is visualized in figure 4.2 below.

[1]Limit temperature is set to 15°C for the case study, but it can be easily re-adapted.

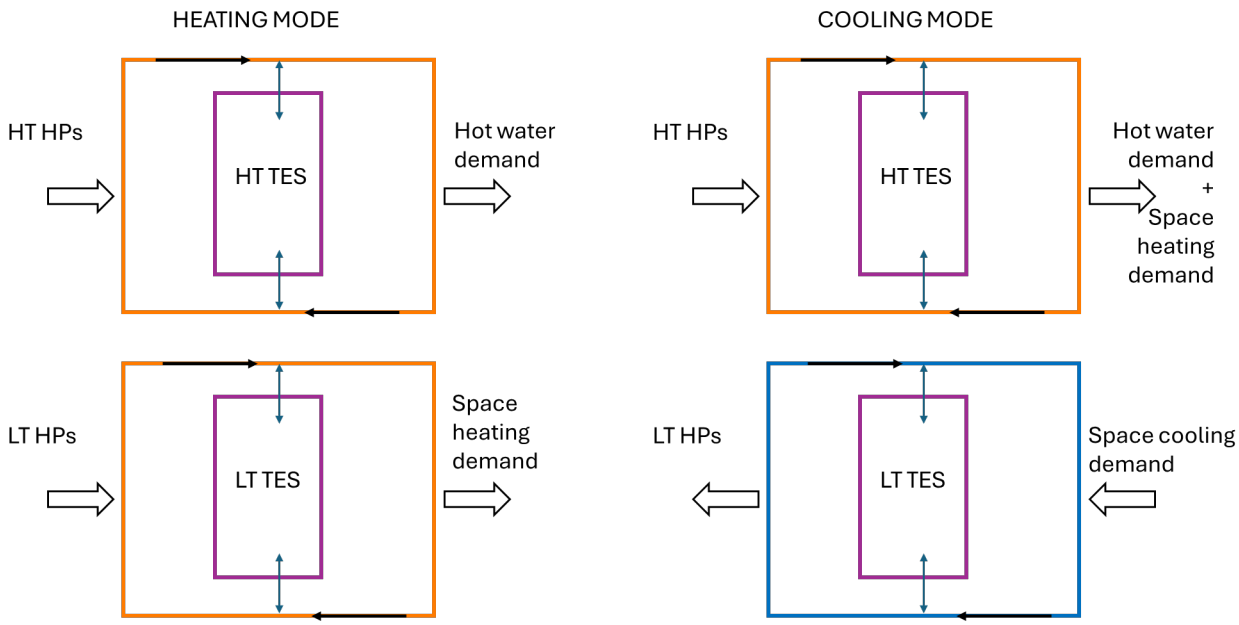

Figure 4.2: 4-pipes change-over heating system

4.2. Data Description

This section describes the data collection process arguing and motivating assumptions in order to provide a clear view of the energy model implemented.

As argued in subsection 3.4.1, the photovoltaic system is modelled based on historical data of irradiance and relative position of PV modules and the sun. Two types of data can be distinguished here: weather data, describing the variation of irradiance and sun position, and PV panel mounting characteristics.

For what concerns the weather data, two sources were found and described in table 4.1

Reference	Database	Year	Time interval	Values	Computation
Pfenninger et al. [62]	MERRA-2 (Global)	2019	Hourly	• PV power output* • DHI • DIF • Air temperature at 2 meters elevation	Ground-level global irradiance and top-of-atmosphere irradiance [62]
Pfeifroth et al. [61]	PVGIS-SARAH2	2020	Hourly	• PV power output* • GHI • DHI • DIF • Sun elevation • Air temperature at 2 meters elevation • Sun azimuth	Satellite-derived irradiance [62]

*for 1 kWp.

Table 4.1: References of weather data.

Thanks to its longer timespan and more accurate data, the database *PVGIS-SARAH2* was chosen [62]. In addition, the reference website provides a tool capable of effectively estimating the power output of a PV system, given the tilt and azimuth angles of installations and estimated system losses. For the solar system in the case study, data regarding the panel's characteristics and mounting was implemented with information given by the owner of the designed system. The module used in the whole system is a JAM72S20 470/MR half-cell, monocrystalline c-Si module of 470 Wp power rated.

For correctly defining the mounting parameters, different combinations of tilt and azimuth[2] were investigated and the total annual energy yield of data retrieved from the database was compared to the one provided by the installer. The correct combination is found when the difference is negligible. The selected mounting parameters are summarized below in table 4.2.

Parameter	Building 00	Building 01	Building 05	Building 09
Tilt angle [°]	20	20	20	20
Azimuth [°]	-40	-30	-40	-40

Table 4.2: Mounting parameters of PV systems.

Another set of data necessary to simulate the energy system's functioning is the load demand. As mentioned in section 4.1, the EC in analysis consists of an agglomerate of buildings in an urban environment, which include dwellings, commercial activities and common areas. Based on the information provided by the system's project, the energy demand is divided into two categories: private households and commercial spaces, each characterized by electrical, space heating, space cooling and hot water demands.

The energy system used for the research considers 1'565 private households distributed in six buildings, all connected to the energy system

The electrical load is expected to have an important impact on the final results and, therefore, the accuracy of data is a crucial parameter. To have an hourly profile similar to what is expected in real systems, the total electrical profile must be obtained with the superposition of single houses profiles and preserve the general daily, weekly, seasonal and yearly patterns. To achieve this, five different household load profiles provided in Quesada et al. [63] are used. This is selected since five different types of dwellings are designed for the case study. This dataset provides the hourly measured electricity demand of more than 20'000 Spanish buildings from 2014 to 2022. Due to the geographical difference, the data is adapted to the case of The Netherlands by the coefficient $c_{electric}$ as explained below:

$$c_{electric} = \frac{E_y}{\sum_{t \in YEAR} \quad e_{t,l}^{data}} \quad , \tag{4.1}$$

where $e_{t,l}^{data}$ is the energy usage of house l at time t in kWh and E_y is the annual average energy yield of a general household in The Netherlands. According to Statistics Netherlands [1], this can be considered 2'860 kWh/yr. This number was measured for the area of Zoetermeer in 2022 and can be generalized to similar living spaces in the country [46]. Therefore, the coefficient $c_{electric}$ is used to scale the electrical profile of each household.

The same procedure is followed for the commercial space electrical profile. A general commercial activity electrical profile is implemented and scaled from Quesada et al. [63]. The designer of the residential area in the study includes a supermarket and other commercial spaces still undefined, for a total area of 1'292 m^2. A study conducted by KTH [65] considers an average yearly electricity consumption of 240 $\frac{kWh}{yr\,m^2}$ for supermarkets, resulting in a total yearly yield of 310'000 kWh/yr. Table 4.3 below resumes the scaling coefficients computed for each house type used.

[2]Basing on the technical drawing provided, azimuth was limited to a range between -10° and -60°

Load type	Scaling coefficient $c_{electric}$
House 1	0.808
House 2	1.076
House 3	2.694
House 4	2.386
House 5	1.285
Commercial spaces	30.060

Table 4.3: Scaling coefficient $c_{electric}$ for electrical load obtained through equation 4.1, in $\frac{kWh_{model}}{kWh_{reference}}$.

Implementation of thermal demands are computed similarly. The data used is found in Ruhnau et al. [67, 68], which provides hourly space heating and hot water demand profiles for a general residential house and commercial space in The Netherlands from 2008 to 2022. In addition, the database provides the Coefficient of Performance (COP) of GSHPs for the same location and timespan, which is then used as discussed in subsection 3.4.2.

To fit the profiles to the case of study, the scaling factor $c_{heating}$ is defined as:

$$c_{heating} = \frac{Q_l^{rated}}{\max_t(Q_{t,l}^{data})} \tag{4.2}$$

in which Q_l^{rated} is the maximum power per house given by the local heating company, and $Q_{t,l}^{data}$ is the maximum heating power registered in the dataset, both in $kW/house$. Therefore, the scaling coefficient $c_{heating}$ is used to obtain the correct profile of space heating and hot water for houses and commercial spaces. These are resumed in table 4.4.

Load type	Scaling coefficient $c_{heating}$
Houses space heating	4.424
Houses hot water	5.609
Houses space cooling	$1.057 \cdot 10^{-4}$
Commercial spaces space heating	0.254
Commercial spaces hot water	0.309
Commercial spaces space cooling	0.056

Table 4.4: Scaling coefficient $c_{heating}$ for heating loads obtained through equation 4.2, in $\frac{kW_{model}}{kW_{reference}}$.

For what concerns space cooling, the used data refers to Mauree et al. [48], which provides demand profiles adapted for the next decade based on records and climate change models for a neighbour energy system. This dataset was chosen in order to obtain reliable results for the upcoming years. Since the energy community in the analysis is still in the construction phase and aims to be an example to future sustainable neighbourhoods, this assumption is valid considering the fast growth of cooling demand predicted in the next years [38]. Therefore, the same procedure of equation 4.2 is followed to determine the cooling scale coefficient, as shown in table 4.4.

The flexibility unit in the heating network is introduced by the Thermal Energy Storage (TES) device. Thanks to its higher efficiency, reliability and controllability, phase-change material has been included in the base system design in two different units, one for each pipe network. As explained in subsection 3.4.2, every PCM TES is characterized by fixed parameters depending on the storage dimension and composite used. Due to a lack of specific information from the system design, general paraffin PCMs are used for the thermal storage units. This choice is related to the many chemical advantages of organic composites over other types, and the relatively cheap cost of paraffin [86]. In order to maximally exploit the bi-phase property of the paraffin, a closer look is given to the temperature constraints of the heating system. According to the information available for the case study, the low-temperature network is limited to delivering water at a temperature between 30°C and 40°C. As a result, the PCM chosen is the RT35HC , with melting temperature T_h^{melt} of 35°C [66]. Similarly, since the high-temperature network must provide hot water at temperatures higher than 58°C, the paraffin RT64HC is selected, with melting temperature of 64°C [66]. Parameters are defined below in table 4.5.

The design variable investigated in this research is the size of the PCM storage, which is determined by the capacity of the composite in use and the time period of design. Following the design procedure of Pans et al. [57], given the specified maximum and minimum temperatures of the heating system, defined as 80°C and 10°C respectively, the total energy capacity per unit of mass results in 0.109 kWh/kg, computed through equation 4.3.

$$\overline{E}^{PCM} = \frac{\overline{T} \cdot c_h^{PCM} + h_h^{PCM}}{3600} - \frac{\underline{T} \cdot c_h^{PCM}}{3600} \tag{4.3}$$

Considering then the heating and cooling demands described before, the peak values registered by the system are 4'389 thermal kW. However, these numbers refer to the worst case in which the HPs cannot be run for the whole selected time period and the demand is fixed to the maximum. Hence, the design decisions for the TES are conservative.

According to the specification given from the current design, the TES has a defined capacity $\overline{E}^{heating}$ of about 1'000 kWh in the base design. As a result, the PCM mass is set to 9'174 kg . Considering a density of 880 kg/m^3, the total volume occupied by a single thermal buffer is about 10.4 m^3 , which corresponds to a 2.2x2.2x2.2 tank.

$$m_h^{PCM} = \frac{\overline{E}^{heating}}{\overline{E}^{PCM}} \tag{4.4}$$

Parameter	Low-temperature TES	High-temperature TES
Specific heat [$\frac{kJ}{kgK}$]	2	2
Latent heat [$\frac{kJ}{kg}$]	240	250
Melting temperature [°C]	35	64
Capacity [kWh]	1'000	1'000
Density [kg/m^3]	880	880

Table 4.5: Properties of the phase-change material (PCM) thermal energy storage (TES) used in the analysis. Reference: [66].

Finally, the parameter $L_{t,h}^{PCM}$ represents the thermal losses of the TES in each time step. Following the thermal storage described in Pans et al. [57], the PCM buffers can be designed under the conservative assumption of 0.95 constant thermal efficiencies for the size mentioned above, meaning a thermal loss of about 50 kWh each time step for the selected size.

As discussed in section 4.1, the case of study's energy system considers possible the installation of a battery storage energy system in the energy community. The integration of such technology is expected to have a strong impact on the final results, and therefore, data must be chosen thoroughly. On a residential neighbourhood level, Pasqui et al. [58] argue that BESS design can go up to 1.5 $kWh/house$ for European dwellings. Considering an annual energy consumption of 2'860 kWh per house, the total EC residential load requires 12'364 kWh per day. Since the TES was designed with a capacity of 1'000 kWh, able to cover about one hour of the average total heating demand, the initial size of BESS analyzed aims to have comparable results of the thermal counterpart, hence, 500 kWh.

Furthermore, besides the battery capacity, other key parameters are the maximum and minimum power of charge-discharge, the so-called C-rate, and the maximum and minimum SOC allowed for preserving the device lifetime. The first is varied from 0.5 to 1, meaning that the BESS can fully discharge 50% and 100% in an hour respectively. While a lower C-rate increases the battery efficiency of operation and reliability, peak reduction can be more easily achieved by a higher value of discharge [25]. Furthermore, the state of charge range is defined to be between 15% and 85% in order to preserve the battery efficiency throughout time [58]. As a result, the battery parameters will be chosen as described in table 4.6.

Parameter	Value
Battery capacity $[kWh]$	500
Maximum SOC [%]	85
Minimum SOC [%]	15
C-rate [%]	0.5

Table 4.6: Parameters of the battery energy storage system (BESS) used in the analysis.

Among the many innovations introduced in the energy system in analysis, flexibility is further increased thanks to the shared EV fleet designed for the neighbourhood. The data used is a confidential collection of records for shared EVs in the Netherlands. It provides the following parameters:

- EV charging volume;
- Time of arrival;
- Time of departure;

It's important to mention that the EV charging volume is measured relatively to the car SOC at the time of connection. In other words, when the EV connects at T_s^{arr}, the charger registers as charging volume the difference between the maximum battery capacity of the vehicle and the initial state of charge. As a result, the SOE profile does not express the whole EV range, but only what the charge is able to read. To reconstruct the full SOC behaviour of each EV, further data is needed. However, this goes out of the scope of the project and only considerations will be made in the results discussion.

Moreover, for what concerns the charger size, a standard level-2 11 kW bi-directional charger is chosen. This allows moderately fast charging (on average 4-6 hours) of the EV and makes it possible to introduce vehicles-to-grid scenarios [41].

Finally, the energy system is connected to the public grid through medium-voltage transformers, with a technical maximum power of withdrawal defined by the transformer type and the contract with the distribution operator. Following the directives of the current system design, one grid connection is planned for each building of the energy community. Hence, a 1 MW point of connection per building is defined, for a total of 6 MW. This assumption can be adjusted according to what the DSO allows. However, for the scope of this project, the maximum power available from the grid, which will be in any case reduced during peak hours, is considered to not affect the congestion management study. Furthermore, the energy system has been designed to be able to ideally operate without any congestion management mechanism. As a result, the transformer limit is initialized high enough to provide feasible solutions to the research.

4.3. Grid Connection Agreements: cases description

The literature analyzed in chapter 1 gave an overview of the existing congestion management mechanisms and frameworks usually applied to energy communities affected by network congestion problems and to projects requesting a new connection. Recalling the details of the case study, the energy system considered falls into this latter category. As a result, given the recent updates on how the Dutch actors are planning to overcome the problem of new connection capacity, we aim to integrate the literature with the results of this research.

To recap, the potential new mechanisms offered in the recently published Draft Decision ATR facilitate new connections if the requesting party can adapt to certain characteristics. By selecting a Time-based Transmission Right (TTR) contract, transmission is guaranteed only during the off-peak hours defined the day ahead. Despite the advantage of having a significant discount, the uncertainties related to this flexible agreement are plenty and difficult to predict.

Conversely, by selecting a Time-Block-based Transmission Right (TBTR) contract, power withdrawal is not guaranteed during predefined periods agreed with the DSO. As a result, the daily uncertainty is relieved in this case.

With a Non-Firm ATO (NFA) contract, instead, the connected party must be able to operate fully off-grid during peak hours, since transmission can be interrupted without prior notice.

Finally, a Capacity Reduction Contract (CBC) agreement invites the connected party to reduce its consumption during peak hours with an economic benefit per kW reduced. However, it requires a normal Connection and Transmission Agreement (CTA) to be applied.

These transmission agreements hardly apply to residential loads, mainly due to the many critical loads that cannot be easily shed. TTR, for instance, is so far applicable only for high-voltage connections, and therefore cannot be considered in an urban environment. The TBTR instead, facilitate the primary connection but requires the system to be able to operate fully off-grid in case no capacity is available. An extended version is the NFA, which predictability is even more challenging. Hence, these contracts appear more inviting for industrial areas or businesses that can easily shift their consumption according to the DSO requirements. However, this problem can be overcome if an initial and reduced CTA is established and a flexible contract is signed for the remaining required capacity. Another option that may be attractive for urban projects is the CBC agreement. The implementation of such a mechanism, though, requires the agreement on a normal full-capacity CTA first, which is currently of short availability. As a result, in this research, we aim to show how the system flexibility can aid the EC to sign the CTA exploiting the advantages introduced by the CBC, TBTR and NFA mechanisms.

Scenario 1: ***no flattening***

Considering the case study's energy system as designed now, the process of obtaining a connection is expected to be challenging and long. To evaluate the improvements proposed in this research, a base case scenario is introduced. This simulates the energy system's current design without any congestion management mechanism implemented. It is used for pure comparison to show the advantages of the other cases. Therefore, it is expected to provide the worst result in terms of the research goal.

In order to set the optimization problem correctly, the base case aims to operate in a hypothetical case, for which EVs are charged as fast as possible and the energy use of the heating system is minimized. Furthermore, leaving degrees of freedom to the system easily leads to a non-unique solution, meaning that the model may return different results every time. This issue is resolved through the secondary objectives of EV fast charging and HP energy saving, as previously discussed in section 3.5.

It is thus crucial to integrate further information to obtain a single-solution optimization problem.

To explore the potential of the energy system flexibility, different scenarios are introduced:

Scenario 2: ***Day-long curve flattening***

As mentioned, the first step is to obtain a Capacity Connection Agreement (CTA) with the DSO, which is sized on the maximum estimated peak power. The lower its value the cheaper and the easier the agreement is to obtain. To address this, the first objective is to reduce the general daily peak power. This is explored in scenario 2, which, as the name suggests, aims to flatten the daily grid power withdrawal curve to facilitate getting the CTA. Referring to the model described in the previous chapter, the peak hours are then defined as $\mathcal{T}^{peak} = [0, 24]$.

Scenario 3: ***Morning peak hours***

In order to assist congestion management and possibly implement the TBTR or CBC contracts mentioned, grid power withdrawal is then to be minimized during the expected peak hours. Therefore, the second case narrows the peak reduction to the sole morning peak window, set as $\mathcal{T}^{peak} = [8, 12]$.

Scenario 4: ***Evening peak hours***

Accordingly, the solely evening peak power reduction is analyzed in the next scenario. Here, the peak hours are defined as $\mathcal{T}^{peak} = [18, 22]$.

Scenario 5: ***Morning and evening peak hours***

Finally, in urban areas, it is likely that grid congestion occurs both in the morning and in the evening. This case aims to explore how the system can adapt to a double peak hours window, defined as $\mathcal{T}^{peak} = [8, 12] \cup [18, 22]$.

In order to achieve these objectives, the flexibility of the energy system must be exploited. Therefore, five different designs were identified in order to explore the potential of each integrated DER.

4.3.1. Base case: no peak reduction

The base case scenario considers the current energy system without any congestion management approach implemented. Therefore, the objective function aims to optimise the energy system's functioning as in equation 4.5 below.

$$\text{O.F.} \quad \min[\, -\varepsilon \cdot (\sum_{s\in\mathcal{S}} \sum_{t\in\mathcal{T}} e^{EV}_{t,s} - \sum_{h\in\mathcal{H}} \sum_{t\in\mathcal{T}} p^{HP}_{t,h})\,] \tag{4.5}$$

It is important to mention that the minimum final EV SOC and the BESS secondary objectives can be neglected since no batteries are included and γ^{EV}_s is constrained to 1.

4.3.2. Current system case: simple peak reduction

The first system design that will be compared to the hypothetical solution shown in the base case considers the simple integration of a demand-side management mechanism. Therefore, the flexibility of the EC as it is designed now is investigated throughout the different scenarios. In this case, the objective function becomes:

$$\text{O.F.} \quad \min[\, p^{peak} - \varepsilon \cdot (\sum_{s\in\mathcal{S}} \sum_{t\in\mathcal{T}} e^{EV}_{t,s} - \sum_{h\in\mathcal{H}} \sum_{t\in\mathcal{T}} p^{HP}_{t,h})\,] \tag{4.6}$$

Besides the implementation of a grid congestion mechanism, the system design may not be sufficiently flexible to withstand the regulations forced by the DSO during peak hours. For this reason, the next cases explore technical changes in the energy system to observe the impact of these on the goal of congestion management.

4.3.3. Moderate EV charging case

The first design exploits the shared fleet of electric vehicles, aiming to increase their flexibility by softening the final charging constraint. Thanks to their non-private nature, consumers in the energy community are expected to prefer vehicles with higher SOC at the booking time. For this reason, the constraint of the final state of charge γ^{EV}_s is set free within 70-100%, exploring how decisive this constraint is on the final results (Equation 4.8). As a result, the objective function follows the expression:

$$\text{O.F.} \quad \min[\, p^{peak} - \varepsilon \cdot (\sum_{s\in\mathcal{S}} \gamma^{EV}_s \cdot \overline{E}^{EV}_s + \sum_{s\in\mathcal{S}} \sum_{t\in\mathcal{T}} e^{EV}_{t,s} - \sum_{h\in\mathcal{H}} \sum_{t\in\mathcal{T}} p^{HP}_{t,h})\,] \tag{4.7}$$

$$\Gamma^{EV}_s = 70\% \tag{4.8}$$

4.3.4. V2G case: integration of vehicle-to-grid

The EC in analysis is expected to become fully inaugurated by the end of 2024 and act as an example to future urban construction areas. Hence, innovative technologies are expected to be tested and integrated into the system, first of all, vehicle-to-grid. This design considers the possible future case for which all EV chargers can operate in a bi-directional manner, allowing the car to behave like a battery. It's important to mention that each vehicle is still subjected to the constraint of full charge by the time of departure. As a result, no relevant negative result is expected compared to the current system design.

In this case, the objective function is once again the one expressed in equation 4.6. The only difference concerns the charging power, $p^{EV}_{t,s}$, which can now be both positive and negative (meaning grid feeding). Hence, the lower bound $\underline{P}^{EV}_s$ of equation 3.53 is now set as negative $\overline{P}^{EV}_s$:

$$\underline{P}^{EV}_s = -\overline{P}^{EV}_s \tag{4.9}$$

4.3.5. TES case: increased size of the thermal storage

Another flexible technology included in the basic system design is Thermal Energy Storage (TES). This design considers the possibility of increasing the capacity of such a device, investigating how this affects the other resources in the system and assisting the primary goal of peak reduction.

In other words, the system design is the same as in the *current system* case, except for a larger size thermal buffer, now set to 50'000 kg, or 5'450 kWh. As a result, the objective function is again as shown in equation 4.6.

4.3.6. BESS case: integration of a battery storage system

Finally, the last design considered in this research includes the installation of battery storage. For the scope of this research, this device is introduced and analyzed with the only scope of assisting grid congestion management. Its characteristics are then set to 500 kWh and 0.5 of C-rate. Although BESS results in an optimal tool for normal rescheduling, the goal is again set for reducing power during peak hours. As a result, the research output doesn't exclude that there may be a more optimal operation method for this device. To avoid this, another secondary objective is included in the objective function, as shown below in equation 4.10. By minimizing the quadratic difference between the BESS SOC and its set goal, the usage of the battery is minimized and a unique solution can be computed.

$$\text{O.F.} \quad \min[\, p^{peak} - \varepsilon \cdot (\sum_{s \in \mathcal{S}} \sum_{t \in \mathcal{T}} e^{EV}_{t,s} - \sum_{h \in \mathcal{H}} \sum_{t \in \mathcal{T}} p^{HP}_{t,h} - \sum_{t \in \mathcal{T}} (SOE^{BESS}_{goal} - e^{BESS}_{t})^2)\,] \tag{4.10}$$

To conclude, in order to make more clear what each design explores, table 4.7 below summarises the different cases while table 4.8 resumes all the scenarios characteristics.

Case name	Fixed final SOC_{EV}	V2G	Increased TES	Integration of BESS	Peak reduction
Base case	✓	x	x	x	x
Current system	✓	x	x	x	✓
Moderate EV charging	x	x	x	x	✓
V2G	✓	✓	x	x	✓
TES	✓	x	✓	x	✓
BESS	✓	x	x	✓	✓

Table 4.7: Summary of differences between the designs.

Scenario:	Peak hours
Base case	-
Day-long curve flattening	from 00:00 to 23:59
Morning peak hours	from 08:00 to 12:00
Evening peak hours	from 18:00 to 22:00
Morning and evening peak hours	from 08:00 to 12:00 and from 18:00 to 22:00

Table 4.8: Summary of the different scenarios considered.

5

Analysis of results

As initially stated in chapter 1, the main scope of the project is to investigate how the flexibility of an energy system can be exploited to tackle the issues related to grid congestion. After having argued the different system designs used for the case study, one-year hourly simulations were performed for the defined scenarios. This chapter provides a deep analysis of the results discussing the findings and comparing the various designs for the different scenarios selected.

In order to provide a clear and organized analysis of results, this section is structured in five subsections as follows: section 5.1 argues the functioning of the base case providing an overview of the system functioning if no congestion occurs. Next, section 5.2 examines the impact of a full-day power reduction on the system behaviour as described in scenario 2. Then, section 5.3 explores the findings for peak reduction during the morning peak while section 5.4 explores the evening counterpart. Finally section 5.5 discusses the results in the case where both morning and evening peaks are managed.

To prove the correct functionality of the model and describe the system behaviour in the real case, the analysis of the results is organized by selecting four representative days, one per season, and the worst-case day, meaning the day with the highest peak power registered. These will be further considered in the report as follows:

- ***Winter day***: for the winter season, 25/01 is chosen as sample day. In cold periods, the system is expected to receive most of the electricity supply from the grid, due to low irradiation, and to register high heating demand from the households. As a result, in terms of grid power demand, this day is expected to plot the highest curve and therefore represent the worst case.
- ***Spring day***: for the spring season, 04/05 is selected. Here, temperatures are expected to be higher and therefore, lower heating demand. Moreover, the higher penetration of solar energy is expected to reduce the dependency on the grid during the central day.
- ***Summer day***: 09/07 is chosen as a sample day for the summer season. In this case, high production of PV power and high temperatures are expected, making the heating system operate mainly in cooling mode. Hence, the change-over heating system is expected to shift all the heating demand to the HT network, while the LT one is responsible for cooling.
- ***Autumn day***: for the fall, 13/10 is considered. Although the results may be similar to the spring case, lower sun radiation is expected to occur. Moreover, being the beginning of October, the heating demand is expected to be lower, resulting then in reduced total grid power withdrawal.
- ***Worst-case***: the highest peak power registered in the base case is on the 23/10. This day is considered thus the design base for the worst-case approach.

For all the scenarios investigated in this chapter, meaning the five cases described in section 4.3, the selected days will have the same solar irradiation as well as the same electrical and thermal demands. These are shown here in figure 5.1.

During each day, different influx of EVs is registered, as shown below in figure 5.2. While *Spring day*, *Summer day* and *Autumn day* show a large fleet of vehicles connected, *Winter day* and *Worst-case* represent anomalous cases, presenting only a few car connections for the whole day. This low influx of EVs can be

attributed to the nature of the data used, which may be a wrong representation of the real case. However, this is expected to strongly influence the results in the cases for which flexibility is attributed to the EV charging plaza and assist in understanding better the role of the different DERs' flexibility.

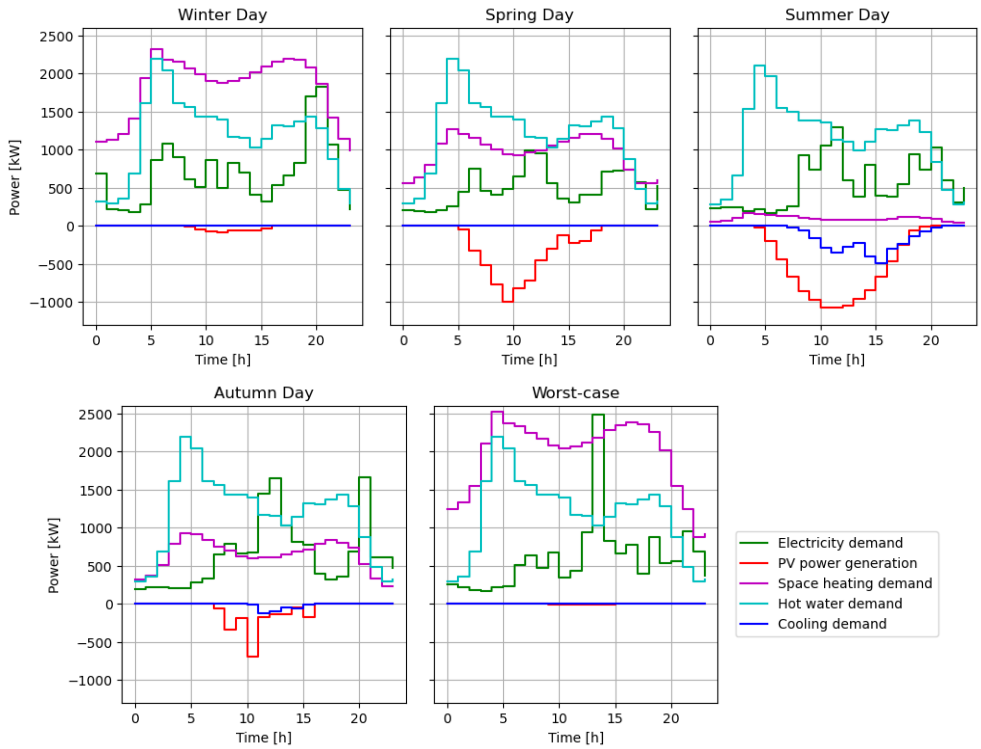

Figure 5.1: PV power generation and demands for the selected days.

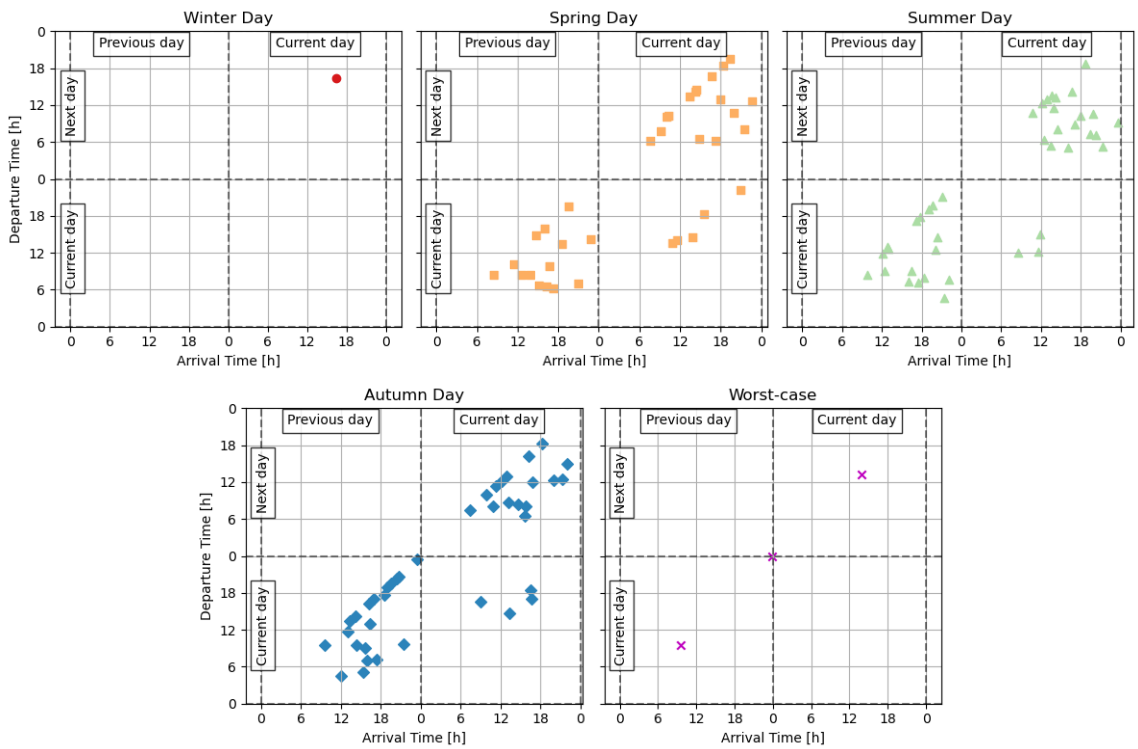

Figure 5.2: Influx of EV in the analyzed days. The plot shows the arrival time on the horizontal axis and the departure time on the vertical axis.

5.1. Base case scenario

The base scenario describes the system operation without any congestion mechanisms integrated. The goal is to describe an ideal case aiming to minimize the heating system energy usage and perform fast charging of the EVs, as specified in the objective in equation 4.5. As a result, scheduling is expected to organize the system behaviour such that a unique solution is found.

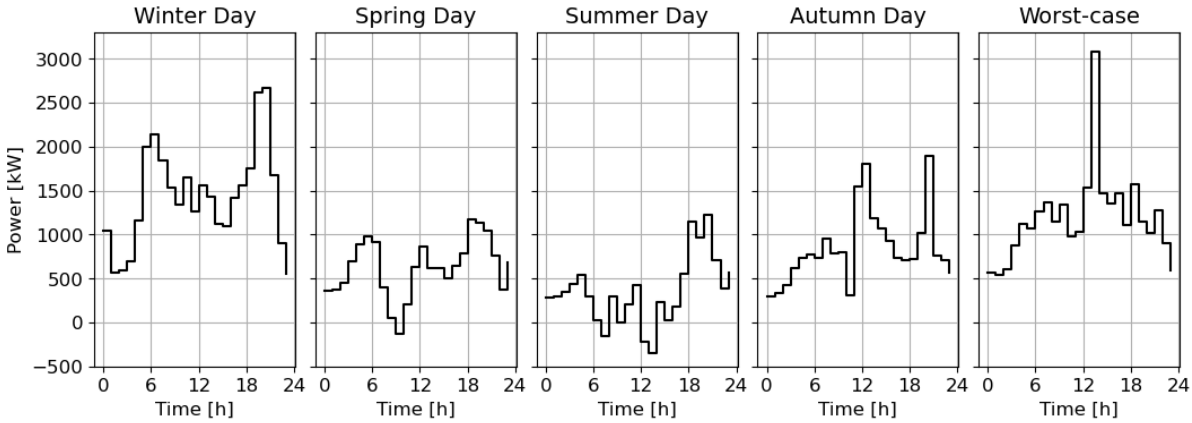

Figure 5.3: p_t^{grid} in the selected sample days for the base case.

Figure 5.3 shows the total grid power withdrawal during the selected days. Comparing these profiles with the demands in figure 5.1, it is possible to notice that the system tends to follow the electrical and heating demand curves, meaning that the EV charging is evenly spread throughout the day and the TES is disconnected.

The EV fleet represents the additional flexible load that must be met during the day in analysis. However, the fast charging objective specified for the base case drives the system to charge each vehicle immediately after arrival. As a result, the grid power demand is expected to spike when many vehicles connect to the system.

Figure 5.2 shows the electric vehicle fleet influx during the selected days. The plots allow us to divide the EV into two groups (visible by the two columns of arrival time): those connected from the previous day and those connecting on the day in analysis. Due to the fast charging objective, the system is expected to mainly take care of the second group, while the first can typically be considered already fully charged within the first few hours of the current day. As a result, the EV fleet charging profile results flat until the start of the second group. This is confirmed in figure 5.4, which shows that the charging profile of the EV fleet begins around the morning hours for the base case.

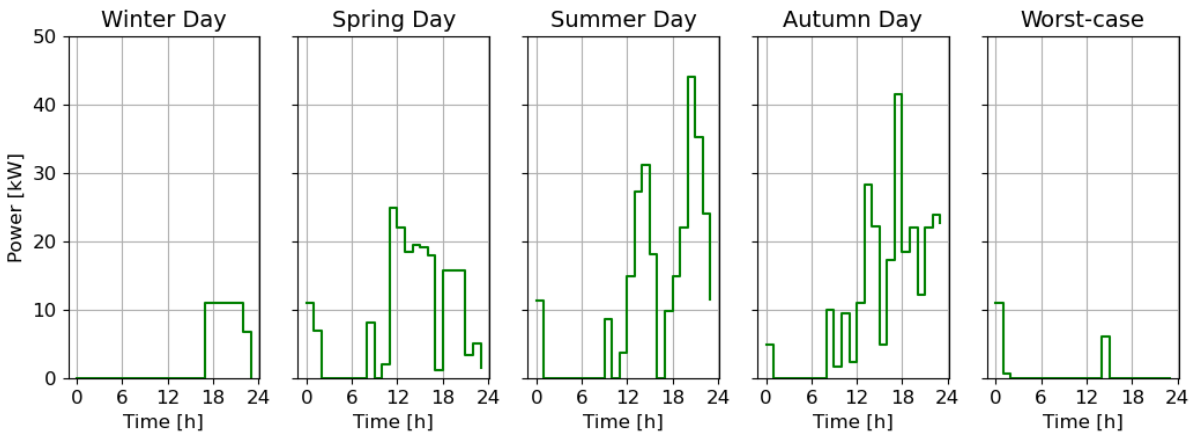

Figure 5.4: $p_{t,s}^{EV}$ in the selected sample days for the base case.

The second objective is to optimize the heat pump operation for minimal energy usage. Due to

significant losses connected to the thermal energy storage unit, its use is minimized in the base case, leading the heat pumps to directly follow the demand profiles.

However, observing the heat pump power profile, shown in figure 5.5, the *Autumn day* experiences a drastic drop in the late morning to then maintain null their involvement for the low-temperature network. This is because the heating system switches to cooling mode. Such behaviour suggests that the thermal energy storage provides sufficient inertia for the heating system to meet the low space cooling demand without need of heat pumps. This mode of operation is less energy-intensive for the low-temperature heat pumps and is therefore preferred by the optimization model.

In addition, the change over system instantaneously transfers the space heating demand to the high-temperature network, which power usage is accordingly increased for the *Autumn day*. This is noticeable in the second half of the day, where the high-temperature heat pump power results higher than the registered hot water demand.

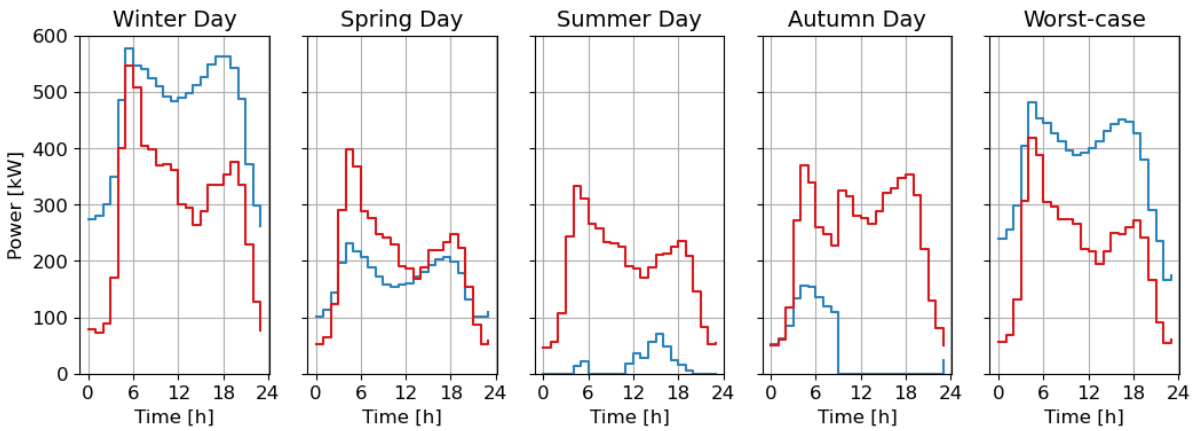

Figure 5.5: $p_{t,h}^{HP}$ in the selected sample days for the base case. The plot shows the high-temperature networks (in red) and the low-temperature network (in blue) power profiles.

Finally, to generalize the observations from the five sample days, the yearly distribution of grid power withdrawal is analyzed. Figure 5.6 below shows the quantile distribution for the year in analysis, from the 5th, in blue, to the 95th percentile, in red, while the mean profile is shown in black. It can be observed that the maximum peak generally occurs during the evening hours, aligning with the findings discussed in the literature. Additionally, a smaller hump is experienced in the early morning, representing the start of the day for residential loads. While the mean curve results quite flat around noon, it is possible to observe that there are a few days in which spikes are experienced also during the middle of the day, shown in red by the 95th percentile. As a result, although the general curve follows the expected behaviour, a few anomalous cases will be registered during the analyzed year.

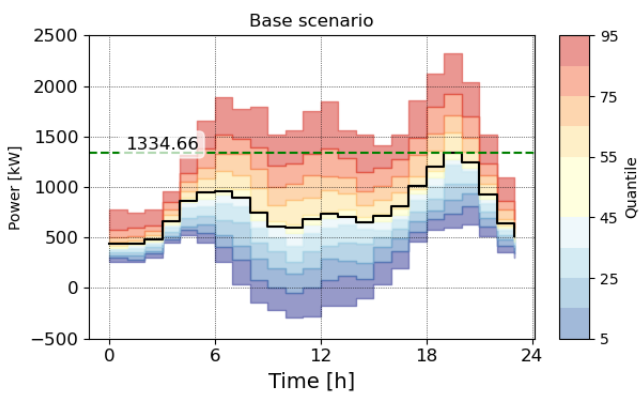

Figure 5.6: Quantile distribution of p_t^{grid} for the base case. The plot shows the daily maximum mean power on the left-hand side.

To conclude, the performance in scenario 1 confirms the correct functioning of the energy system model, simulating the optimal operation of the current EC design as if no congestion is experienced.

Morning and/or evening peaks are registered on all selected days. As a result, the different congestion management methods discussed in this research are expected to significantly improve the system in the next scenarios.

5.2. Scenario 2: day-long curve flattening

In scenario 2, a day-long minimization of grid power withdrawal is performed, aiming to flatten the curve and extinguish the peaks regardless of when these occur. The goal is to observe how the system flexibility can assist in minimizing the maximum power expected, which is used to design the Capacity Transmission Agreement (CTA) with the DSO for primary connection.

To do so, the worst-case approach is followed. In figure 5.7 below the daily peak estimated for the base case scenario is shown along the year. The graph shows the power in kW on the left axis while on the right axis, in orange, the percentage of reduction compared to the maximum peak registered in the base case scenario, resulting in 3'072.62 kW. As expected, the days with the highest peak power registered fall in the winter season, with the highest value registered on the 23rd of December. This day is thus considered representative for the whole system and the following arguments will be referring to it.

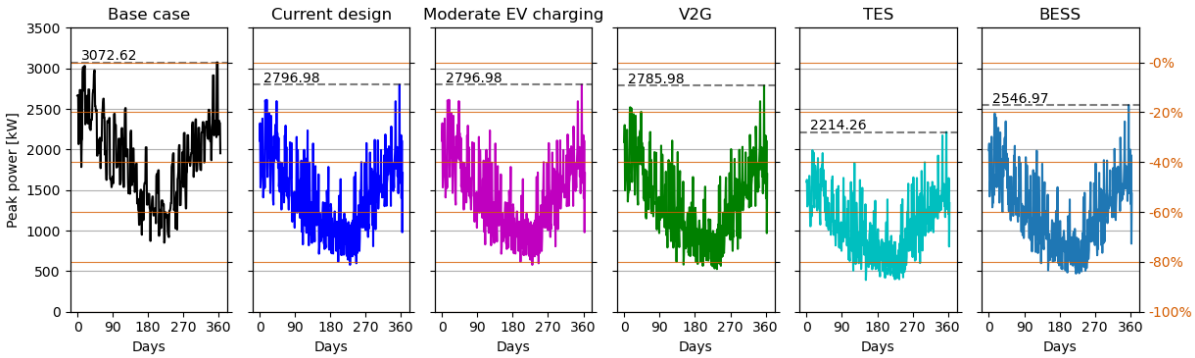

Figure 5.7: Daily maximum peak power registered during the analyzed year. The figure shows the base case (black) compared to the other five different designs for the day-long curve flattening scenario. On the left-hand axis, the power in kW is shown while on the right-hand axis the percentage of reduction compared to the base case yearly maximum is expressed.

First, the *Current system* design explores the impact of the simple Demand-Side Management (DSM) on the current system design without considering further investments. The goal is to observe the potential of the project as it is currently drafted.

Figure 5.8 shows the grid power withdrawal profile compared to the base case scenario for the selected *worst-case*. The plot clearly pictures that implementing peak power minimization helps reduce peaks of a significant value. The maximum peak is experienced in the early afternoon and clearly stands out compared to the rest of the curve. This can be attributed to an anomalous spike in the demands, which generates a spike that accordingly requires high power supply from the grid. In the *current system* design, the improvement is related to the two flexible energy resources: the EV fleet and the TES.

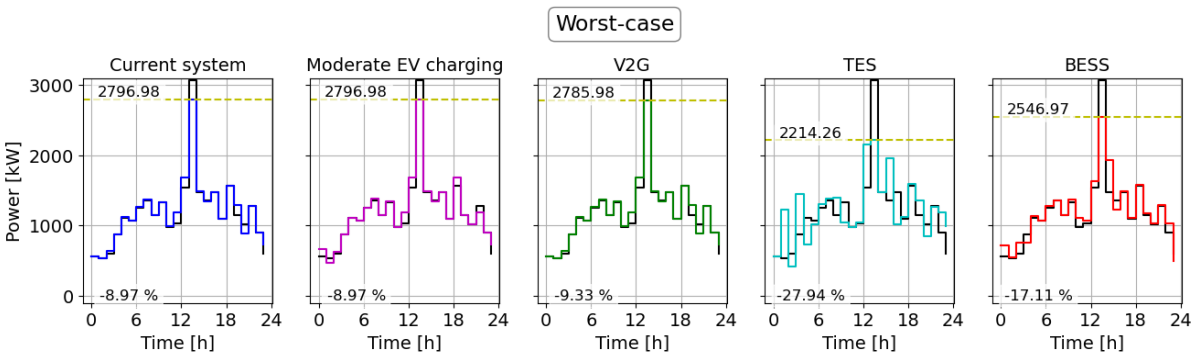

Figure 5.8: p_t^{grid} in the different system designs for day-long curve flattening (scenario 2) in the selected sample day (worst case). The plot includes the maximum registered power (next to the yellow line) and the percentage of reduction compared to the base case (on the bottom-left corner of each plot)

First, looking at the charging power of electric vehicles, the primary objective of peak power reduction overcomes the fast charging and therefore re-scheduling is performed. While in the base scenario, the evening peak was strongly increased by the EV charging need, implementing simple DSM shows how the same final goal can be achieved by shifting the charging schedule by a few hours. However, the day in analysis registers only 3 vehicle connections, of which only one results connected during the mentioned peak. Hence, the full reduction cannot be only attributed to the EV fleet flexibility.

As a result, it becomes evident that the main contribution to peak reduction comes from the flexibility of the heating system, particularly thanks to thermal storage. Both High-Temperature (HT) and Low-Temperature (LT) networks register higher power usage right before the peak occurrence, to then drastically drop during the peak indicating charging and discharging the TES units. The reason why charging occurs in the immediate previous time step of the peak is related to the thermal losses defined in the TES model.

Despite the selected day representing the worst-case scenario, the spike behaviour observed in the demand could be related to an incorrect value. If this is the case, the final peak power used for the CTA agreement will result in overestimation. To overcome this problem, the analysis can be extended to the yearly distribution of the grid power withdrawal throughout the whole considered year. This is depicted in figure 5.9 below, which shows the registered yearly distribution for scenario 2. It is important to mention that while the power of interest is detected in the *Worst-case* day in analysis, the probability of occurrence of this is quite rare and can be considered an anomalous case.

Observing the plot, a clear overall improvement from the base case is evident, especially in the evening peak. However, the limited flexibility of the current system does not provide enough room to efficiently flatten the curve. Hence, further improvement can be achieved when flexibility is increased.

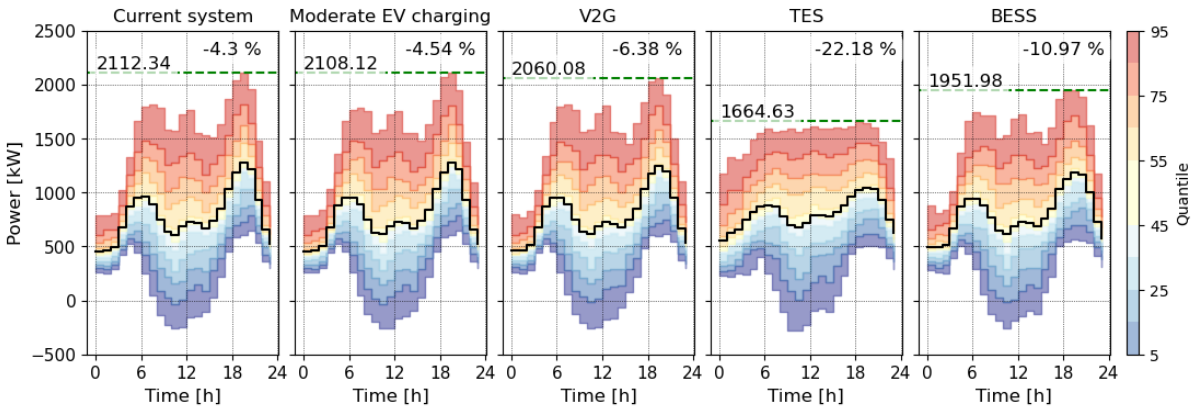

Figure 5.9: Quantile plots of p_t^{grid} for day-long curve flattening (scenario 2), including the highest power of the 95th percentile (next to the green line) and the percentage of reduction compared to the base case (on the top-right corner of each plot)

To explore the role of EV flexibility, the second design case with moderated EV charging is analyzed. Here, the final State Of Charge (SOC) constraint is softened to allow more freedom in the charging rescheduling and thus further curve flattening.

However, the peak registered in the selected day does not prove any further improvement compared to the previous case. Such a conclusion is then confirmed by the yearly distribution plot, which shows only a very slight improvement by softening the EV final SOC constraint.

This narrow difference can be attributed to the nature of the data used in the energy system model. As discussed in the literature, the average connection time of each vehicle significantly increases when considering a shared EV fleet. This can be observed in figure 5.10, which shows an average dwell time of 24 hours for the used data. Coupled with an average EV charging volume of about 14 kWh , as expressed by the bottom plot in figure 5.10, the general EV can fully charge in less than 3 hours. As a result, the soft-constrained final SOC introduced in this system design results ineffective for the shared EV business model.

To conclude, the flexibility improvement introduced in the moderate EV charging case results in negligible benefit and may even lead to a disadvantage for users than a benefit for curve flattening.

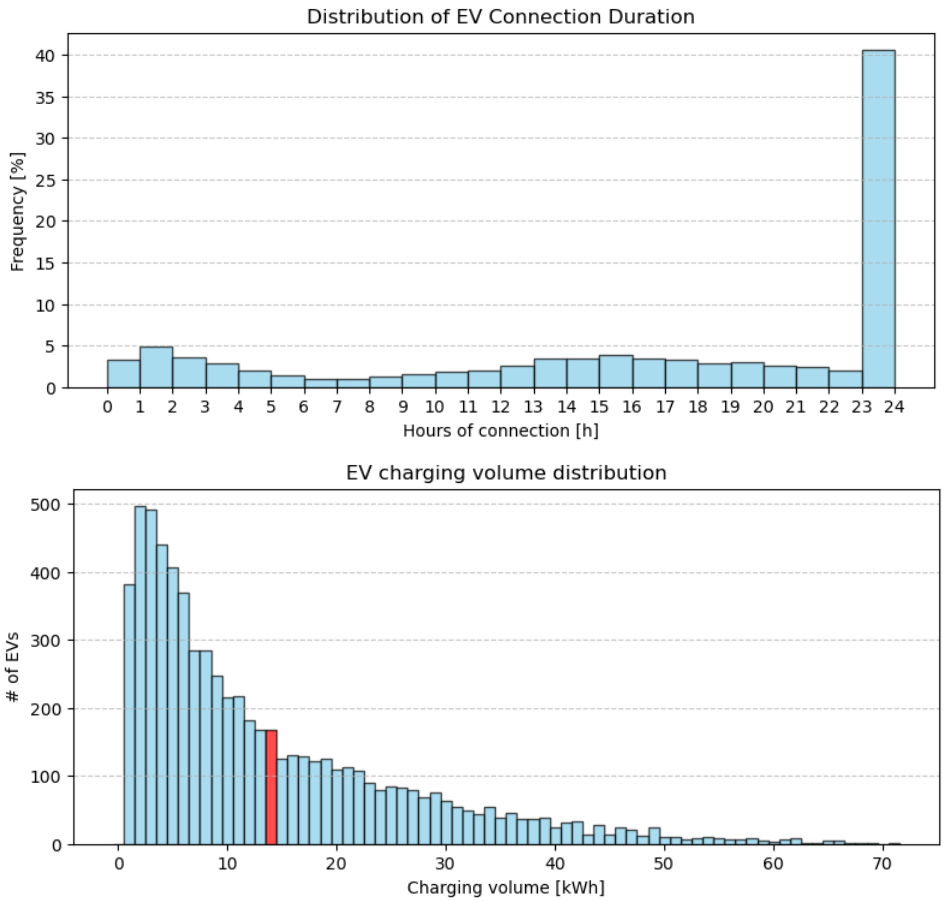

Figure 5.10: EV fleet duration of connection (top) and charging volume distribution (bottom). In red, the second plot highlights the average charging volume.

It is thus proven that the flexibility of EV fleet charging has limitations in flattening the grid power curve. However, the increased time of connection resulting from shared vehicles can prove more effective if vehicle-to-grid (V2G) integration is implemented. This is explored through the system design *V2G*, shown in green in *worst-case* plot (figure 5.8).

As expected, further improvement is registered compared to the first two designs. The system now utilizes the connected EV as a form of electrical storage, charging them before the peak occurs and thus supplying power to the grid during it.

However, as noted for the *Current system* and *Moderate EV charging* designs, the extent of grid power reduction is strictly related to the influx of vehicles during the selected day. For instance, when peak management is required in the early morning, the connected EVs are typically close to their maximum State Of Charge (SOC), since they charged during the previous night, and therefore provide good potential for reduction. Conversely, if the peak occurs in the evening, the second group of EVs can contribute by delaying their charging later in the night, thus providing a good potential for electricity supply. Moreover, there might be some days when very low influx of EVs is registered, due to holidays or weekends for instance, strongly reducing the power assistance V2G can provide. This is proven in the selected day, which observes only a single vehicle during the peak. As a result, the maximum potential improvement the V2G can provide is the size of a single charger, hence 11 kW.

It is though expected that the magnitude of reduction is largely improved when higher EV influx is registered. When looking at the yearly distribution of grid power withdrawal, the peak difference with the simple DSM design is improved by a good 40 kW, showing the potential of V2G for the goal in this scenario.

Therefore, the flexibility introduced by vehicle-to-grid technology fully exploits the advantages of the shared EV fleet business model. Thanks to the long average connection time of each vehicle, the EV fleet can assist effectively in day-long curve flattening but providing only a small reduction. However, the uncertainty related to the EV influx makes this case unreliable for strong peak reduction, hence

inadequate for the goal in scenario 2.

Exploring the flexibility of the other distributed energy resource mentioned, the *TES* system design aims to investigate the impact of increased thermal energy storage capacity on scheduling for grid power curve flattening.

As mentioned earlier in section 4.2, the phase-change material mass is increased by a factor of five in this case, thus extending the system's operational range. The aim is to understand to what extent a larger thermal buffer can assist in grid power flattening.

From the central graph in the *worst-case* power plot, the peak power reduction is observed significantly improved, registering a drop of about 800 kW compared to the base case.

Considering then the yearly distribution, the grid power withdrawal curve appears much flatter in this case compared to the other designs. This suggests that the size of the TES significantly influences the system's response to the objective of day-long power reduction. As a result, it is possible to conclude that for the goal curve flattening, the flexibility associated with the TES has a much greater impact compared to that of the EVs.

Proven the potential of energy storage for the goal of curve flattening, integration of a Battery Energy Storage System (BESS) is expected to overcome the EV influx fluctuation issue observed in the *V2G* case. This is explored in the last *BESS* system design.

As mentioned in section 4.2, the BESS size and C-rate are selected to cover the electrical demand for a few hours to have a comparable demand covering to what discussed for the *TES* design. Hence, for the initial analysis, a battery unit of 500 kWh with a C-rate of 0.5 is considered.

From the single-day grid power curve, we can observe that battery storage provides a smaller degree of flexibility compared to the thermal energy storage counterpart. This is evident in the plot, which shows a system behaviour in between the *Current system* design and the *TES* design.

Due to the secondary objective specified in equation 4.10, the usage of the battery storage system is minimized and activated only for peak reduction. This is confirmed by the battery power profile, depicted in figure 5.11, which shows charging and discharging occurring only around peak hours while remaining at zero during the rest of the time.

Considering the yearly distribution, we can confirm that the fixed size and the C-rate of electricity storage provided in the *BESS* design have a strong impact on the final peak reduction goal. Indeed, the parameters specified in this case allow a maximum peak reduction of 250 kW, which requires about 23 EVs to be connected at the same time for the *V2G* competitor design. Hence, a higher C-rate or higher BESS size is expected to provide even further reduction.

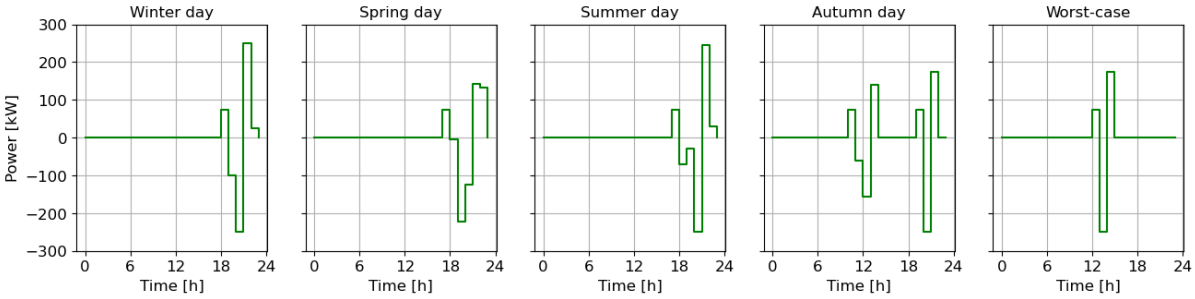

Figure 5.11: Charging and discharging power of BESS in the selected days.

It is thus confirmed the dependency of the final peak power on the storage unit size. In order to investigate this further, sensitivity analyses are conducted for the selected day.

The left plot in figure 5.12 below shows the relationship between peak power and Thermal Energy Storage (TES) size. As expected, increasing storage capacity improves the final outcome, resulting in a lower peak power value. It is possible to observe that the curve becomes flat after a certain TES capacity. This suggests that there exists an optimal size after which no further improvement can be achieved.

Conversely, when observing the sensitivity analysis for the battery storage, on the right in figure 5.12, also the electrical demand can be covered by the BESS unit, allowing thus further potential reduction than in the *TES* design. Moreover, it is possible to notice that the difference between the two analyzed

C-rates is visible only for low battery capacities. This is because the higher the BESS size, the larger the maximum discharge power and consequently the peak reduction potential. For example, if the peak reduction requires 500 kW of battery supply, the rate of discharge will be no different for batteries larger than 1'000 kWh.

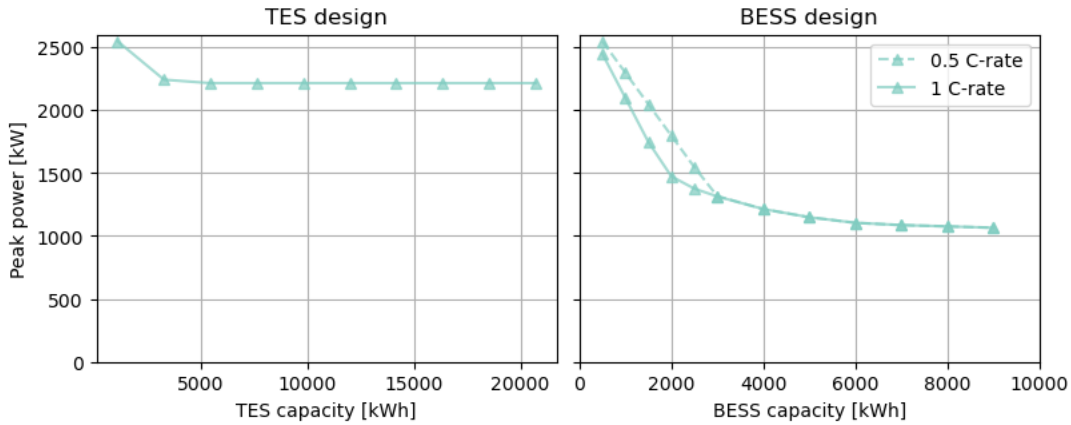

Figure 5.12: Sensitivity analysis for the day-long curve flattening case in the selected day (worst-case), for the *TES* design (left) and for the *BESS* design (right).

In summary, The goal in scenario 2 is to minimize the CTA design parameter, the maximum peak power, for the whole year. Hence, the worst-case approach was followed in this analysis. While EV flexibility and V2G integration offer some benefits, fixed storage solutions such as BESS and increased TES are more reliable and effective options for curve flattening. The sensitivity analysis highlights the importance of optimizing storage size to achieve the best performance for achieving the goal. Hence, to identify the optimal solution, further considerations must be considered. This will be discussed later in chapter 6.

5.3. Scenario 3: morning peak hours

Although having a flat curve throughout the entire day strongly helps the energy community in obtaining grid connection, the distribution grid experiences congestion especially during the morning and evening peaks [16]. In this case, a more targeted approach is followed and the goal becomes to focus the minimization of grid power withdrawal only to the morning hours. This has been defined from 08:00 to 12:00, as discussed previously in section 4.3.

Unlike the previous scenario, this and the next cases explore how the system flexibility may invite the implementation of the Capacity Limitation Contract (CBC) or the Time-Block-based Transmission Right (TBTR) agreements and assist the system in better operation than the simple CTA. As a result, the following analysis aims to describe the typical system behaviour and therefore will consider the four sample days, one per season, to investigate the effectiveness of each design throughout the whole year.

The *Current system* design applies a simple Demand-Side Management (DSM) mechanism for peak power minimization to the base case energy system. The total power withdrawal for the four selected days is shown in figure 5.13 below. Compared to the base case, the reduction provided by the system's flexibility is relatively narrow.

As discussed in the previous scenario, the current system design offers flexibility through the heating system and EV fleet. However, due to the lower influx of EVs during the morning hours selected, rescheduling cannot effectively contribute to power reduction. This is evident in the charging power profile, which shows a minimal difference compared to the base case, resulting in a limited improvement potential for this design. It is thus possible to conclude that the peak reduction potential related to the EV fleet is extremely low for the morning peak hours scenario.

Observing the behaviour of the heating system, the flexibility introduced by the small Thermal Energy Storage (TES) results helpful for shifting heat pump power usage from hour to hour. This can be observed in the heat pump power profile, which shows high utilization of heat pumps just before the peak hour window to then drop during it. Unlike the all-day minimization performed in scenario 2, the focused peak reduction in this case relives limitations on power spikes outside the selected window. As a result,

the system can rapidly charge the TES right before the start of peak hours without further restrictions on off-peak periods.

Therefore, as discussed in the previous scenario, the nature of shared EVs is non-optimal for the moderate EV charging case. Indeed, due to the long average connection time, it is rare to observe cases in which this flexibility is used.

Such a conclusion is then confirmed by the yearly distribution plots of both *Current system* and *moderate EV charging* designs in this morning peak scenario 3. As pictured in figure 5.14, the difference between the two can be considered negligible, emphasising the limited potential of EVs in this scenario.

While scenario 2 demonstrated that integrating vehicle-to-grid was effective for flattening the grid power curve, applying the *V2G* system design to morning peak reduction leads to different conclusions.

As mentioned previously, the number of vehicles connected during the morning peak is reduced compared to the night and evening periods. In addition, the constraints set on the EV fleet, as defined in section 3.5, require that vehicles must be fully charged by their departure time. Since many EVs register the scheduled to disconnect during the morning peak, vehicle-to-grid cannot be performed for these vehicles. As a result, the effectiveness of V2G is further reduced for morning peak reduction performed in scenario 3.

Nevertheless, when observing the yearly distribution, final results register a further reduction of 5% for the *V2G* design, although the final peak power value results quite close to the findings in *Current system* and *moderate EV charging* cases. This suggests that even though a very slight help can be attributed to the vehicle-to-grid technology, the EVs flexibility can be maximally exploited by its implementation.

On the other side, the thermal energy storage flexibility is proven to be optimal for this scenario. This is confirmed by the results of implementing the *TES* design, which shows a clear flattening and reduction in grid power withdrawal during the morning period. This trend is evident in both single-day analysis and the yearly grid power withdrawal distribution. Moreover, the fast charging of the TES units becomes clear in the latter. This means that shifting the heat pump usage from the peak hours to the immediately before the TES provides longer autonomy when its size is increased.

Furthermore, the effectiveness of fast charging for TES units becomes more clear in the latter analysis, which shows a spike right before the start of the peak hours. This indicates that shifting heat pump usage to just before the TES charging period provides longer autonomy when the TES size is increased.

However, the slower response of the system becomes more clear in this case. Comparing the yearly distribution of the *TES* design with the other, it is possible to notice that the curve behaviour is also different for a few hours before and after the defined time window. This effect is related to the modelling of the heating system, which is characterized by a complex relation between the flowing water temperatures and the phase change material temperature.

To conclude, system design *TES* confirms the effectiveness of thermal energy storage. However, its final result is once again related to the size.

Having discussed the disadvantages related to the EV fleet in this scenario, it is shown that integrating electrical storage into the *BESS* system design leads to a significant improvement, comparable to the thermal storage counterpart. The yearly distribution plot shows a flat behaviour during the peak time window, resulting in a lower and more constant power interaction with the electricity grid. Additionally, while the *TES* experiences a significant spike before the time window starts, the battery storage design shows the reduced losses allow a more optimal behaviour in flattening the morning peak.

As discussed earlier for scenario 2, the effectiveness of both *TES* and *BESS* designs strongly depends on the storage size. Hence, sensitivity analysis is once again needed for this case. Figure 5.15 and figure 5.16 below show in beige how the different storage capacity influences the final peak power value in this scenario.

Considering first the thermal storage case, we observe that even a slight increase in capacity from the base case leads to a strong power reduction for most of the cases. However, different behaviours can be observed from the four different selected days. While on the winter day the curve decreases gradually, the other plots show a much steeper drop followed by stabilization at relatively small TES sizes. This suggests that the thermal buffer is much more effective for warm days, while winter days result more challenging to manage. Therefore, sizing based on the winter season is expected to be sufficiently large to cover also the other season's average day.

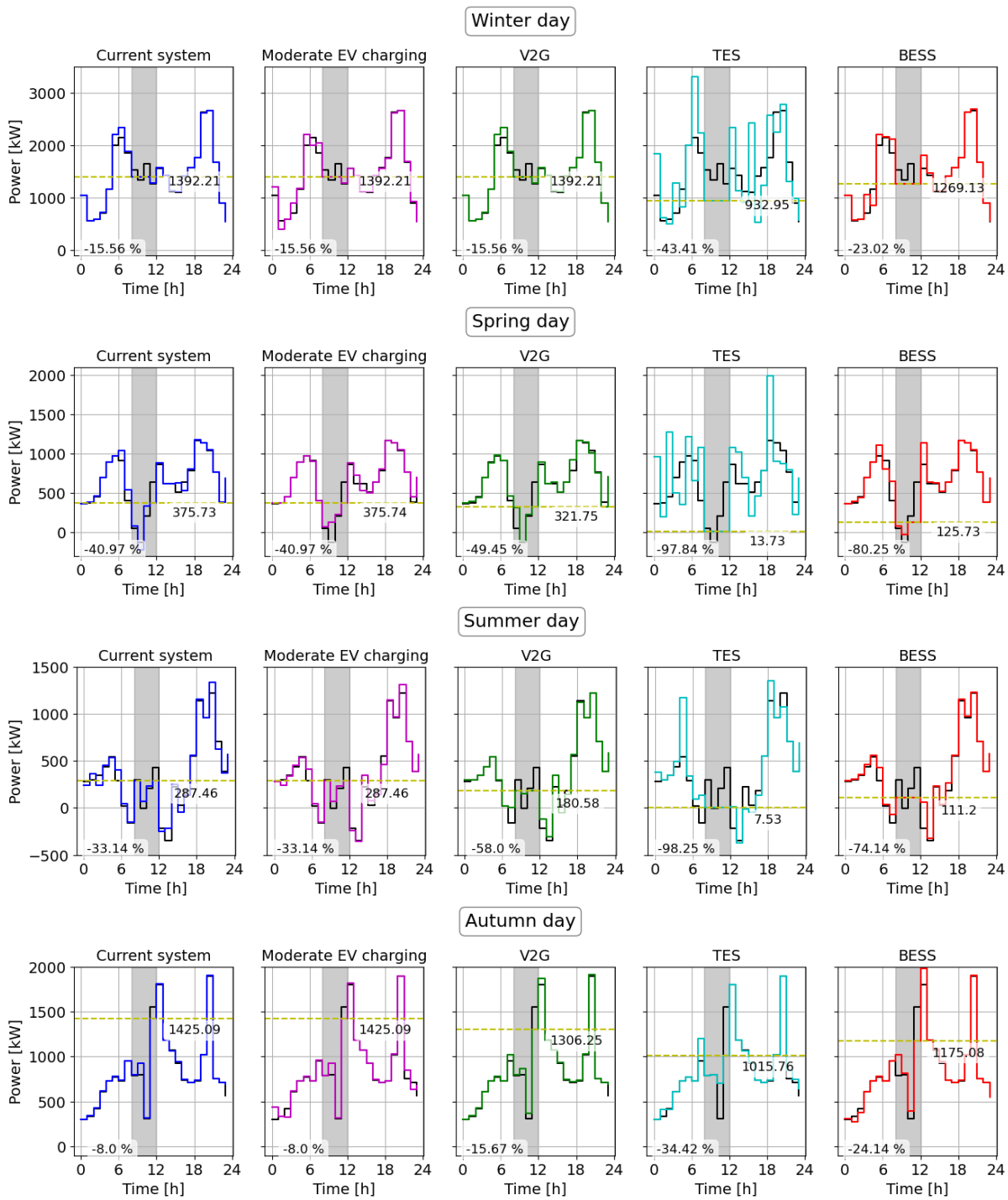

Figure 5.13: p_t^{grid} for morning peak reduction (scenario 3), including the maximum average power (on the left-hand side of each plot) and the percentage of reduction compared to the base case (at the bottom of each plot).

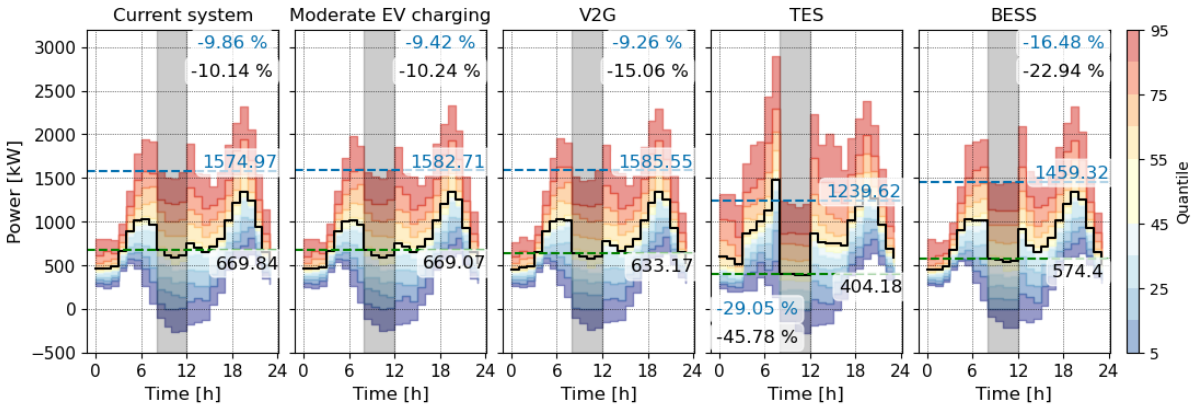

Figure 5.14: Quantile plots of p_t^{grid} for morning peak reduction (scenario 3), including the maximum power and the percentage of reduction compared to the base case for both the mean (in black) and the 95th percentile (in blue).

Next, the BESS size and discharge rate are investigated in a figure 5.16. From the graphs, we observe similar trends to what described earlier in the day-long curve flattening scenario, with a further improvement for large BESS units. Besides the curve decreasing linearly in all the selected days, the plots show that the grid power withdrawal can be potentially set to zero if the system integrates a certain battery capacity. This is observed mainly on the days with the lowest demand and highest PV production. Hence, sizing based on the winter season results once again convenient for covering the whole year.

In addition, when significant spikes are registered during peak hours, a higher C-rate shows a better performance in power reduction. This is attributed to the battery's capability to discharge faster and thus cover a larger area of the peak. Such effect can be observed, for instance, in the *Autumn day*, where changing the C-rate from 0.5 to 1 results in an additional reduction of 200 kW.

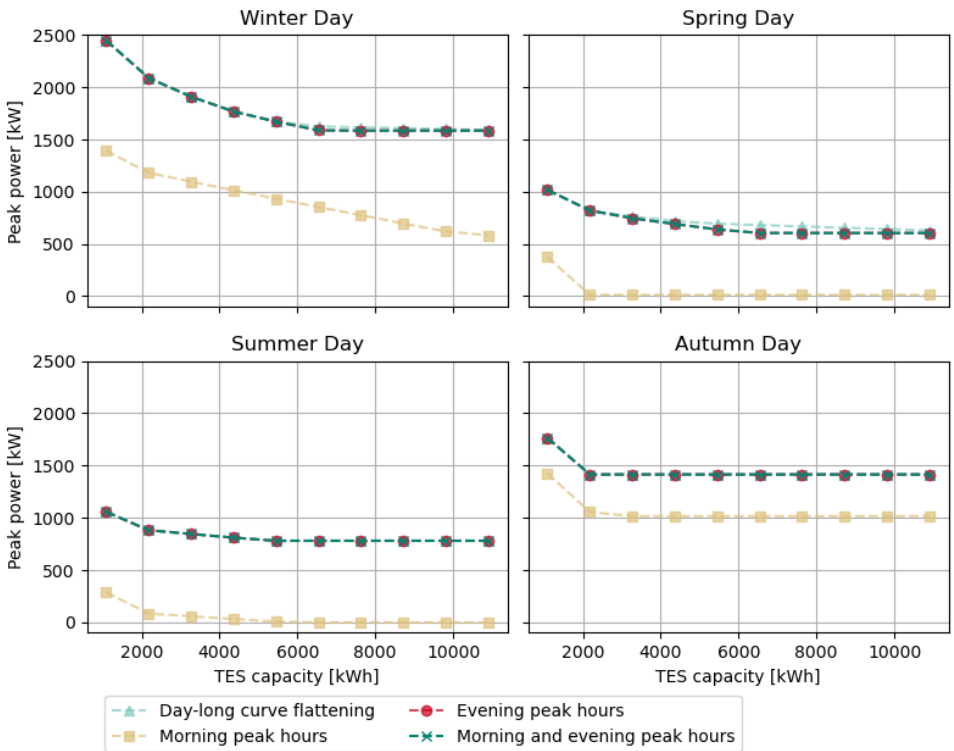

Figure 5.15: Sensitivity analysis for correlation between peak power and the thermal storage capacity for the *TES* design in the four sample days.

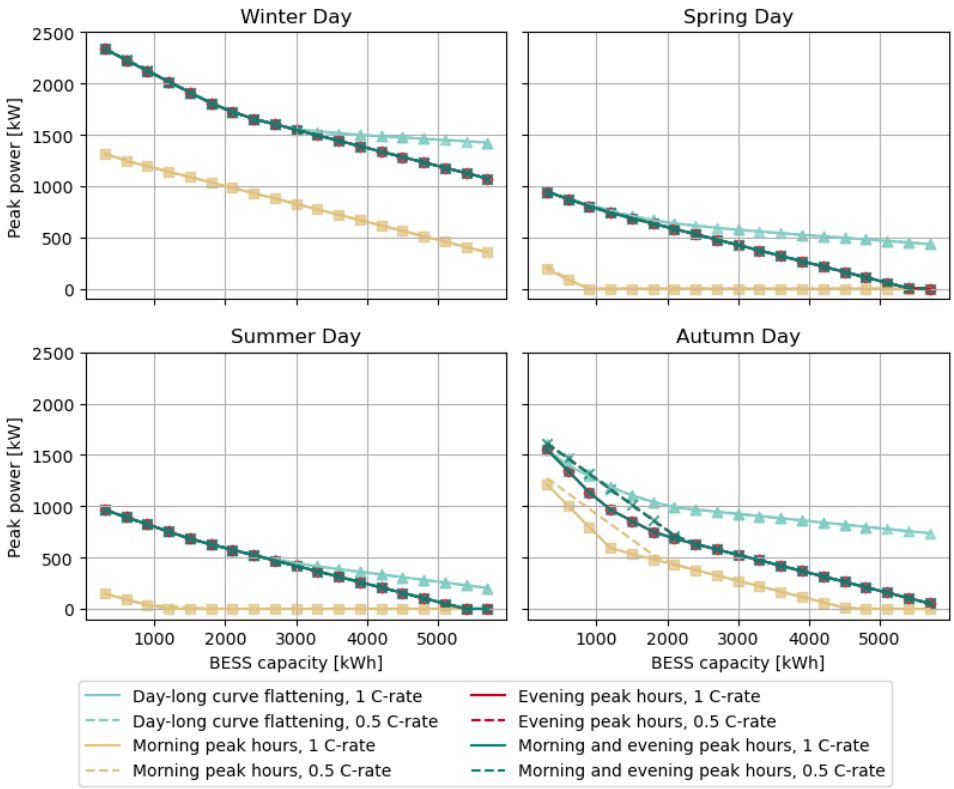

Figure 5.16: Sensitivity analysis for correlation between peak power and the battery storage capacity for the *BESS* design in the four sample days.

In summary, when performing peak power reduction from 08:00 to 12:00, the EV fleet showed limited potential and scarce results. This was attributed to the lower influx of EVs and the vicinity of the connected ones to the departure time, unable to perform V2G. Conversely, the definition of a smaller time window suggested the usage of TES, which allows great reduction with large sizes thanks to its autonomy. However, the best results were found with the *BESS* design. Thanks to the relatively low demand and the high PV integration, battery storage was proven to allow significant reduction during the morning peak, potentially making the whole system fully independent from the electricity grid. Similar conclusions can be drawn when considering the 95th percentile, showing how the different designs equally treat the peak reduction regardless of the peak size.

5.4. Scenario 4: evening peak hours

Similarly, the arguments discussed for the morning peak can be extended to the evening peak. As indicated in the literature and as observed from the base case scenario, residential loads typically experience their highest demand during this second peak, making congestion in distribution more probable to occur in this period. For this reason, this section discusses the results of target peak minimization in the time window of 18:00 to 22:00.

When observing the grid power interaction in figure 5.17, the *Current system* design leads results very close to what was observed in scenario 2. This similarity can be attributed to the nature of the base case profile. Indeed, for all selected days, the maximum peak is always registered during the evening peak. As a result, whether the focus is on the entire day or only on the evening time window, the system flexibility will act on the maximum detected peak only. Therefore, applying simple demand-side management results in the same peak power value as in scenario 2.

However, differences are noticeable for the *Autumn day*. Since the focus is set only on the evening peak, the model has no incentive to apply reductions during the mid-day peak, which in fact remains untouched. Consequently, by concentrating peak reduction on the evening window, the system behaviour during off-peak hours will be driven by the secondary objectives, making it close to what observed in the base case.

Therefore, this scenario reinforces the conclusion drawn from the day-long curve flattening. While

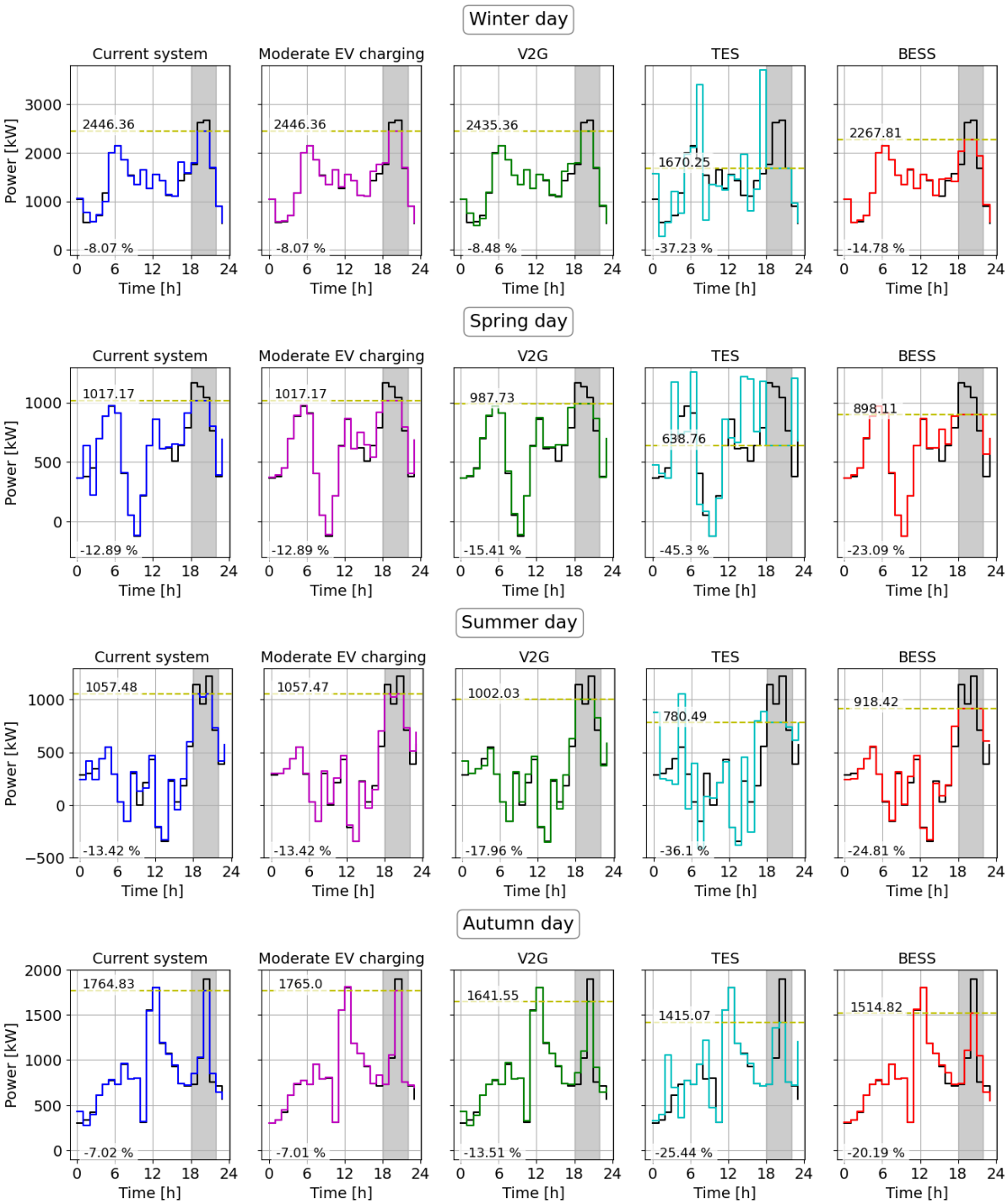

Figure 5.17: p_t^{grid} for evening peak reduction (scenario 4), including the maximum average power (on the left-hand side of each plot) and the percentage of reduction compared to the base case (at the bottom of each plot).

the flexibility of the current system design offers considerable potential for peak power reduction, it is limited to efficiently mitigating the evening peak. Therefore, further analysis on both EV fleet and heating system flexibility is explored.

While poor EV influx is registered in the morning, the evening hours typically see residents returning home and connecting vehicles to the chargers. Then, according to the registered EV influx, most of the cars are expected to stay connected throughout the whole night, allowing the system to delay the charging and thus reduce the evening peak. Despite this bringing an advantage for the EV fleet flexibility, no further improvement can be introduced by the *moderate EV charging* system design. This is confirmed by both single-day analysis and yearly distribution, shown in figure 5.18. The latter especially shows a very slight improvement related to a few particular cases. Thus, the charging flexibility of the EV fleet does not improve evening peak minimization, confirming the observations from previous scenarios.

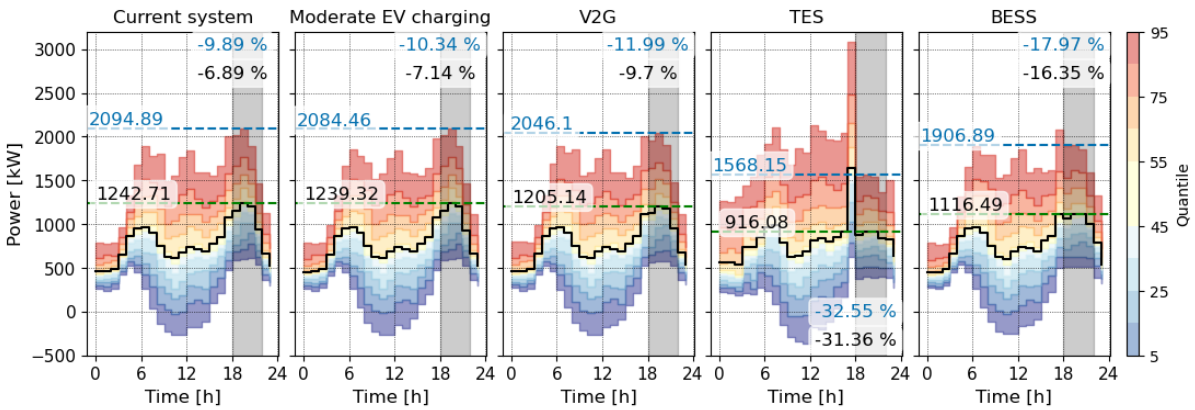

Figure 5.18: Quantile plots of p_t^{grid} for evening peak reduction (scenario 4), including the maximum power and the percentage of reduction compared to the base case for both the mean (in black) and the 95th percentile (in blue).

Furthermore, the large number of vehicles returning home before the peak hours and remaining connected through it increases the EV storage capacity than compared to the morning peak.

The additional storage capacity provided by the connected EVs enables a more substantial reduction in peak power withdrawal, as the system can utilize the stored energy in the vehicles to supply power to the grid during peak hours. As a result, the *V2G* system design case can reduce further the grid power withdrawal during the evening peak. This result is better observed in the yearly grid power profile distribution, showing a potential average reduction of 40 kW.

The *TES* design was proven to have a high potential for power reduction in both scenarios 2 and 3. This can be extended also to the evening peak case, where the heating system efficiently charges the TES units right before the start of peak hours to then flatten the curve during the selected window.

This is evident in the single-day analysis and becomes more clear in the yearly quantile distribution, in figure 5.18. The latter expresses that the analyzed TES size provides results that can be generally considered lower even than the morning peak. Having now more freedom during the early day, the heating system can reschedule the heat pump functioning to reduce even more the evening grid interaction. Therefore, despite the thermal buffer may experience more losses compared to the other designs, the final peak reduction achieved is significantly improved.

However, the magnitude of such is again strictly related to the storage capacity, which invites further investigation.

Observing thus the sensitivity analysis performed in figure 5.15, it is evident that the curve follows a decreasing trend, becoming then constant after a certain TES capacity, as observed in scenario 2. The only difference that can be pointed out is in the *Winter day* and *Spring day*, which registered a more or less constant power interaction with the grid in scenario 2. As a result, when DSM is focused only on the evening peak, further reduction can be achieved.

Lastly, the effectiveness of the *BESS* system design for the evening peak reduction is proven in the single-day plot. Here, the size and more particularly the C-rate of the battery system are expected to significantly affect the result.

This can be observed in the trade-off offered in figure 5.16. This sensitivity analysis shows with higher BESS capacity, the evening peak can be efficiently flattened and reduced.

In addition, the C-rate is observed to make a difference for small BESS, showing again a point after which both discharge rates, 0.5 and 1, deliver the same result. This relates once again to the conclusions drawn for the morning peak reduction scenario, discussed in the previous section.

In conclusion, the current energy system design showed good potential in evening peak reduction. Even with the simple *Current system* case, an important evening flattening can be achieved when compared to the base case. The implementation of vehicle-to-grid technology matches with the EV-shared business best, significantly improving the result. Conversely, the *moderate EV charging* case proved once again ineffective for achieving the set goal.

Both electrical and thermal storage designs showed strong potential in load shifting. While increasing the TES capacity shows effectiveness in power reduction, it requires a significant spike right before the start of the evening window. Conversely, thanks to the lower energy losses, the *BESS* design is able to charge the battery for more hours, reducing the aforementioned spike.

5.5. Scenario 5: morning and evening peak hours

Finally, the last case considered in this research involves the combination of scenarios 3 and 4. Hence, both morning and evening time windows are simultaneously considered in the minimization objective. The results are expected to align with the findings discussed so far and confirm the correct functioning of the model. However, due to the definition of two separate time windows, the operational schedule of the energy system in the periods between the peaks may vary, potentially leading to different outcomes. Therefore, the peak hours windows in this scenario are defined from 08:00 to 12:00 and from 18:00 to 22:00.

Considering the *Current system* design, the single-day analysis shown in figure 5.19 clearly shows that rescheduling is applied mainly to the evening peak, as this results in the global maximum during the selected days. Except for the *Autumn day*, which experiences a spike at the end of the morning time window, it is possible to notice that the morning registers much lower gird power withdrawal compared to the evening one for all the days in analysis. As a result, for this scenario, the single-day analysis can be considered less relevant in highlighting the overall system performance.

Conversely, when observing the entire year, some days are expected to have the highest peak within the morning peak hours. These cases are captured during the yearly distribution analysis as shown in figure 5.20. However, the *current system* design observes a profile very similar to the base case scenario in the first half of the day. This means that the flexibility of the existing system's draft is not sufficient to effectively reducing the average morning power withdrawal. On the other hand, improvement is clearly shown for the higher and more probable evening peak reduction, leading to a very similar result as the one discussed in the previous scenario. Therefore, we can conclude that there is no strong evidence that the *Current system* case is generally effective for morning peak reduction, while, differently, it is for the evening counterpart.

These conclusions are further confirmed by the *moderate EV charging* design. Hence, it is possible to irrevocably state that this design does not introduce any significant improvement for the research.

Observing then the *V2G* system design, vehicle-to-grid technology is demonstrated effective primarily during the evening peak. This is once again connected to the higher influx of EVs registered towards the end of the day, as mentioned earlier.

Conversely, when considering the *TES* design, the strongly targeted reductions observed for morning-only and evening-only peak scenarios efficiently combine in this scenario. Despite the minimization mainly focusing on the evening peak, the morning time window is also reduced and flattened. This is mainly observed in the rare cases that fall within the high percentiles. This suggests that the earlier peak hours are efficiently managed only if the average evening peak is reduced to such an extent that the peak power value intersects the morning curve.

Moreover, the rapid charging of the TES can be clearly observed in the hours right before the peak window for both cases. This indicates that the system response is sufficiently fast to manage the two windows more or less independently. However, when comparing these results to those found for the

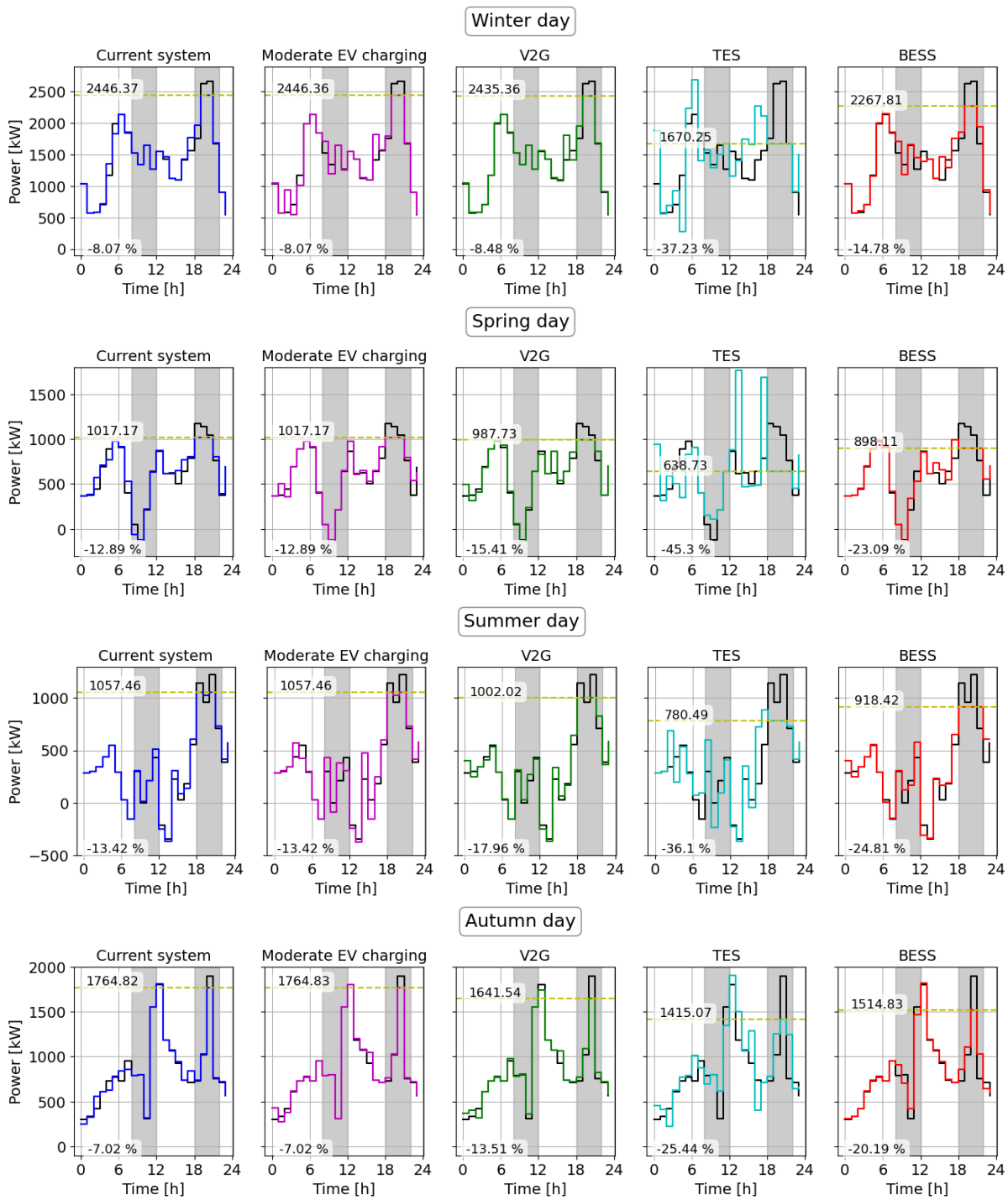

Figure 5.19: p_t^{grid} for morning and evening peak reduction (scenario 5), including the maximum average power (on the left-hand side of each plot) and the percentage of reduction compared to the base case (at the bottom of each plot).

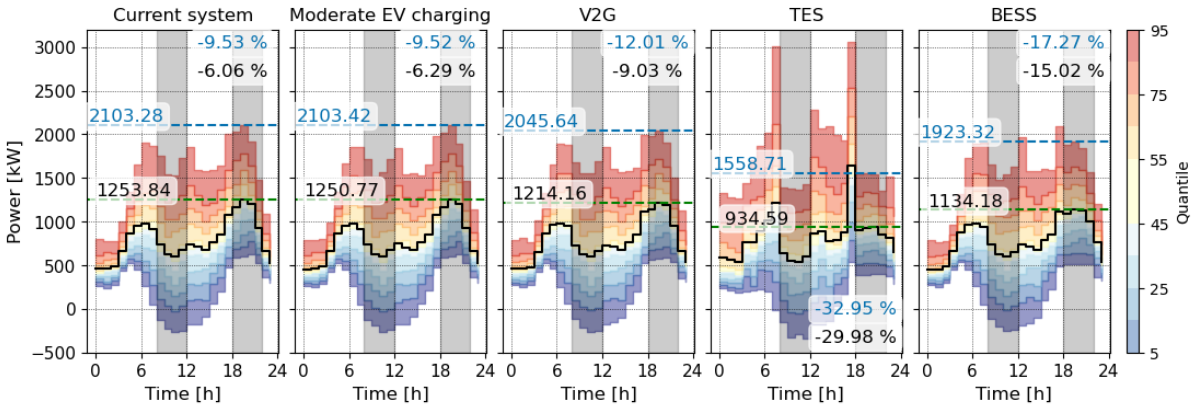

Figure 5.20: Quantile plots of p_t^{grid} for morning and evening peak reduciton (scenario 5), including the maximum power and the percentage of reduction compared to the base case for both the mean (in black) and the 95th percentile (in blue).

single peak reduction, a slightly higher average peak is observed. This suggests that having two peak hours may be less effective than focusing on a single one.

When investigating the correlation between TES size and peak power value, in figure 5.15, similar trends to those observed in scenario 4 are noted for the four selected days. This suggests that the heating system responds sufficiently fast to efficiently address the evening peak without making worse off the morning one. Furthermore, given that this scenario combines aspects of scenarios 3 and 4, and considering that the average morning maximum is lower than the evening counterpart, the same optimal TES size designed for evening minimization is expected to efficiently cover the morning one. As a result, each TES capacity selected for evening minimization will work well for morning peak reduction as well.

Finally, considering the *BESS* design, the results observed suggest a similar but improved outcome compared to the *V2G* case. Additionally, as discussed in the previous analysis, this gap is expected to increase when the battery capacity increases. Indeed, the sensitivity analysis for scenario 5, proposed in figure 5.16, shows the exact same profile to that observed for evening-only peak minimization, for all four selected days. Hence, the rapid response of the electrical storage offered in *BESS* allows effective reduction of both evening and morning peaks, similar to what was observed for the thermal counterpart. Accordingly, the system design with BESS included is expected to efficiently work the other way around, lowering the evening peak if the power results higher in the morning.

To conclude, scenario 5 aims to exploit the system's DER flexibility for both morning and evening peak minimization, combining the cases discussed in scenarios 3 and 4. While the effectiveness of the *Current system* case for morning peak reduction remains inconclusive, the results are more clear for evening peak reduction. The *moderate EV charging* design was once again proven ineffective for the shared EV fleet considered in the case study, while the *V2G* one showed good potential by treating the morning and evening peak completely separate, thanks to the EV influx nature. The *TES* design demonstrated significant improvement for reducing both morning and evening peaks, highlighting how an accurate size of the thermal buffer assists in achieving the final goal. Similarly, the *BESS* design showed how integrating electrical storage results in an efficient tool for grid congestion management, especially when targeting both morning and evening peaks, as it provides a rapid response for considering the two time periods independently.

5.6. Conclusions of results analysis

To conclude, this chapter focused on describing the results and discussing the findings of the simulation run for the energy system in the case study. The base case showed how the system would operate in the optimal scenario where no grid congestion is experienced. The results showed that the system tends to follow the thermal and electrical demands, avoiding the use of storage facilities and rapidly charging the EVs close to their arrival. The grid power interaction was found following the expected duck curve, showing a small hump in the morning and a bigger peak in the evening. To address the different nature of congestion, four scenarios were analyzed and compared to the base case.

First, scenario 2 performed a day-long power minimization, aiming to flatten the grid power withdrawal curve and thus reduce the size of the Connection and Transmission Agreement (CTA) with the DSO. In this case, the flexibility of the existing system proved a good capacity for peak reduction, showing how the current system flexibility can already potentially assist in obtaining connection. The reduction is then further improved by the integration of vehicle-to-grid technologies, which though are strictly related to EV influx. The best performance was achieved by the integration of storage facilities. Both large Thermal Energy Storage (TES) and Battery Energy System Storage (BESS) resulted in effective curve flattening. However, the size of the reduction was found strongly dependent on the storage size, which requires further consideration.

Secondly, targeted peak reduction was performed in the morning by scenario 3 and in the evening by scenario 4. Here the goal was shifted to describe a more general case instead of considering the worst day. It was observed that the limited influx of EVs in the morning time window strongly reduced the peak reduction potential related to the flexibility of this part of the system. Conversely, its potential was increased when only the evening peak was considered, making again the *V2G* design a good fit for the grid congestion management in this period. However, the lowest values were again found with the integration of thermal and electrical storage. While the first one was observed to strongly affect the hours right before the peak window, the lower losses registered by battery storage showed a less fluctuating grid interaction. Moreover, the sensitivity analysis conducted marked the potential of reducing to zero the power interaction during the peak hours, especially in the already low morning period. Thus, the *BESS* design emerged as optimal for these two scenarios. However, before drawing final conclusions, techno-economic considerations must be added to the research.

Finally, reduction for both morning and evening peaks was investigated in scenario 5. Due to the magnitude difference between the two, observed in the base case, the power reduction was performed mainly only during the evening peak, leaving untouched the morning period. Such observation led to the conclusion that the *V2G* system design has good potential for the selected objective, but struggled in the few cases where low influx matched morning peaks. On the other hand, the *TES* design offered results as a superposition of scenarios 3 and 4. However, the slower response of the large thermal buffer proved dependency between the morning and the evening time windows. Conversely, the *BESS* case showed a faster response and was able to manage the two periods independently.

However, while it is easy to identify the best system design based solely on simulation results, other factors must be discussed before drawing definitive conclusions for the case study of this research.

6 Discussions

In the previous chapter 5, the results obtained from the various simulations performed were discussed, highlighting the advantages and disadvantages in all the scenarios studied.

Accordingly, this chapter discusses how the findings can answer the research questions. First, a brief recap of the scope of the research is argued, showing how the analysis performed can contribute to the research goal. Then, techno-economical considerations are discussed, providing a deeper view of the problem in the case study. The chapter closes the thesis with considerations regarding limitations and further research.

Recalling the main research question introduced in chapter 1, this study aims to explore how different Distributed Energy Resources (DERs) integrated into an energy system can improve its flexibility and thus support grid congestion management and thus reduce the system's impact on the electricity grid. Specifically, this project focused on investigating how to address the implications of congestion on residential Energy Communities in the urban scene.

To prove the results found, a real case study is considered. The project involves a new residential area in the city of Utrecht, which is currently considering different options for connection to the distribution grid. This section provides an overview of potential solutions across the four different scenarios analyzed, aiming to show how the findings can assist the case study in obtaining grid connection and mitigate the congestion issues.

6.1. Techno-economic considerations

Chapter 5 showed how the different DERs integrated into the energy system respond to peak power minimization for various definitions of peak hours explored in the different cases. It is then essential to further explore each design to reveal additional factors to consider. Hence, each system design and scenario will be technically and economically evaluated.

To briefly review the case study, the current energy system project has been designed to ensure that the building's electrical load is entirely met through direct grid interaction, supplemented by PV power supply on days with high solar radiation. Additionally, the EV fleet charging operates independently, aiming to minimize the waiting time for each vehicle to achieve a full charge. Space heating, cooling, and hot water demands are satisfied through two separate heating networks, powered by dedicated heat pumps and phase-change material thermal buffers. In the different designs explored, the congestion management mechanism of demand-side management is applied, aiming to reduce the interaction with the grid during peak periods.

6.1.1. Financial Considerations

The energy system was analyzed in five different designs, each focusing on a specific type of flexibility. Besides the technological considerations, economic investment is expected to play a crucial role in the final design decision. Regarding this, the following can be argued.

As discussed in the literature, the integration of congestion management mechanisms typically requires the installation of smart meters and sensors near the load location [74]. These devices provide accurate data to control the operation, enabling more efficient load shifting and rescheduling. However,

given that the energy system under analysis is still in the design phase, the cost of implementing such technologies is relatively small compared to the overall system realization expenses and can be considered included in the project budget. Therefore, the technological investment required for the *Current system* design, as well as for the *moderate EV charging* case, can be considered null.

Conversely, when introducing vehicle-to-grid into the energy system, two key factors must be discussed. First, the charger that in the base design can operate only mono-directionally must now enable grid feeding from the connected EVs. However, being the system still in the design phase, new chargers would have to be installed in any case and the additional price for including V2G can be assumed negligible if compared to the whole investment. Hence, the additional technology required for V2G can be considered a limited cost. Similar can be concluded for what concerns the EV fleet. Nowadays, the EV market considers only a few models that include V2G, indicating that the technology state of progress is still in the development phase. However, their price is yet no much different compared to the average cost of a normal EV and is expected to drop in the next decade [30]. As a result, also the integration of the *V2G* for the design can be considered quite small for this case study.

Differently can be concluded for the last two designs. Increasing the Thermal Energy Storage (TES) units as in the *TES* system design is expected to consider significant initial investment. This will be mainly related to the mass of phase-change material selected, the insulated tank to contain it, the volume the storage would occupy and the relative cost of realization, the pipes for connecting it to the water system and the permits and regulations, for instance, for underground installation. Considering the *current system* design, the PCM thermal buffer was sized according to the given details, enabling a total capacity of about 1'000 kWh for each heating network, as described in section 4.2. For such a design, the data analysis performed estimated a total volume of about 10.4 cubic meters per TES, making its size moderate and simple to install in the heating room, close to the heat pumps, reducing the connected piping costs. However, the sensitivity analysis shown in figure 5.15 expressed a negative exponential correlation between the final peak power and the TES mass employed, flattening after a certain saturation value. Moreover, this was observed to give different results in all four selected days. Therefore, given the costs and benefits of both peak power reduction and TES capacity as well as chosen a representative sample day(s), an optimal solution can be found.

Due to a lack of detail, such estimation cannot be conducted in this research. However, indicative considerations are argued in the following. For simplicity, we can consider that the DSO sets a fixed price C_{peak} for each kW of power withdrawn during the peak hours and there exists a cost C_{TES} for each kWh of TES added, which includes both variable costs based on the size (PCM price, cost for expanded volume, etc.) and semi-variable costs (piping, land allowance, security standards, etc.). Then, a trade-off can be computed and the optimal design can be identified through equation 6.1 below, which identifies the slope m of the trade-off line to apply to figure 5.15 or a similar graph.

$$m_{TES} = -\frac{C_{TES}}{C_{peak}} \qquad m_{BESS} = -\frac{C_{BESS}}{C_{peak}} \tag{6.1}$$

If, for instance, the cost of a larger TES is much lower than the set cost of higher peak power, then it results convenient to invest in a bigger thermal unit size. Conversely, if the higher peak power withdrawal is relatively cheap, it is interesting to explore the return of investment rate, or payback time period in case of benefit, before investing in expanding the heating system.

Similarly can be discussed for the *BESS* design. While the thermal storage cost per kWh can be considered quite limited, about 20 €$/kWh_{TES}$, battery storage is generally more expensive [9]. Depending on the market and the type of battery, the price per kWh can go up to 130 €$/kWh_{BESS}$ for Li-Ion battery units [10]. Hence, BESS requires higher investment per unit of capacity added. On the other side, electrical storage is proven to have a higher energy density per unit of volume. Indeed, while a battery unit typically requires 0.005 m^3/kWh_{BESS}, the PCM material counterpart registers an energy density of 0.01 m^3/kWh_{TES} [55, 66].

Therefore, if from one side the *TES* design may offer a cheaper option, the *BESS* case proves to occupy a smaller volume for the same energy content. Moreover, the size of storage needed for the same power reduction may be different from the analysis of the results. Considering, for instance, the *winter day* selected in the analysis for the day-long curve flattening, in figure 5.15 and figure 5.16, we can observe that a final peak power of 2'000 kW can be achieved either with 1'300 kWh battery storage or with 3,000 kWh of TES. According to the estimation mentioned before, this results in 169'000 € and 6.5 m^3 for the *BESS* design and 60'000 € and 30 m^3 for the *TES* design. Therefore, this suggests that for what concerns

the straightforward investment, the *TES* design is estimated cheaper than the *BESS* counterpart, although the latter requires less space of installation.

However, such analysis must be further considered including marginal costs and potential constraints set by the case study. For example, while the TES requires high insulation in order to minimize losses, battery storage necessitates a ventilation system to reduce the room temperature and increase the device's efficiency and lifetime. In addition, while the heating system is expected to be concentrated in a single heating room, in order to reduce the pipeline length and thus losses, the *BESS* design may consider batteries spread around the residential area. Such design becomes interesting also considering the potential vicinity to the electrical load, EV charging plaza or heat pumps.

To summarize, there is a very large room for discussion between the two *TES* and *BESS* designs, making it difficult to estimate which result performs best in terms of techno-economical investment. On the other hand, the system designs offered in *Current system*, *moderate EV charging* and *V2G* were observed to provide quite small power reduction but with basically null investment.

6.1.2. Scenario Analysis

Besides the challenge of estimating the benefit of investment for each design proposed, it is essential to make separate considerations for each scenario analyzed. As discussed in the literature, the Netherlands is currently facing significant issues with new connection capacity due to grid congestion. Specifically, the case in this research involves the urban area of Utrecht, strongly congested as mentioned in chapter 2 [53]. As a result, the case study project is currently in the queue with the local DSO to obtain a Connection and Transmission Agreement (CTA) for then connecting to the distribution grid. Consequently, the initial challenge for the case study is to demonstrate to the system operator that its system design is sufficiently flexible to be eligible for connecting without increasing the congestion issue. In other words, to prove the need for a smaller CTA. For this reason, the day-long optimization conducted in scenario 2 provides an overview of how a flatter curve can be achieved, aiming to convince the system operator to provide the first connection.

As discussed in chapter 5, the existing energy system design, explored through the *current system* case, provided a good reduction compared to the base case. This flexibility was found to be connected to both the heating system and the EV fleet.

The strategy of shifting EV charging to nighttime hours is performed in all the analyzed designs and efficiently assisted the peak power reduction, showing, though, a maximum peak power reduction of only 4%. However, the shared business case of the EV fleet integrated in the case study showed how fragile its flexibility is, primarily due to the dependency on EV influx during the day. Despite a small improvement is achieved through the *V2G* design, the final grid power profile remained similar to the base case, suggesting that no efficient flattening can be provided by the current system design.

Additionally, the varying influx of EVs makes the sizing challenging. Following a worst-case approach, the EV fleet is characterized by high uncertainty, making these designs unreliable for designing the CTA contract.

Conversely, the thermal energy storage in the base design efficiently supports the heat pump in meeting demand during the peaks. Thus, while the load profile remains unchanged, the generation of thermal energy is shifted to the adjacent hours.

Furthermore, this research did not explore the potential of electrical and thermal load shifting, considering these as fixed and essential loads that must be met under all circumstances. Therefore, there is potential for further reduction if more data is provided, such as washing machine scheduling, common space heating and cooling or potential storage units in proximity of the houses. The latter, in particular, presents significant potential for flattening the demand curve, especially for hot water demand. In typical dwellings, hot water is provided by privately owned boilers, whereas the system in analysis considers a centralized heating system. Although this latter offers various advantages in terms of investment and energy efficiency, it also reduces the overall flexibility of the heating system. Hence, further research could be conducted exploring the decentralized heating system design.

As observed in the results analysis, a more constant and reliable grid interaction was achieved with the *TES* and *BESS* designs. The first was observed to efficiently flatten the grid power withdrawal curve in the winter days while showing a more oscillating behaviour during the warm days. This fluctuation is attributed to the change-over nature of the heating system, which switches on and off the cooling mode. As a result, the *TES* system proved to be more efficient on colder days, when overall demand is higher.

Two key observations can be discussed from these findings. First, if the system sizing is performed following the worst-case approach, the highest grid power profile is chosen. This is expected to occur

during the winter cases, due to high thermal demand, less daylight and consequently lower PV generation. In such cases, the *TES* design responds efficiently and results in optimal curve flattening.

Secondly, the operational characteristics of the thermal buffer suggest a more balanced behaviour compared to the BESS case. Indeed, unlike electrical storage, which can either charge or discharge at any given time, the TES is modelled to charge and discharge simultaneously, as shown in chapter 3. This perfectly matches the goal of making the grid power interaction as constant as possible throughout the whole day.

On the other side, the trade-off between the thermal storage and the electrical counterpart showed a much stronger reduction with the *BESS* case when considering the worst day, in figure 5.12. This suggests that the difference in investment is much lower for the same magnitude of reduction. This is due to the fact that, unlike TES, battery storage can act also on the electrical demand. However, this is proven for single spikes with high values. For the other sample days considered, for instance, the trade-off suggests the *TES* design as more convenient.

As a result, the final choice depends on the approach method followed as well as the accuracy of the data used. If the sizing is investigated for the very worst day, which may be a wrong representation of reality, the *BESS* case results optimal. Otherwise, the *TES* design becomes more and more attractive as more days are considered. In any case, both designs provide a reliable tool to reduce the maximum peak power and facilitate to obtain the CTA agreement with the local DSO.

The case explored in scenario 2 is expected to result effective primarily for obtaining the initial connection, showing that the system can be considered as a constant base load from the grid perspective. During normal daily operations, however, the energy grid is not expected to be congested for the whole 24 hours but, as viewed in the literature, research suggests that this event occurs mainly during the morning and the evening. Hence, it is possible that the DSO requires power reduction only during the selected periods instead of for the whole day. Such cases were discussed in scenarios 3 and 4, respectively.

Considering first the morning peak reduction case, the analysis showed how low influx of EVs directly suggests that implementing *moderate EV charging* and *V2G* designs may be disadvantageous. However, further consideration can be made for the latter. Given that the EV fleet in the case study is shared among residents, it is not necessarily the case that all vehicles are used every day. Hence, the accuracy of data becomes crucial in determining whether this design can effectively assist in reducing the morning peak.

Furthermore, thanks to the generally lower power value observed in the base case during this time window, the integration of vehicle-to-grid technology could potentially reduce the peak power with the EV fleet operating as a small battery system. However, the lack of connected vehicles during this period makes such a design impractical. This challenge may be overcome by designating a few EVs to remain stationary and cover the morning peak, thus increasing the storage system size. It becomes interesting to compare such a case with the fixed storage designs proposed in *TES* and *BESS*.

While the increased thermal storage case showed good peak reduction, the nature of TES limits its flexibility in meeting thermal demands only. Conversely, since the heating system is directly powered by heat pumps, electrical battery storage was proven better since it can also meet the electrical demand and potentially bring the grid power to zero. Furthermore, following the same sizing procedure discussed before, the smaller the storage size the closer the difference between the cost of the two technologies. Therefore, we can conclude that the *BESS* design is a more effective storage choice for morning peak reduction.

Having selected electrical storage as a better option for morning peak reduction, the discussion between the *V2G* and *BESS* designs is still open. To design an energy system capable of efficiently reducing the morning peak throughout the entire year, the worst-case scenario procedure is recommended.

Considering, for instance, that the initial investment is chosen in a battery system, it is likely that this will be oversized for summer days due to its generally lower demand compared to winter. Conversely, investing in a few stationary EVs that remain stationary and provide storage assistance during winter, but are available for use during summer, shows potential for maximizing the investment also when grid congestion is not a concern. However, the cost per kWh in the *V2G* design is significantly higher compared to the *BESS* option, since includes the whole vehicle.

The optimal solution can be achieved through accurate data on EV availability and demand forecasting as well as clear costs of implementation of both designs. Hence, the installation of smart meters and data collection devices is once again suggested. Moreover, the optimal design decision is expected to strongly depend on the cost/benefit per reduced kW set by the system operator. If, for instance, this is very low, implementing V2G is likely to be more effective. Otherwise, if the price of additional morning power withdrawal is high, the integration of battery storage would make the *BESS* design more attractive.

Therefore, depending on the level of reduction required, the *V2G* design combined with the designation of stationary EVs for critical days is expected to compete against the *BESS* option for morning peak minimization.

If, instead, the goal is to minimize grid power interaction during the evening peak, different conclusions can be drawn.

While considerations discussed in the morning peak hours case also apply to this scenario, the magnitude of power experienced during the evening peak is generally much higher than in the morning. As a result, implementing the *V2G* design would require a significantly higher investment, as more stationary EVs would be needed. In addition, while the difference in investment between the *TES* case and the *BESS* case was estimated lower, when looking at the evening peak, both capital and space required for such technologies become a crucial decision factor. More considerations can be discussed for these two designs.

First, as viewed in the literature, grid congestion in urban areas is expected to occur more frequently and with greater intensity during the evening. This means that on many days of the year, the power withdrawal will exceed the hypothetical threshold set by the DSO, resulting in higher fees (or lower benefits) for the case study. Hence, the optimal storage design is expected to be significantly large. In this case, the design approach recommended is once again the worst-case scenario, with the winter season being chosen for its typically higher demand.

In addition, as discussed in the analysis of results in section 5.4, the thermal energy storage experienced an important spike just before the start of the peak hours. This represents the high demand from heat pumps needed to sufficiently charge the TES units, for then being shut off in the next hours.

Here, the energy loss term plays a crucial role in distinguishing between electrical storage and its thermal counterpart. Indeed, while the BESS can consider energy losses over time to be negligible, the thermal buffer experiences significant heat dissipation through the tank shell, making it convenient to charge it only the time step before the start of the evening window. Conversely, battery storage offers higher flexibility, allowing charging to happen gradually from several hours earlier.

Although this is not an issue in the first place, considerations about the uncertainty of peak hours definition must be brought into this case. Re-analysing the objective of scenario 4, the goal is to minimize the evening peak in order to reduce congestion in the network. This concerns also the surrounding area. Being in an urban environment, it is expected that the surrounding connections would follow a similar profile to that of our case study. As a result, the DSO aims to flatten the curve during the whole evening and avoid spikes. For simplicity of implementation, this research considered this time window fixed from 18:00 to 22:00. However, in reality, this window could shift earlier or later according to the forecasted demand and system operator's decision. As a result, the existence of the charging spike registered in the *TES* scenario may cause problems for grid congestion management in this case. Although this is not a direct economic problem for the EC, the system operator is likely to prefer a less fluctuating grid power interaction.

Considering this, we can conclude that if the DSO sets a defined peak hours window in the evening and what happens outside of this is no concern of the EC, the *TES* potentially offers a cheaper design. However, for the goal of mitigating grid congestion, the system operator seeks a more constant power curve. In this case, the *BESS* system results more attractive, although it may require larger initial investments for the energy system planner. While the first case perfectly aligns with the contract of the Time-Block-based Transmission Right (TBTR) discussed, the latter is better represented by the Non-Firm ATO (NFA) agreement.

To recap, electrical storage emerged as the optimal tool for morning peak power minimization, showing how the *V2G* design can be a better investment compared to the *BESS* case depending on the magnitude of reduction. Conversely, for evening peak reduction, EV flexibility was discarded as a viable solution due to limited effectiveness connected to the magnitude of power demand in this time period. Instead, the *BESS* system emerged as optimal for managing evening grid congestion. Despite requiring higher investment, it provided a more consistent grid power withdrawal profile compared to the *TES* design.

When combining the two peak periods, as in scenario 5, it is assumed that the same weight is placed on both the morning and evening peaks. In this case, due to its typically higher magnitude, the evening peak drives the optimization process without affecting the morning peak in most of cases.

However, it is possible that the DSO requires minimization of both peak periods independently but within the same day. Therefore, the results are expected to be a sort of superposition of the two single

cases argued earlier. As a result, the system may consider implementing the *V2G* design with stationary vehicles to mitigate congestion during the morning peak, while incorporating the *BESS* for managing the evening peak. As observed earlier, the battery system provided better final results for the morning peak, but its investment was not optimal due to limited use during summer days. However, with consideration for both morning and evening peaks, this issue disappears, making the *BESS* design the best fit for morning and evening peak reduction.

As a result, the *BESS* is confirmed as the best option for minimizing both evening and morning peak loads.

6.2. Role of Flexibility in Different Connection Agreements

Recalling from the literature viewed in subsection 2.1.7, standard Connection and Transmission Agreements (CTAs) soon will have more flexible versions in the Netherlands. The Alternative Transmission Rights (ATR) and Non-Firm Agreement (NFA) agreements that will become active in the coming year show great potential when targeted minimization is performed. These contracts stipulate that during predefined peak hours, transmission is not guaranteed for the connected system, meaning that the connected party may have reduced or no grid power supply at all [42]. Therefore, if the energy system flexibility is such that islanded operation can be efficiently performed, these ATR and NFA become very attractive, especially thanks to their discount in price. Applying this to the designs discussed, it was observed that only the electrical storage options can potentially set the peak power to zero. As a result, the potential of the *V2G* and *BESS* designs can be discussed.

Considering the case where the DSO defines peak hours only in the morning time block, the analysis performed in scenario 3 shows how the electrical storage is a reliable tool that can potentially set the power to zero if designed of the correct size. The first option considers an extended EV fleet with some stationary cars to cover the winter days. However, when increasing the size, this latter appears more expensive than the battery option. As a result, the decision becomes a three-dimensional trade-off with the two considered designs competing against the benefit of implementing the flexible CTA contract.

Conversely, if the DSO defines peak also the evening time block, the *BESS* design emerged as most optimal, mainly due to the high magnitude of reduction needed. In this case, though, installing a BESS sufficiently large to ensure reliability to cover the whole district may become too expensive.

However, a further consideration must be discussed. While a CBC contract can be applied only after a first CTA is signed, the implementation of TBTR or NFA does not require any existing connection. On the other side, these two contracts do not ensure any grid power supply during the defined periods, forcing the system to operate independently.

However, this problem can be solved by a combination of the two approaches. The findings of this analysis show that reducing power during selected time windows allows the system to schedule the DERs functioning to off-peak hours without affecting the final users. This suggests that, if possible, signing a fixed CTA for the maximum reduced power and combining this with a TBTR or NFA contract allows the system to have certain transmission rights capable of covering the minimized peak hours demand and still meet the demands. As a result, obtaining a base load connection through a small CTA and then the extra connection via a flexible contract allows the DSO to accommodate the system in the distribution grid and optimally organize its usage. This concept is visualized in figure 6.1 below.

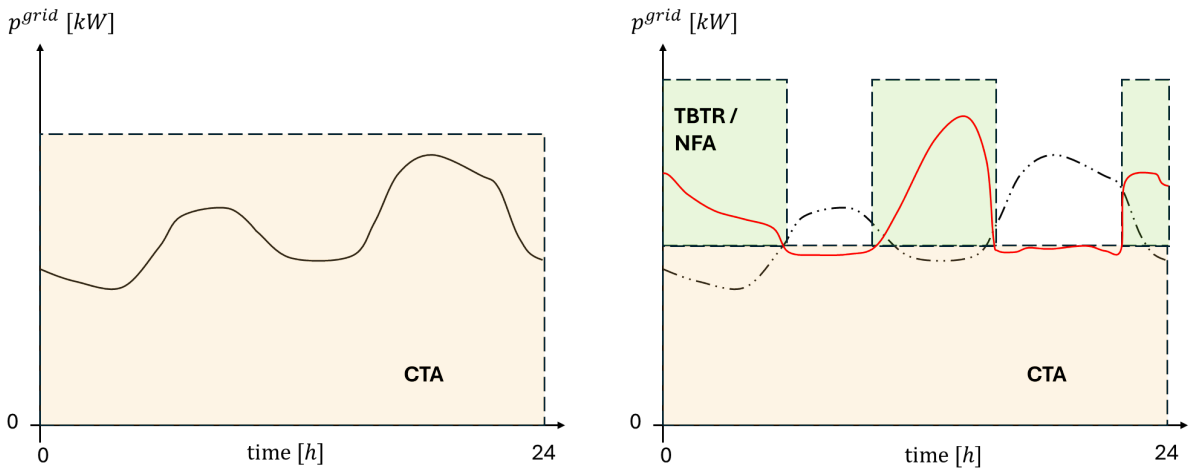

Figure 6.1: Implementation of a full CTA contract to cover the grid power profile, shown in black (left) and implementation of a reduced CTA contract and a TBTR / NFA contract for the remaining capacity to cover the re-scheduled demand, shown in red (right).

Therefore, two options can be identified:

- Implementation of a full capacity CTA with the integration of a CBC contract;
- Implementation of a reduced capacity CTA and a flexible contract, TBTR or NFA, to cover the remaining.

In the first option, the DSO agrees to provide the full right of transmission to the EC. It is then up to the local system to reschedule its functioning and receive a monetary return. Depending on the CBC details, meaning the hours, size and tariff of the reduction, the local system receives compensation. In other words, the DSO incentivizes the connected party to reduce their connection, thus reducing congestion. However, obtaining this kind of connection is expected to be more challenging and expensive. To reduce the total initial cost, the *V2G* design with possible stationary vehicles offers the best investment.

Conversely, the second option results more attractive for the system operator, since the transmission right during peak hours is no longer guaranteed. Hence, obtaining a connection will be easier and cheaper, thanks to the discount provided by these types of contracts. However, no compensation is stipulated for power reduction during these periods. This means that the local community is forced to reschedule its operation according to the peak hours definition agreed with the DSO. As a result, the EC must be fully sure of its DERs' flexibility and reliability properties. If TBTR is chosen, the *TES* design offers a strong reduction and reliable technology. Nonetheless, the charging spikes observed before peak hours are incompatible with the uncertainty of the NFA contract, suggesting the *BESS* design as a better alternative.

6.3. Limitations and data sensitivity

Before conclusions, it is important to mention that the results found are a rough estimation of the energy system based on many assumptions.

First, the energy system has been modelled through a simplistic approach to maintain the optimization problem linear and with low computational costs, possibly representing a system response far from real. This especially applies to the thermal energy storage system, whose non-linear nature makes precise modelling challenging and highly computationally expensive. Therefore, for more accurate results, more detailed models can be designed and implemented in each DER included in the energy system.

In addition, the accuracy of data is identified as a crucial factor for the final results. Despite the demands being thoroughly adjusted and shaped for describing the case in analysis, the system response strongly depends on their profiles and patterns. For instance, the analysis performed in the day-long curve flattening scenario focused on a day characterized by a huge spike in electrical demand. This can be correlated, for instance, to a fault or an anomalous measurement that should not considered representative of the whole year's functioning. It is thus expected that much more precise results can be achieved by implementing real measurements.

Furthermore, the lack of information about techno-economical constraints leaves space for discussion when applying the results to the case study. One example can be the space limitations for expanding the storage facilities. Indeed, being a residential neighbourhood located in a highly dense populated area thigh in space, as the one in analysis, the volume of DERs is expected to play a crucial role in the final design method.

6.4. Further studies

The goal of this master thesis was to explore the role of flexibility in large capacity connection for urban living spaces, aiming to exploit the DERs characteristics to address the problem of grid congestion. However, as mentioned in the literature. This issue is too broad to be fully covered in a single project.

Considering the energy system modelling discussed in chapter 3, a simplistic and deterministic approach was followed in this project. Such a method allows a fast and efficient representation of the energy system but fails to carefully address the uncertainties and it is sensitive to the input data. Therefore, further research could consider an improvement of the model, integrating more precise constraints and larger simulations.

Moreover, the findings were proved to be strongly affected by the assumptions and data argued in chapter 4. Due to a lack of specifications, some modelling parameters have been estimated and could be largely improved. In addition, the data used have been scaled and adapted from the reference to the case study, potentially missing to describe correctly the real system's behaviour.

Besides the improvement of the current research, the research can be continued in different directions. To address more in-depth the current problem of the case study, further techno-economic analysis can be performed. First, the development of the flexible transmission agreements currently in progress may vary or be redesigned in the next years. Hence, a more careful analysis of the policies and regulations can better assist the residential community in obtaining grid connection faster.

Secondly, this research focused the research only on five system designs, describing the flexibility of the different resources in a semi-independent way. Therefore, further analysis may consider the implementation of hybrid systems, exploring, for instance, the potential of battery storage and vehicle-to-grid together or integration of back-up generators.

Finally, potential research involves a closer collaboration with the Distributor System Operator (DSO), exploring, for instance, the potential of grid feeding by PV or electrical storage and related subsidies or discounts. In other words a deeper view of how the EC can cooperate with the grid operators to solve grid congestion in exchange of easier connection and cheaper energy bills.

7 Conclusions

The research presented in this master's thesis aimed to explore the role of flexibility in grid connection capacity planning for urban residential areas. The focus was specifically posed on how integrated scheduling frameworks can optimize the design of neighbourhood energy systems through the flexibility of its Distributed Energy Resources (DERs) to mitigate the issues related to grid congestion. The study focused on a new residential area currently under construction in the city of Utrecht, the Netherlands, characterized by a shared EV fleet and a district heating system. However, due to the congested nature of the distribution network in the area, limited capacity is available for new large projects like the one considered and the energy community is currently in the process of obtaining a grid connection. Through the development and application of a comprehensive optimization model, several key results have been found, providing valuable insights for both energy community and grid operator.

Grid congestion is a critical challenge in the context of urban energy systems. It occurs when the electricity demand exceeds the capacity that the grid infrastructure can handle, leading to inefficiencies and potential disruptions. This research clarified the implications of grid congestion, emphasizing its impact on reliability, cost, and the overall sustainability of energy supply. By exploiting the flexibility of integrated DERs, such as Electric Vehicles (EVs), Vehicle-to-Grid (V2G) systems, Thermal Energy Storage (TES), and Battery Energy Storage Systems (BESS), it is possible to alleviate congestion and enhance grid performance.

The modelling of DERs was computed through a mixed-integer linear optimization model, using Python-based open-source optimization (*Pyomo*) as implementation tool. The research highlighted five different scenarios: a base case for comparison, day-long curve flattening, morning peak hours, evening peak hours, and combined morning and evening peak hours. For each scenario, five system designs were evaluated: the *current system*, *moderate EV charging*, *V2G*, *TES*, and *BESS* designs. This comprehensive approach enabled a thorough analysis of how different designs and their inherent flexibility affect the energy system functioning for minimization of grid power withdrawal during peak hours.

From the analysis, it was evident that EV flexibility is highly dependent on the availability and usage patterns of the shared EV fleet. Due to the long average time of connection, the *moderate EV charging* design proved to be ineffective for all considered scenarios. Conversely, the shared EV business model showed potential for vehicle-to-grid implementation. Integration of large storage facilities as in the *TES* and *BESS* designs, demonstrated significant potential for peak reduction. While thermal storage units provide more stable results for day-long curve flattening, battery storage systems stand out in targeted peak hours thanks to their rapid response and minimal losses. However, the size of the reduction was observed to be strongly related to the storage unit size and integrating these technical findings with techno-economic considerations revealed important trade-offs. While the *current system*, *moderate EV charging*, and *V2G* consider limited costs, *TES* and *BESS* are more expensive and require substantial space. The analysis suggested thermal storage as the cheaper solution whereas battery storage as the less cumbersome. This underscores the importance of balancing technical performance with economic feasibility and spatial constraints in designing urban energy systems.

Given the case study's primary challenge of obtaining a grid connection, the research identified two viable options for managing grid capacity:

- **Standard full capacity CTA with CBC Contract**: This option involves securing full connection rights through a standard Connection Transmission Agreement (CTA) and compensating for peak reduction via a Capacity Reduction Contract (CBC). While this approach makes it harder and more expensive to obtain the initial connection, it provides monetary return to the local community. The cheap V2G design is particularly attractive in this scenario, as it offers a cost-effective solution for peak management;
- **Reduced CTA with TBTR or NFA Contract**: This alternative involves a reduced CTA agreement supplemented by a Time-Block-based Transmission Right (TBTR) or a Non-Firm ATO (NFA) contract for the remaining capacity. This option simplifies the connection process but requires the energy system to rely heavily on its flexibility to meet demand during periods when grid supply is limited. In this context, the *TES* and *BESS* designs emerge as the best option due to their high flexibility and rapid response capabilities.

The findings of this thesis highlight the significant role of DER flexibility in mitigating grid congestion and optimizing the design of urban energy systems. The research points out the need for a thorough study that can consider technical performance, economic considerations, and spatial constraints. As urban areas continue to grow and evolve, the insights provided in this thesis will be instrumental in guiding the development of resilient, efficient, and sustainable energy systems.

References

[1] 125 Statistics Netherlands. *Energy consumption private dwellings: type of dwelling and regions*. Oct. 2023. URL: https://www.cbs.nl/en-gb/figures/detail/81528ENG#shortTableDescription.

[2] International Energy Agency. "Solar Energy". In: (2023). URL: https://www.iea.org/energy-system/renewables/solar-pv.

[3] Jamshid Aghaei et al. "Multiobjective generation expansion planning considering power system adequacy". In: *Electric Power Systems Research* 102 (2013), pp. 8–19. DOI: https://doi.org/10.1016/j.epsr.2013.04.001.

[4] Ardak Akhatova et al. "Agent-based modelling of urban district energy system decarbonisation—a systematic literature review". In: *Energies* 15.2 (2022), p. 554. DOI: https://doi.org/10.3390/en15020554.

[5] Tobi Michael Alabi, Lin Lu, and Zaiyue Yang. "A novel multi-objective stochastic risk co-optimization model of a zero-carbon multi-energy system (ZCMES) incorporating energy storage aging model and integrated demand response". In: *Energy* 226 (2021), p. 120258. DOI: https://doi.org/10.1016/j.energy.2021.120258.

[6] Jonas Allegrini et al. "A review of modelling approaches and tools for the simulation of district-scale energy systems". In: *Renewable and Sustainable Energy Reviews* 52 (2015), pp. 1391–1404. ISSN: 1364-0321. DOI: https://doi.org/10.1016/j.rser.2015.07.123. URL: https://www.sciencedirect.com/science/article/pii/S1364032115007704.

[7] Mehdi Attar, Sami Repo, and Pierre Mann. "Congestion management market design-Approach for the Nordics and Central Europe". In: *Applied Energy* 313 (2022), p. 118905. DOI: https://doi.org/10.1016/j.apenergy.2022.118905.

[8] Edoardo Barabino et al. "Energy Communities: A review on trends, energy system modelling, business models, and optimisation objectives". In: *Sustainable Energy, Grids and Networks* 36 (2023), p. 101187. ISSN: 2352-4677. DOI: https://doi.org/10.1016/j.segan.2023.101187. URL: https://www.sciencedirect.com/science/article/pii/S2352467723001959.

[9] Ashley Bland et al. "Buildings PCMs for Residential Building Applications: A Short Review Focused on Disadvantages and Proposals for Future Development". In: *Buildings* 7 (Aug. 2017), p. 78. DOI: https://doi.org/10.3390/buildings7030078.

[10] BloombergNEF. *Lithium-Ion Battery Pack Prices Hit Record Low of* $139/kWh|BloombergNEF$. Nov. 2023. URL: https://about.bnef.com/blog/lithium-ion-battery-pack-prices-hit-record-low-of-139-kwh/.

[11] Natural Resources Canada. "Heating and Cooling With a Heat Pump". In: (Aug. 2022). URL: https://natural-resources.canada.ca/energy-efficiency/energy-star-canada/about/energy-star-announcements/publications/heating-and-cooling-heat-pump/6817.

[12] Hongbing Chen et al. "Experimental study on heat and moisture transfer in soil during soil heat charging for solar-soil source heat pump compound system". In: *Applied Thermal Engineering* 70.1 (2014), pp. 1018–1024. ISSN: 1359-4311. DOI: https://doi.org/10.1016/j.applthermaleng.2014.06.030. URL: https://www.sciencedirect.com/science/article/pii/S1359431114005109.

[13] Wenxin Chen, Hongtao Ren, and Wenji Zhou. "Review of multi-objective optimization in long-term energy system models". In: *Global Energy Interconnection* 6.5 (2023), pp. 645–660. DOI: https://doi.org/10.1016/j.gloei.2023.10.010.

[14] Dean Chuang. "Back to the Basics: A Simple Analogy to Visualize the Evolution of the Modern Grid". In: *Energy Central* (May 2020). URL: https://energycentral.com/c/um/back-basics-simple-analogy-visualize-evolution-modern-grid.

[15] Consumer and Markets Authority. *Decision of the Netherlands Authority for Consumers Markets of 25 January 2024, reference ACM/UIT/610965 final decision to amend the tariff structures and conditions as referred to in Articles 27 and 31 of the Electricity Act 1998 concerning the non-firm transport agreement, Case number: ACM/22/180165*. Jan. 2024. URL: https://zoek.officielebekendmakingen.nl/stcrt-2024-2951.html#.

[16] Netherlands Authority for Consumers and Markets. *ACM: flexible utilization opens up more possibilities on congested grid, projects with social functions prioritized*. Apr. 2024. URL: https://www.acm.nl/en/publications/acm-flexible-utilization-opens-more-possibilities-congested-grid-projects-social-functions-prioritized#:~:text=The%20problem%20of%20grid%20congestion%20predominantly%20occurs%20during%20peak%20hours,there%20is%20still%20sufficient%20capacity..

[17] Drury B Crawley et al. "Contrasting the capabilities of building energy performance simulation programs". In: *Building and environment* 43.4 (2008), pp. 661–673. DOI: https://doi.org/10.1016/j.buildenv.2006.10.027.

[18] J.F. DeCarolis et al. "Modelling to generate alternatives with an energy system optimization model". In: *Environmental Modelling Software* 79 (2016), pp. 300–310. ISSN: 1364-8152. DOI: https://doi.org/10.1016/j.envsoft.2015.11.019. URL: https://www.sciencedirect.com/science/article/pii/S1364815215301080.

[19] Gordon W. F. Drake. "thermodynamics". In: *Encyclopedia Britannica* (Mar. 2024). URL: https://www.britannica.com/science/thermodynamics.

[20] European Parliament and Council of 11 December 2018. *DIRECTIVE (EU) 2018/2001 OF THE EUROPEAN PARLIAMENT AND OF THE COUNCIL of 11 December 2018 on the promotion of the use of energy from renewable sources*. 2018. URL: https://eur-lex.europa.eu/legal-content/EN/TXT/PDF/?uri=CELEX:32018L2001&from=EN.

[21] Shahin Farahani. "Chapter 6 - Battery Life Analysis". In: *ZigBee Wireless Networks and Transceivers*. Ed. by Shahin Farahani. Burlington: Newnes, 2008, pp. 207–224. ISBN: 978-0-7506-8393-7. DOI: https://doi.org/10.1016/B978-0-7506-8393-7.00006-6. URL: https://www.sciencedirect.com/science/article/pii/B9780750683937000066.

[22] P. Favre-Perrod. "A vision of future energy networks". In: *2005 IEEE Power Engineering Society Inaugural Conference and Exposition in Africa*. 2005, pp. 13–17. DOI: 10.1109/PESAFR.2005.1611778.

[23] Siyu Feng, Hongtao Ren, and Wenji Zhou. "A review of uncertain factors and analytic methods in long-term energy system optimization models". In: *Global Energy Interconnection* 6.4 (2023), pp. 450–466. DOI: https://doi.org/10.1016/j.gloei.2023.08.006.

[24] Rafael Martinez-Gordon Francois Briens. *IEA - Heating*. July 2023. URL: https://www.iea.org/energy-system/buildings/heating.

[25] Roby Gauthier et al. "How do depth of discharge, C-rate and calendar age affect capacity retention, impedance growth, the electrodes, and the electrolyte in Li-ion cells?" In: *Journal of The Electrochemical Society* 169.2 (2022), p. 020518. DOI: 10.1149/1945-7111/ac4b82.

[26] Vladimir Z. Gjorgievski, Snezana Cundeva, and George E. Georghiou. "Social arrangements, technical designs and impacts of energy communities: A review". In: *Renewable Energy* 169 (2021), pp. 1138–1156. ISSN: 0960-1481. DOI: https://doi.org/10.1016/j.renene.2021.01.078. URL: https://www.sciencedirect.com/science/article/pii/S0960148121000859.

[27] Srinivasulu Gumpu, Balakrishna Pamulaparthy, and Ankush Sharma. "Review of congestion management methods from conventional to smart grid scenario". In: *International Journal of Emerging Electric Power Systems* 20.3 (2019), p. 20180265. DOI: https://doi.org/10.1515/ijeeps-2018-0265.

[28] Gurobi Optimization, LLC. *Gurobi Optimizer Reference Manual*. 2023. URL: https://www.gurobi.com.

[29] Gonca Gürses-Tran, Hendrik Flamme, and Antonello Monti. "Probabilistic Load Forecasting for Day-Ahead Congestion Mitigation". In: *2020 International Conference on Probabilistic Methods Applied to Power Systems (PMAPS)*. 2020, pp. 1–6. DOI: 10.1109/PMAPS47429.2020.9183670.

[30] Toby Hagon. "Price driven: electric cars have never been cheaper." In: (June 2024). URL: https://www.theguardian.com/australia-news/article/2024/jun/01/ev-electric-vehicle-sales-prices-australia.

[31] Long He et al. "Charging an electric vehicle-sharing fleet". In: *Manufacturing & Service Operations Management* 23.2 (2021), pp. 471–487. DOI: https://doi.org/10.1287/msom.2019.0851.

[32] Roman J Hennig, Laurens J de Vries, and Simon H Tindemans. "Congestion management in electricity distribution networks: Smart tariffs, local markets and direct control". In: *Utilities Policy* 85 (2023), p. 101660. DOI: https://doi.org/10.1016/j.jup.2023.101660.

[33] Christina E Hoicka and Julie MacArthur. "The infrastructure for electricity". In: *The Oxford Handbook of Energy Politics*. Oxford University Press, 2021. Chap. 4. DOI: https://doi.org/10.1093/oxfordhb/9780190861360.013.33.

[34] Dan Hu and Sarah M Ryan. "Stochastic vs. deterministic scheduling of a combined natural gas and power system with uncertain wind energy". In: *International Journal of Electrical Power & Energy Systems* 108 (2019), pp. 303–313. DOI: https://doi.org/10.1016/j.ijepes.2018.12.047.

[35] Muhammad Tayyab Hussain et al. "Optimal Management Strategies to solve issues of Grid Having Electric Vehicles (EV): A Review". In: *Journal of Energy Storage* 33 (2021), p. 102114. DOI: https://doi.org/10.1016/j.est.2020.102114.

[36] IEA. *Electricity generation mix - Germany*. 2022. URL: https://www.iea.org/countries/germany.

[37] IEA. *Electricity generation mix - The Netherlands*. 2022. URL: https://www.iea.org/countries/the-netherlands.

[38] IEA. "Space Cooling". In: (July 2023). URL: https://www.iea.org/energy-system/buildings/space-cooling.

[39] Mohammad Javadi et al. "A multi-objective model for home energy management system self-scheduling using the epsilon-constraint method". In: *2020 IEEE 14th International Conference on Compatibility, Power Electronics and Power Engineering (CPE-POWERENG)*. Vol. 1. IEEE. 2020, pp. 175–180. DOI: https://doi.org/10.1109/CPE-POWERENG48600.2020.9161526.

[40] James Keirstead, Mark Jennings, and Aruna Sivakumar. "A review of urban energy system models: Approaches, challenges and opportunities". In: *Renewable and Sustainable Energy Reviews* 16.6 (2012), pp. 3847–3866. DOI: https://doi.org/10.1016/j.rser.2012.02.047.

[41] Saadullah Khan et al. "Recent Development in Level 2 Charging System for xEV: A Review". In: *2018 International Conference on Computational and Characterization Techniques in Engineering Sciences (CCTES)*. 2018, pp. 83–88. DOI: 10.1109/CCTES.2018.8674068.

[42] Léone Klapwijk and Noortje van Bergeijk. "Alternative and flexible transmission capacity rights: a step closer to a more efficient use of the electricity grid in the Netherlands". In: *Van Doorne* (2024). URL: https://www.vandoorne.com/en/artikelen/alternative-and-flexible-transmission-capacity-rights-a-step-closer-to-a-more-efficient-use-of-the-electricity-grid-in-the-netherlands/.

[43] Aaron Kolleck. "Does Car-Sharing Reduce Car Ownership? Empirical Evidence from Germany". In: *Sustainability* 13.13 (2021). ISSN: 2071-1050. URL: https://www.mdpi.com/2071-1050/13/13/7384.

[44] Henrik Lund et al. "Simulation versus optimisation: Theoretical positions in energy system modelling". In: *Energies* 10.7 (2017), p. 840. DOI: https://doi.org/10.3390/en10070840.

[45] Montaser Mahmoud et al. "Recent advances in district energy systems: A review". In: *Thermal Science and Engineering Progress* 20 (2020), p. 100678. ISSN: 2451-9049. DOI: https://doi.org/10.1016/j.tsep.2020.100678. URL: https://www.sciencedirect.com/science/article/pii/S2451904920301980.

[46] Bardia Mashhoodi, Dominic Stead, and Arjan van Timmeren. "Local and national determinants of household energy consumption in the Netherlands". In: *GeoJournal* 85.2 (2020), pp. 393–406. DOI: https://doi.org/10.1007/s10708-018-09967-9.

[47] Fabian Voswinkel Mathilde Huismans. *Electrification - Energy System - IEA*. July 2023. URL: https://www.iea.org/energy-system/electricity/electrification.

[48] Dasaraden Mauree et al. "A new framework to evaluate urban design using urban microclimatic modeling in future climatic conditions". In: *Sustainability* 10.4 (2018), p. 1134. DOI: https://doi.org/10.3390/su10041134.

[49] Richard McAllister et al. *New approaches to distributed pv interconnection: Implementation considerations for addressing emerging issues*. Tech. rep. National Renewable Energy Lab.(NREL), Golden, CO (United States), 2019. DOI: https://doi.org/10.2172/1505553.

[50] Dev Millstein et al. "Solar and wind grid system value in the United States: The effect of transmission congestion, generation profiles, and curtailment". In: *Joule* 5.7 (2021), pp. 1749–1775. DOI: https://doi.org/10.1016/j.joule.2021.05.009.

[51] Mohammad Mohammadi et al. "Energy hub: From a model to a concept–A review". In: *Renewable and Sustainable Energy Reviews* 80 (2017), pp. 1512–1527. DOI: https://doi.org/10.1016/j.rser.2017.07.030.

[52] M Granger Morgan and David W Keith. "Improving the way we think about projecting future energy use and emissions of carbon dioxide". In: *Climatic Change* 90.3 (2008), pp. 189–215. DOI: https://doi.org/10.1007/s10584-008-9458-1.

[53] Nederland Netbeheer. *Capacity map in the electricity grid*. May 2024. URL: https://capaciteitskaart.netbeheernederland.nl/.

[54] Netbeheer Nederland. *Position paper Groeps-transportovereenkomst (Groeps-TO)*. Aug. 2023. URL: https://www.netbeheernederland.nl/sites/default/files/2024-03/position_paper_groeps-to_v1.0_-_augustus_2023.pdf.

[55] Nigel. *Battery pack volume*. May 2024. URL: https://www.batterydesign.net/battery-pack-volume/#:~:text=Often%20it%20is%20difficult%20to,a%20volume%20of%20500%20litres..

[56] Nanda K. Panda and Simon Tindemans. "Quantifying the Aggregate Flexibility of EV Charging Stations for Dependable Congestion Management Products: A Dutch Case Study". In: (Mar. 2024). DOI: https://doi.org/10.48550/arXiv.2403.13367.

[57] M.A. Pans, G. Claudio, and P.C. Eames. "Modelling of 4th generation district heating systems integrated with different thermal energy storage technologies – Methodology". In: *Energy Conversion and Management* 276 (2023), p. 116545. ISSN: 0196-8904. DOI: https://doi.org/10.1016/j.enconman.2022.116545. URL: https://www.sciencedirect.com/science/article/pii/S0196890422013231.

[58] Mattia Pasqui et al. "Community Battery for Collective Self-Consumption and Energy Arbitrage: Independence Growth vs. Investment Cost-Effectiveness". In: *Sustainability* 16.8 (2024). ISSN: 2071-1050. DOI: 10.3390/su16083111. URL: https://www.mdpi.com/2071-1050/16/8/3111.

[59] Moritz Paulus and Frieder Borggrefe. "The potential of demand-side management in energy-intensive industries for electricity markets in Germany". In: *Applied energy* 88.2 (2011), pp. 432–441. DOI: https://doi.org/10.1016/j.apenergy.2010.03.017.

[60] Tim T Pedersen et al. "Modeling all alternative solutions for highly renewable energy systems". In: *Energy* 234 (2021), p. 121294. DOI: https://doi.org/10.1016/j.energy.2021.121294.

[61] Uwe Pfeifroth et al. *Surface Radiation Data Set - Heliosat (SARAH) - Edition 2*. 2017. DOI: 10.5676/EUM_SAF_CM/SARAH/V002. URL: https://wui.cmsaf.eu/safira/action/viewDoiDetails?acronym=SARAH_V002.

[62] Stefan Pfenninger and Iain Staffell. "Long-term patterns of European PV output using 30 years of validated hourly reanalysis and satellite data". In: *Energy* 114 (2016), pp. 1251–1265. ISSN: 0360-5442. DOI: https://doi.org/10.1016/j.energy.2016.08.060. URL: https://www.sciencedirect.com/science/article/pii/S0360544216311744.

[63] Carlos Quesada et al. "An electricity smart meter dataset of Spanish households: insights into consumption patterns". In: *Scientific Data* 11.1 (2024), p. 59. DOI: https://doi.org/10.1038/s41597-023-02846-0.

[64] Benjamin Rausch, Philipp Staudt, and Christof Weinhardt. "Transmission grid congestion data and directions for future research". In: *Proceedings of the Tenth ACM International Conference on Future Energy Systems*. 2019, pp. 443–446. DOI: https://doi.org/10.1145/3307772.3331018.

[65] Royal Institute of Technology (KTH). *Eco-friendly Supermarkets - an Overview*. Tech. rep. 2016. URL: https://ec.europa.eu/research/participants/documents/downloadPublic?documentIds=080166e5adf40ec8&appId=PPGMS#:~:text=It%20is%20shown%20that%20supermarkets,of%20the%20total%20energy%20use..

[66] Rubitherm GmbH. *PCM RT-LINE*. URL: https://www.rubitherm.eu/en/productcategory/organische-pcm-rt.

[67] Oliver Ruhnau, Lion Hirth, and Aaron Praktiknjo. "Time series of heat demand and heat pump efficiency for energy system modeling". In: *Scientific data* 6.1 (2019), pp. 1–10. DOI: https://doi.org/10.1038/s41597-019-0199-y.

[68] Oliver Ruhnau and Jarusch Muessel. *Update and extension of the When2Heat dataset*. eng. Tech. rep. Additional information: This is an update and extension of the original When2Heat dataset described in: Ruhnau, O., Hirth, L., Praktiknjo, A., 2019. Time series of heat demand and heat pump efficiency for energy system modeling. Sci Data 6, 189. https://doi.org/10.1038/s41597-019-0199-y. Kiel, Hamburg, 2022. URL: https://hdl.handle.net/10419/249997.

[69] Sandia National Laboratories. *Isotropic Sky Diffuse Model*. 2024. URL: https://pvpmc.sandia.gov/modeling-guide/1-weather-design-inputs/plane-of-array-poa-irradiance/calculating-poa-irradiance/poa-sky-diffuse/isotropic-sky-diffuse-model/.

[70] Hans Schermeyer, Claudio Vergara, and Wolf Fichtner. "Renewable energy curtailment: A case study on today's and tomorrow's congestion management". In: *Energy Policy* 112 (2018), pp. 427–436. ISSN: 0301-4215. DOI: https://doi.org/10.1016/j.enpol.2017.10.037. URL: https://www.sciencedirect.com/science/article/pii/S0301421517307115.

[71] Katrin Schmietendorf, Joachim Peinke, and Oliver Kamps. "The impact of turbulent renewable energy production on power grid stability and quality". In: *The European Physical journal. B* 90.11 (Nov. 2017). DOI: 10.1140/epjb/e2017-80352-8. URL: https://doi.org/10.1140/epjb/e2017-80352-8.

[72] Mattia Secchi et al. "Multi-objective battery sizing optimisation for renewable energy communities with distribution-level constraints: A prosumer-driven perspective". In: *Applied Energy* 297 (2021), p. 117171. DOI: https://doi.org/10.1016/j.apenergy.2021.117171.

[73] Noman Shabbir et al. "Congestion control strategies for increased renewable penetration of photovoltaic in LV distribution networks". In: *Energy Reports* 8 (2022), pp. 217–223. DOI: https://doi.org/10.1016/j.egyr.2022.10.184.

[74] Pierluigi Siano. "Demand response and smart grids—A survey". In: *Renewable and sustainable energy reviews* 30 (2014), pp. 461–478. DOI: https://doi.org/10.1016/j.rser.2013.10.022.

[75] Arno Smets et al. *Solar Energy: The physics and engineering of photovoltaic conversion, technologies and systems*. Bloomsbury Publishing, Jan. 2016. URL: https://ocw.tudelft.nl/course-readings/readings-solar-energy/.

[76] Ankur Srivastava et al. "Development of a DSO support tool for congestion forecast". In: *IET Generation, Transmission & Distribution* 15.23 (2021), pp. 3345–3359. DOI: https://doi.org/10.1049/gtd2.12266.

[77] Stedin. *COngestie en congestiemanagement*. URL: https://www.stedin.net/zakelijk/energietransitie/beschikbare-netcapaciteit/congestie-en-congestiemanagement.

[78] Peter Tozzi Jr and Jin Ho Jo. "A comparative analysis of renewable energy simulation tools: Performance simulation model vs. system optimization". In: *Renewable and Sustainable Energy Reviews* 80 (2017), pp. 390–398. DOI: https://doi.org/10.1016/j.rser.2017.05.153.

[79] C.P. Underwood. "14 - Heat pump modelling". In: *Advances in Ground-Source Heat Pump Systems*. Ed. by Simon J. Rees. Woodhead Publishing, 2016, pp. 387–421. ISBN: 978-0-08-100311-4. DOI: https://doi.org/10.1016/B978-0-08-100311-4.00014-5. URL: https://www.sciencedirect.com/science/article/pii/B9780081003114000145.

[80] Laetitia Uwineza, Hyun-Goo Kim, and Chang Ki Kim. "Feasibility study of integrating the renewable energy system in Popova Island using the Monte Carlo model and HOMER". In: *Energy Strategy Reviews* 33 (2021), p. 100607. DOI: https://doi.org/10.1016/j.esr.2020.100607.

[81] Remco A. Verzijlbergh, Laurens J. De Vries, and Zofia Lukszo. "Renewable Energy Sources and Responsive Demand. Do We Need Congestion Management in the Distribution Grid?" In: *IEEE Transactions on Power Systems* 29.5 (2014), pp. 2119–2128. DOI: 10.1109/TPWRS.2014.2300941.

[82] Karl Vilén and Erik O Ahlgren. "Linear or mixed integer programming in long-term energy systems modeling–A comparative analysis for a local expanding heating system". In: *Energy* 283 (2023), p. 129056. DOI: https://doi.org/10.1016/j.energy.2023.129056.

[83] Werner van Westering and Hans Hellendoorn. "Low voltage power grid congestion reduction using a community battery: Design principles, control and experimental validation". In: *International Journal of Electrical Power & Energy Systems* 114 (2020), p. 105349. DOI: https://doi.org/10.1016/j.ijepes.2019.06.007.

[84] Ralph A Wurbs. "Reservoir-system simulation and optimization models". In: *Journal of water resources planning and management* 119.4 (1993), pp. 455–472. DOI: https://doi.org/10.1061/(ASCE)0733-9496(1993)119:4(455).

[85] Le Xie et al. "Toward carbon-neutral electricity and mobility: Is the grid infrastructure ready?" In: *Joule* 5.8 (2021), pp. 1908–1913. URL: http://www.elsevier.com/open-access/userlicense/1.0/.

[86] Guijun Yang et al. "Carbon-filled organic phase-change materials for thermal energy storage: A review". In: *Molecules* 24.11 (2019), p. 2055. DOI: https://doi.org/10.3390/molecules24112055.

[87] Xuanjun Zong, Yue Yuan, and Han Wu. "Multi-objective optimization of multi-energy flow coupling system with carbon emission target oriented". In: *Frontiers in Energy Research* 10 (2022), p. 877700. DOI: https://doi.org/10.3389/fenrg.2022.877700.